Diffusion Bonding Aluminium Alloys and Composites:

New Approaches and Modelling

Amir A. Shirzadi

King's College
Cambridge

A thesis submitted for the degree of
Doctor of Philosophy at the University of Cambridge

December 1997

Declaration

This thesis describes work undertaken in the Department of Materials Science and Metallurgy at the University of Cambridge between April 1994 and December 1997.

The work is entirely my own and includes nothing which is the outcome of work done in collaboration, except where reference is explicitly made to the work of others. The work has not been submitted, either in whole or in part, for any degree or qualification at any other university and does not exceed 60,000 words.

This work was financially supported by the Ministry of Higher Education of Iran, the Committee of Vice-Chancellors and Principals of the Universities of the United Kingdom (ORS Award Scheme), and King's College, the University of Cambridge.

Amir A. Shirzadi
Cambridge
December 1997

Acknowledgement

I am wholeheartedly grateful to my supervisor, Dr Rob Wallach, for his guidance, encouragement and invaluable friendship during my research period in Cambridge. It is a pleasure for me to acknowledge Dr Sue Jackson for her advice and ever friendly support. Also, I would like to thank Dr Ian Bucklow for the useful discussions I had with him on my work.

I sincerely thank Dr Hamid Assadi for his advice and help throughout my research, and also Fataneh who provided an enjoyable atmosphere for Hamid and me to carry on with our discussions. I am also grateful to Mohammed Balamdi for "tidying" my room frequently and Kaveh Chamandar who kept correcting my English accent so patiently. Thanks are also due to my friends at King's College: Clea for her kind friendship and food-wise logistic; Liz, Ken, Kai and Paul for improving my knowledge to the single currency issue during our outings.

I am grateful to Professor Alan Windle, the Head of the Department, for providing laboratory facilities, and I express my gratitude to my research colleagues, academic and technical staff in the Department who helped me so sincerely in the course of my research. Finally, thanks to the staff in my college for their help and many others who made my time in Cambridge so enjoyable.

Abstract

Development of a suitable joining technique for advanced aluminium alloys and composites will enable them to be more widely used. The aim of this Ph.D. research was to develop new joining methods for these materials for which conventional welding methods have been unsuccessful. The research led to six new bonding methods and also to an analytical model which may be applicable to all transient liquid phase (TLP) bonding processes.

In the early stage of the research, two new methods for TLP diffusion bonding of aluminium-based composites (aluminium alloys with silicon carbide particles as reinforcement) were developed. The methods were based on applying isostatic pressure (rather than conventional uniaxial compression), and bonds were fabricated with shear strengths as high as 242 MPa which is 92% of the shear strength of the parent material. This value is far greater than the highest bond strength reported to date for these aluminium-based composites.

Based on simple finite element analysis modelling, a third method was developed which allows the joining of superplastic alloys/composites with minimal deformation. This method is based on a combination of conventional TLP diffusion bonding and hot isostatic pressing without encapsulation. It allows the fabrication of intricate parts with virtually no deformation during the bonding process so that dimensional tolerances are preserved.

A fourth method, which is based on a new approach to TLP diffusion bonding by introducing a temperature gradient, is capable of producing reliable bonds with shear strengths as high as those of the parent alloys. The use of this method led to the formation of non-planar interfaces, compared to planar interfaces associated with

conventional diffusion bonding methods. Therefore the strength and reliability of the bonds, made using this method, were improved considerably. This fourth method has already been patented in the United Kingdom (UK 9709167.2).

A comprehensive analytical model was developed to predict the bonding time and the microstructure of the bond line when using temperature gradient TLP diffusion bonding. The model has been experimentally verified. The model also may be applicable to all TLP diffusion bonding approaches.

The fifth method, developed in the current research, is capable of fabricating reliable bonds in air with shear strengths as high as 90% of those of the parent material. This is the highest bond strength, reported to date, for diffusion-bonded aluminium joints made in air. The approach overcomes the limitations associated with bonding aluminium-based materials in vacuum; this has been a major restriction in exploitation of the process. Patent protection has been sought (UK 9811860.7).

Based on a combination of the fourth and fifth methods, a sixth method is proposed to improve the reliability of bonds made in air (temperature gradient TLP diffusion bonding in air). Preliminary results are very promising and some suggestions for further work on this method are proposed.

Table of Contents

1. Introduction 1

Summary of the work in this dissertation 2

2. Literature survey 4

2.1 Theoretical aspects of solid-state diffusion bonding 7

2.2 Theoretical aspects of transient liquid phase (TLP) diffusion bonding 10

Modelling of TLP diffusion bonding 12

Modelling of TLP diffusion bonding of composites 16

2.3 Solid-state diffusion bonding of aluminium alloys 18

Imposing macroscopic plastic deformation 18

Enhancing microplastic deformation of the surface asperities 18

Use of interlayers and the effect of alloying elements 20

Non-conventional bonding and testing methods 21

2.4 TLP diffusion bonding of aluminium alloys 24

Zinc based interlayers 24

Silver interlayers 25

Copper interlayers 25

2.5 Joining aluminium metal matrix composites 27

2.6 Diffusion bonding of aluminium-based materials in air 31

2.7 Summary 33

Appendix 35

3. Experimental procedure 37

3.1 Parent materials and interlayers 37

3.2 Bond fabrication 39

3.2.1 Pre-bonding procedure 39

3.2.2 Bonding procedure 40

Method I: *Isostatic TLP diffusion bonding 42*

Method II: *Low pressure conventional TLP diffusion bonding followed by isostatic solid-state diffusion bonding in air 42*

Method III: *Low pressure conventional TLP diffusion bonding followed by hot isostatic pressing (HIP) without encapsulation 44*

Method IV: *Temperature gradient TLP diffusion bonding 44*

Method V: *High heating rate TLP diffusion bonding in air 44*

Method VI: *Temperature gradient TLP diffusion bonding in air 47*

3.2.3 Post bond heat treatment 49

3.3 Bond testing and evaluation 51

3.3.1 Mechanical testing 51

3.3.2 Metallographic examination 52

4. Methods I, II and III: New methods for TLP diffusion bonding aluminium-based composites 55

4.1 Introduction 55

4.2 The aim of using isostatic pressure for TLP diffusion bonding of aluminium MMCs 58

4.3 Results and discussion 60

4.3.1 Methods I and II 60

4.3.2 Bonds in Al-Li alloy (UL-40) 71

4.3.3 Method III 73

4.4 Case study: The role of reinforcement particles when diffusion bonding Al-MMCs 77

4.5 Summary 81

5. Method IV: Temperature gradient TLP diffusion bonding.....83

5.1 Introduction.....83

5.2 Theoretical aspects of temperature gradient TLP diffusion bonding.....84

5.3 Numerical simulation of temperature gradient TLP diffusion bonding.....87

5.4 Results and discussion.....89

5.4.1 Microstructure examination.....89

5.4.2 Shear test results.....93

5.4.3 Chemical analysis and hardness testing results.....97

5.5 Summary.....99

Appendix.....100

6. Analytical modelling of temperature gradient TLP diffusion bonding (method IV).....101

6.1 Background.....102

6.2 Precise analytical solution.....103

6.3 Geometrical approach: conservation of mass.....108

6.4 Combination of analytical and mass conservation approaches....111

6.5 Experimental verification of modelling.....118

6.5.1 Experimental procedure and results.....118

6.6 Summary.....123

7. Methods V and VI: New methods for TLP diffusion bonding aluminium alloys in air.....124

7.1 Introduction.....124

7.2 Method V: High heating rate TLP diffusion bonding in air.....126

7.2.1 Results of method V and discussion 128

7.3 Method VI: Temperature gradient TLP diffusion bonding in air 135

7.3.1 Results of method VI and discussion 136

7.4 Summary 138

8. Conclusions and proposal for future work 140

8.1 Experimental results 140

Method I *140*

Method II *140*

Method III *141*

Method IV *141*

Method V *142*

Method VI *142*

Al-Li (UL-40) bonds *143*

Summary *143*

8.2 Modelling of method IV 146

8.3 Future work 147

References 150

Chapter 1

1. Introduction

In the last three decades, the development of advanced materials with superior mechanical properties has underpinned rapid progress in manufacturing of new products. The ever increasing demand for high performance materials has spurred research into the development of advanced alloys and composites. Transport industries, particularly aerospace and more recently car manufacturers, have been interested particularly in materials with high strength-to-weight ratios as these can provide significant performance benefits.

Since the development of the first heat-treatable aluminium alloy in the early years of this century, aluminium alloys have been of interest because of their high strength-to-weight ratio, formability, corrosion resistance and long-term durability. The first all-aluminium aeroplane was manufactured in 1920 and since then, despite significant advances in non-metallic composites and titanium-based materials, aluminium alloys are still the major materials for aerostructures, *Staley et al. (1997).* Aluminium metal matrix composites (Al-MMCs) possess even better mechanical properties compared to un-reinforced aluminium alloys (especially their high stiffness, strength and wear resistance). Following the recent development of low cost manufacturing processes, Al-MMCs with silicon carbide or alumina particle reinforcement (i.e. discontinuously reinforced aluminium, DRA) are now available commercially. The use of Al/SiC composites has reduced the production costs and improved the performance of aircraft components, *Materials Progress (1997).*

However, despite substantial improvements in the range and properties of such

advanced aluminium-based materials, the lack of a reliable and economic joining method has restricted their full potential.

Due to the high temperatures inherent in fusion welding processes, the use of these methods for joining some of the advanced aluminium-based materials (e.g. Al-Li alloys and Al/SiC MMCs) proved unsuccessful. Detrimental reactions are reduced when joining using solid or liquid state diffusion bonding as these processes are carried out at lower temperatures than fusion welding processes.

Unfortunately, the results of more than three decades of research on diffusion bonding aluminium-based materials have not convinced design engineers that diffusion bonding is a reliable and commercial method for joining these materials. A particular discouraging feature when diffusion bonding aluminium-based materials is the wide scatter in the results. Also, in most cases either the bond strengths are well below the strength of the parent material, or the bonding process is associated with intolerable plastic deformation which is required to achieve reasonable bond strengths. Some of the approaches tried rely on sophisticated pre-bonding processes and equipment which restrict considerably the application of the method.

In order to overcome the problems associated with the diffusion bonding of aluminium based materials, six new methods for liquid-state diffusion bonding of aluminium-based materials have been developed in the current work. An analytical model for the fourth method is proposed and verified experimentally. This model also has the potential to predict bonding times in other liquid-state diffusion bonding approaches.

Summary of the work in this dissertation

In **Chapter 2,** the basic definitions and theoretical aspects of solid and liquid state diffusion bonding are detailed. Previous investigations on solid and liquid state diffusion bonding of aluminium alloys have been categorised and compared by considering the basis of the technique or the type of interlayer used. Joining methods developed for Al-MMCs are reviewed, and the diffusion bonding of aluminium-based materials in air is reviewed in the final section. The experimental procedures for the

new liquid-state diffusion bonding methods and the techniques used for bond evaluation are described in **Chapter 3.**

In **Chapter 4**, the first three methods (methods I, II and III), developed for joining Al-MMCs, are explained. Methods I and II are based on applying isostatic pressure (rather than conventional uniaxial compression), and bonds were fabricated, using method II, with shear strengths as high as 242 MPa which is 92% of the shear strength of the parent material. Based on simple finite element analysis modelling, a third method was developed which allows the joining of superplastic alloys/composites with minimal deformation. This method is based on a combination of conventional TLP diffusion bonding and hot isostatic pressing (HIP) without encapsulation. It allows the fabrication of intricate parts with virtually no deformation during the bonding process so that dimensional tolerances are preserved. Patent protection is being investigated for this method (Method III).

A fourth method, which is based on a new approach to TLP diffusion bonding, is capable of producing reliable bonds with shear strengths as high as that of the parent material. This method is described in **Chapter 5**, and has been patented in the United Kingdom (UK 9709167.2). A comprehensive analytical model, capable of predicting the bonding time and the microstructure of the bond line, is presented in **Chapter 6**. The model has been verified experimentally.

The fifth method is capable of fabricating reliable bonds in air with shear strengths as high as 90% that of the parent material. This approach overcomes the limitations associated with bonding aluminium-based materials in vacuum which has been a major restriction in exploitation of the process. The method is outlined in **Chapter 7**. Patent protection has been applied for. The preliminary results of the most recent method (method VI) are also presented in **Chapter 7**. This method is based on a combination of the fourth and fifth methods and was developed to improve the reliability and strength of the bonds made in air. Finally, the results of the current work are summarised in **Chapter 8** and also suggestions for future work are proposed.

Chapter 2

2. Literature survey

Welding techniques are generally classified into two categories: fusion welding processes (e.g. arc welding) and solid-state welding processes (e.g. pressure welding). In the former case, bonds are established by the formation and solidification of a liquid phase at the interface while, in the latter case, the applied pressure has a key role in bringing together the surfaces to be joined within interatomic distances. Although precise details are not known about the actual methods used by early blacksmiths and craftsmen, it is evident that solid-state welding has been used for more than a thousand years, *Singer et al. (1958).*

Diffusion bonding, as a subdivision of both solid-state welding and liquid-phase welding, is a joining process wherein the principal mechanism is interdiffusion of atoms across the interface. The International Institute of Welding (IIW) has adopted a modified definition of solid-state diffusion bonding, proposed by *Kazakov (1985).*

Diffusion bonding of materials in the solid state is a process for making a monolithic joint through the formation of bonds at atomic level, as a result of closure of the mating surfaces due to the local plastic deformation at elevated temperature which aids interdiffusion at the surface layers of the materials being joined.

Solid-state diffusion bonding is normally carried out at high temperatures, about 50%-70% of the absolute melting point of the parent material. Longer times than those used in conventional pressure welding processes, e.g. roll or forge welding, are used in order to allow creep processes to contribute to bonding and to lead to a reduction in the

pressure required for intimate contact between the faying surfaces. Thus, in contrast to most solid-state welding processes, diffusion bonding is not normally associated with large amounts of deformation.

In contrast, liquid-state diffusion bonding relies on the formation of a liquid phase at the bond line during an isothermal bonding cycle. This liquid phase then infuses the base material and eventually solidifies as a consequence of continued diffusion at constant temperature. Therefore, this process is called Transient Liquid Phase (TLP) diffusion bonding. The liquid phase in TLP diffusion bonding generally is formed by inserting an interlayer which forms a low melting point phase, e.g. eutectic or peritectic, after preliminary interdiffusion of the interlayer and the base metal at a temperature above the eutectic temperature $T_{eutectic}$. Note that the liquid phase could, alternatively, be formed by inserting an interlayer with an appropriate initial composition e.g. eutectic composition which melts at the bonding temperature $T_{bonding}$. The diffusion rate in the liquid phase enhances dissolution and/or disruption of the oxide layer and so promotes intimate contact between the faying surfaces. Therefore, the presence of a liquid phase reduces the pressure required for TLP diffusion bonding in comparison with solid-state diffusion bonding and may overcome the problem associated with solid-state diffusion bonding of the materials with a stable oxide layer.

Achieving high integrity joints with minimal detrimental effects on the parent material in the bond region and also the possibility of joining dissimilar materials are the most promising features of diffusion bonding. Accordingly, interest in diffusion bonding has been growing in the last forty years. The combination of diffusion bonding and superplastic forming for producing complex structures (e.g. honeycomb structures) has also played a part in increasing the use of this process as a commercial joining method. A number of advantages and limitations of diffusion bonding are listed in the appendix at the end of this chapter, although not all apply to the diffusion bonding of all materials.

Diffusion bonding of most metals is conducted under a vacuum of 10^{-3}-10^{-5} mbar or in an inert atmosphere (normally dry nitrogen, argon or helium) in order to reduce detrimental oxidation of the faying surfaces. Bonding of the few metals which have

oxide films that are thermodynamically unstable at the bonding temperature (e.g. silver) may be achieved in air.

Variants of solid-state diffusion bonding are also referred to by the following terms:

- diffusion welding;
- solid-state bonding;
- pressure bonding;
- isostatic bonding;
- hot press bonding;
- pressure joining;
- auto-vacuum welding;
- thermo-compression welding.

Liquid-state diffusion bonding is referred to as “transient liquid phase (TLP) diffusion bonding” or simply “TLP diffusion bonding” in this work.

2.1 Theoretical aspects of solid-state diffusion bonding

The aim, when diffusion bonding, is to bring the surfaces of the two pieces being joined sufficiently close that interdiffusion can result in bond formation. In practice, because of inevitable surface roughness greater than an atomic scale, it is not possible to bring the surfaces of two pieces within interatomic distances by simple contact. Even highly polished surfaces come into contact only at their asperities and the ratio of contacting area to faying area is very low. Thus the mechanism of solid-state diffusion bonding can be classified into two main stages.

During the first stage, the asperities on each of the faying surfaces deform plastically as the pressure is applied. These asperities arise from the grinding or polishing marks that have been produced in the surface finishing stage. The microplastic deformation proceeds until the localised effective stress at the contact area becomes less than the yield strength of the material at the bonding temperature. In fact, initial contact occurs between the oxide layers that cover the faying surfaces. As the deformation of asperities proceeds, more metal-to-metal contact is established because of local disruption of the relatively brittle oxide films which generally fracture readily. At the end of the first stage, the bonded area is less than 10% and a large volume of voids and oxide remains between localised bonded regions.

In the second stage of bonding, thermally activated mechanisms lead to void shrinkage and this increases further the bonded areas.

There are several hypotheses to explain how a bond is formed in the solid state, *Kazakov (1985)*. The “Film Hypothesis” emphasises the effect of surface film characteristics on the joining process. According to this hypothesis, the observed differences in weldability of various metals are attributed to the different properties of their surface films and all metals are assumed to bond if thoroughly cleaned surfaces are brought together within the range of interatomic forces. A different theory, the “Recrystallisation Hypothesis”, suggests that the strain hardening of the faying surfaces

during plastic deformation causes atoms to move from one side to the other of the interface at high temperature. Subsequently, new grains grow at the interface and the bond is established. The "Electron Hypothesis" is based on the formation of a stable electron configuration as a result of metallic bond formation. In the "Dislocation Hypothesis", exposure of dislocations to the free surface, as a result of plastic deformation, breaks up the oxide film and produces steps on an atomic scale which enhance the seizure of the joining parts. Finally, the "Diffusion Hypothesis", the most commonly accepted hypothesis, considers the contribution of interatomic diffusion during bond formation. The difference in the energy level of surface atoms and of bulk atoms is the basis of this hypothesis.

All attempts at modelling diffusion bonding have two main aims. The first is to optimise the process variables e.g. surface finish, bonding temperature, pressure and time so that the proper bonding conditions for a particular material can be identified. Secondly, a model attempts to obtain a reasonable and profound understanding of the mechanisms involved and their relative contributions not only for different bonding conditions but also for different materials being joined.

Various models for solid-state diffusion bonding have been reviewed by *Wallach (1988)*. See figure 2-1 for a chronological summary of the proposed models up-dated to include recent approaches. However, as solid-state diffusion bonding is not a major part of the current work, this topic is not considered further.

1966
Cline
A two-stage model assuming localized plastic deformaion followed by the diffusion-controlled process, using the recrystallisation model of Parks (1953).

1967
King and Owczarski
Similar to Cline's model except that the migration of interface away from the voids was assumed to occur during the second stage and the remaining isolated voids are removed by volume diffusion in the third stage.

1973
Hamilton
The first quantitative model, based on creep dominant mechanisms.

1975
Garmong et al.
Similar to the Hamilton's model but including diffusion mechanisms and superimposing two different wavelengths (corresponding waviness and roughness of the joining surfaces). Removal of the voids was modelled by using the sintering equations derived by Coble (1970).

1982
Derby and Wallach
Based on an intensive use of the sintering equations assuming six different diffusion mechanisms.

1984
Derby and Wallach
Modification of the previous model (1982) in order to reduce the existing discontinuity in bonding rate between the second and final stage.

1984
Pilling et al.
A diffusive creep cavitation model adopted for fine grain superplastic alloys, based on creep model of Chen and Argon (1981).

1987
Guo and Ridley
Using the same mechanisms as the Derby and Wallach model but assuming two concomitant modes of void closure.

1989
Hill and Wallach
Assuming elliptic voids with successive incremental changes in shape to circular in order to overcome some of the limitations of previous models.

1992
Takahashi and Inoue
An overview of the void shrinkage models including the models proposed by Takahashi et al. (1988 & 1991) based on diffusional flow of atoms, assuming successive mechanisms when interface diffusion is slower than surface diffusion or vice versa.

1995
Takahashi and Tanimoto
Finite element analysis of interfacial contact process due to power law creep; no diffusional mechanisms for void shrinkage are taken into account.

Fig. 2-1: Summary of solid-state diffusion bonding modelling.

2.2 Theoretical aspects of transient liquid phase (TLP) diffusion bonding

Figure 2-2 shows a simple eutectic phase diagram where A represents a pure parent material and B is the diffusing solute (i.e. the originally solid interlayer) with limited solubility in A. Basically, TLP diffusion bonding consists of three major stages as follows.

- dissolution of the base metal;
- isothermal solidification;
- solid-state homogenisation.

The dissolution stage can be divided into two hierarchical sub-stages in which filler metal melting is followed by widening of the liquid zone, *Tuah-poku et al. (1988)*. However, if the melting process occurs as a result of interdiffusion of A and B, then melting of the interlayer and widening of the liquid phase may occur simultaneously.

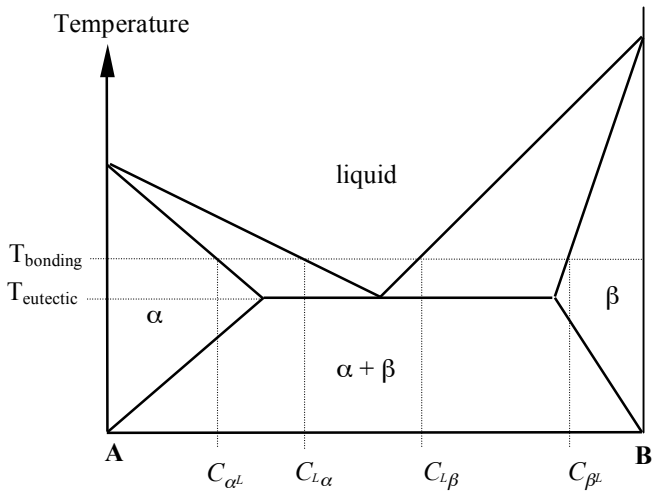

Fig. 2-2: A simple binary phase diagram; A and B represent the parent material and the interlayer in transient liquid phase diffusion bonding, respectively.

According to the phase diagram, equilibrium in the liquid can be established by dissolution of A atoms into the supersaturated B-rich liquid to decrease its concentration to $C_{L\alpha}$. During this stage, homogenisation of the liquid phase continues and the width of the liquid zone increases, see figure 2-3a, until the composition profile in the liquid phase levels out, i.e. diffusion in the liquid ceases. The rate of this homogenisation is controlled mainly by the diffusion coefficient in the liquid phase and, therefore, this stage takes a short time to be completed.

In the next stage, isothermal solidification occurs as B atoms start to diffuse into the solid phase, and the liquid zone shrinks in order to maintain the equilibrium compositions of $C_{L\alpha}$ and $C_{\alpha L}$ at the solid/liquid moving boundaries, figure 2-3b. The interdiffusion coefficient in the solid phase (α) controls the rate of solidification and, because diffusivity in the solid is low, the annihilation of the liquid phase is very slow compared to the initial rapid dissolution stage for which diffusivity in the liquid controls the rate of the reaction. It should be mentioned that solidification may occur before reaching the bonding temperature if the heating rate between the eutectic temperature and the bonding temperature is too low. This situation normally happens when the filler material contains a melting point depressant with high diffusivity in the solid phase. This phenomenon was modelled by *Nakagawa et al. (1991*) for TLP diffusion bonding of a nickel-based alloy using a Ni-P interlayer.

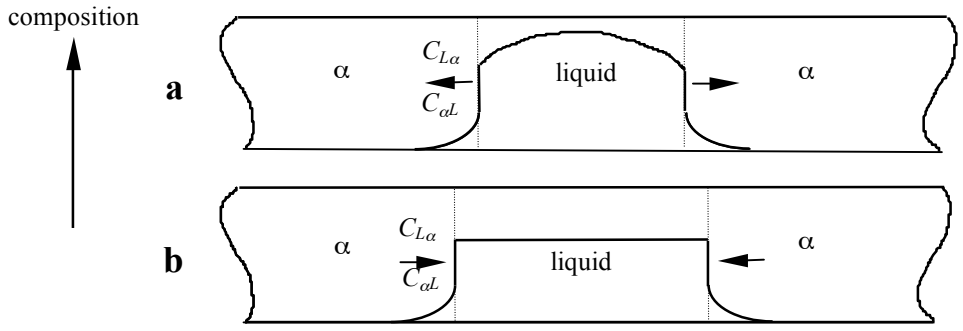

Fig. 2-3: Dissolution of base metal and homogenisation of liquid phase (a), and onset of isothermal solidification (b) in TLP diffusion bonding. Arrows show the direction of movement of the solid/liquid interfaces.

In the solid-state homogenisation stage, the concentration gradient of solute around the interface declines. This is due to further diffusion of solute into the base material. Theoretically, the chemical composition of the area adjacent to bond line could approach that of the parent material.

In addition to the stages mentioned above, *MacDonald & Eagar (1992)* introduced another stage, termed stage 0, which accounts for the effects of a low heating rate, discussed by *Niemann & Garrett (1974a) and Nakagawa et al. (1991*). They showed that a low heating rate may lead to insufficient liquid formation due to diffusion of the filler material into the bulk of base metal before the eutectic temperature is reached.

Finally note that there is a difference between conventional brazing and TLP diffusion bonding processes. The liquid phase in a brazing process wets the base metal and solidifies only when the interface temperature decreases. In TLP diffusion bonding, however, interdiffusion between the liquid phase and the base metal leads to a change in the composition of the liquid phase and, consequently, to isothermal solidification. The bonding temperature is usually determined by the temperature at which the liquid phase forms, i.e. it is slightly above the corresponding eutectic temperature.

Modelling of TLP diffusion bonding

In light of the increasing use of TLP diffusion bonding for joining heat resistant materials and titanium alloys in recent years, some attempts have been made to model this process using analytical and numerical approaches. Some are reviewed below.

As mentioned before, TLP bonding uses the reduced liquidus temperature that occurs in eutectic or peritectic alloy systems. *Tuah-poku et al. (1988)* analysed theoretical aspects of TLP bonding associated with a simple eutectic phase diagram, using the binary system of silver-copper. Based on earlier work of *Lesoult (1976)* and *Sekerka (1975)*, they studied TLP diffusion bonding in four distinct stages wherein the composition of each phase was determined by the phase diagram, assuming local equilibrium at the solid/liquid interface. However, for the sake of simplicity in this mathematical calculation, the interdiffusion coefficients were assumed to be independent of chemical composition. Also, the difference between the partial molar volumes of each element in

existing phases was neglected, so it was possible to use *Fick's* diffusion laws in terms of mole fractions. Finally, because of the small thicknesses of the interlayers used in this process (normally not more than 100 μm), the effect of convection in the liquid phase was neglected.

In the first stage, interdiffusion of A (base material) and B (interlayer) atoms at the interface results in a composition $C_{\alpha L}$ (figure 2-2) and consequently melting starts. The dissolution of A and B atoms in the liquid phase is very rapid since there is a high concentration gradient ($C_{L\beta}$–$C_{L\alpha}$) across the interface. Accordingly, complete dissolution of the interlayer occurs rapidly and the rate is controlled by the diffusion rate in the liquid phase, D_L. If the interlayer is assumed to be thick enough (such that the concentration at its centre does not change) then the amount of solute at the interface is constant, and the solution to *Fick's* second law for this case is the well-known error function equation:

$$C_L = E + F \times erf\left(\frac{x}{\sqrt{4D_L t}}\right) \tag{2-1}$$

where x is the distance across the bond region, t is the time, E and F are constants determined by the specific boundary conditions. Hence the interface displacement Y obeys a general square root law:

$$Y = K_1\sqrt{4D_L t} \tag{2-2}$$

For typical values of the constant K_1, between 0.13 to 1.18 for different systems *(Lesoult 1976)*, dissolution is completed in less than a minute.

In the second stage, homogenisation of the liquid phase occurs. As the liquid phase is supersaturated, equilibrium is established by the dissolution of A atoms and meanwhile the width of the liquid zone increases. Depending on the alloy system, the width of the molten zone can be several times the original width of the interlayer being used. The diffusion phenomenon in this stage is complicated and no simple analytical approach has been proposed. This stage normally takes several minutes to be completed and the effective diffusion coefficient D_e is related to a combination of the diffusion coefficients

in both the liquid and solid phases. It is worth noting that the effect of pressure on the width of the liquid zone has been neglected in this analysis; see discussion in Chapter 6.

Isothermal solidification occurs in the third stage and the liquid zone starts to shrink as B atoms diffuse into the solid A. Then, the interdiffusion coefficient D_α in the α phase controls the rate of solidification. Hence, this stage is much slower than the two previous stages. Based on the original work of *Sekerka (1975)*, the time required for complete solidification and the effect of the bonding temperature on it were also investigated by *Tuah-poku et al. (1988)*. The solute distribution during the homogenisation stage can be modelled using the basic equations for diffusion in a solid phase.

An alternative approach was proposed by *Kuriyama (1992)* and is based on a thin film model. The bond is assumed to be the same as a diffusion couple with initial composition equal to the interlayer composition. In this case the general solution for *Fick's* law would be:

$$C = \frac{A}{\sqrt{t}} exp\left(\frac{-x^2}{4Dt}\right) \tag{2-3}$$

This is called the profile equation in which A is a constant. The total amount of diffusing solute M is constant and equal to the initial amount of interlayer, hence:

$$M = \int_{-\infty}^{\infty} C dx = 2A\sqrt{\pi D} \tag{2-4}$$

Therefore substituting M for A in the profile equation (2-3) yields:

$$C = \frac{M}{2\sqrt{\pi Dt}} exp\left(\frac{-x^2}{4Dt}\right) \tag{2-5}$$

Thus, the solute concentration profile can be calculated as a function of time and distance from the initial position of the interlayer. *Kuriyama (1992)* reported good agreement between experimental results and the theoretical predictions based on this model when TLP diffusion bonding titanium alloys, using copper interlayers.

The analytical approaches describe the bonding process using a number of hierarchical and discrete stages. Actually, some of these steps occur simultaneously. For example solute homogenisation in the bulk of the base metal starts immediately after the solidification of a few atomic layers at each of the two interfaces, while the liquid phase still exists at the centre of the bonding region. Also, these approaches rely on the approximate solutions for diffusion equations, e.g. error function equations. *Zhou et al. (1995*) reviewed the analytical approaches and proposed numerical simulations for TLP diffusion bonding. They concluded that, in contrast to analytical solutions, a numerical simulation has a key advantage in treating the bonding stages (i.e. dissolution, solidification and homogenisation) as interdependent sequential processes.

Nakagawa et al. (1991) developed a numerical analysis in which the base metal dissolution between the melting temperature and the bonding temperature of nickel, using Ni-P filler metal, was studied. An explicit finite difference method was employed, using a mass balance technique, to determine the location of the solid/liquid interface. According to their work, at very low heating rates, isothermal solidification of the liquid phase can occur between the melting temperature of the filler material and the bonding temperature. *Zhou (1994)* developed a fully implicit finite difference model to calculate the solute distribution and the location of the solid/liquid interface when TLP diffusion bonding nickel base metal using a Ni-P 19 at.% interlayer. The well-known *Fick's* first and second diffusion laws were used as the governing differential equations in order to determine the interface movement and the solute diffusion field, respectively. The finite difference expression for the nodes near to the moving boundary were estimated using *Crank's* approximation.

The results of both of these numerical approaches showed that the surface areas under the curves of solute versus distance from the centreline remained constant during the base metal dissolution and isothermal solidification. This is a direct and obvious consequence of the use of *Fick's* laws which is based on the conservation of solute during a diffusion process. However, the use of these equations in terms of atomic or weight percents could be justified only if the partial molar volumes of phosphorus in all three involved phases (i.e. the filler material with eutectic microstructure, the liquid phase and the solidified single phase) are regarded as reasonably close. The molar

volume of pure phosphorus is more than 2.5 times higher than that of pure nickel. Therefore, this assumption that the partial molar volumes of phosphorus in all phases are almost equal should have been more fully justified or explained since it can result in unacceptable errors when calculating the locations of the solid/liquid interface. Note that in *Tuah-poku et al.*'s approach, the molar volumes and physical properties of the filler and base metals (i.e. copper and nickel) are almost the same, therefore the basic equations could be expressed in terms of mole fractions without introducing a substantial error.

Despite the advantages of numerical simulations for TLP diffusion bonding, the results of these methods depend on the choice of arbitrary constants and parameters which are used in the algorithm. Also, the numerical approaches generally are not reproducible nor verifiable by other researchers. This is in contrast to analytical solutions, the accuracy of which can be assessed directly without having to introduce additional parameters necessary when running the numerical program, assuming the program itself is accessible.

Modelling of TLP diffusion bonding of composites

Unfortunately, there are very few publications which consider the theoretical aspects and modelling of the TLP diffusion bonding processes for composite materials. A theoretical approach is required not only to optimise the bonding conditions but also to ensure that any interfacial reactions between matrix and reinforcement are minimised.

In most metal matrix composites, diffusion of solute through the reinforcement particles is expected to be negligible and these particles effectively reduce the cross sectional area available to the diffusing elements. Thus, the effective diffusion coefficient of the solute may depend on the volume fraction of reinforcement. Consequently, the diffusion-controlled bonding mechanisms are affected by the reinforcement. This hypothesis is in contrast to the results of a kinetic study on TLP diffusion bonding of Al-6061/SiC composite, reported by *Sabathier et al. (1994)*. They found out that the presence of short-circuit paths for diffusion such as grain boundaries, subgrain

boundaries, dislocations and ceramic/matrix interfaces enhanced the diffusion rate, and the activation energy for atomic transport declined considerably.

Kuriyama (1992) investigated the effect of reinforcement on the TLP bonding of titanium/SiC composites using a thin layer of copper to achieve bonding. In this system, the high percentage of copper around the joint stabilised the β titanium phase. On the other hand, the matrix further away from the bond line (where no copper was present) transformed at the bonding temperature to the α titanium phase due to the diffusion of carbon (an α stabiliser) out of the SiC particles. The solubility and diffusivity of copper in the β phase are much higher than in the α phase and, therefore, the copper became concentrated in the area close to the joint where the β phase was present and could diffuse into the parent material (α phase) only very slowly. In contrast when TLP diffusion bonding pure titanium, the absence of carbon did not allow the formation of the α phase at the bonding temperature.

Accordingly, for the titanium/SiC composite, the profile of the copper distribution became step-like in the region near to the bond line and then followed an error function distribution further away. In contrast, in pure titanium with a single β phase structure, the copper distribution followed an error function profile. Therefore, the bonding behaviour of composites can be quite different from the corresponding un-reinforced alloys and should be investigated individually.

2.3 Solid-state diffusion bonding of aluminium alloys

Oxide layers on the faying surfaces may affect the ease of solid-state diffusion bonding certain materials. Some oxide films either dissolve in the bulk of the metal or decompose at the bonding temperature (e.g. those of many steels, copper, titanium, tantalum and zirconium), and so metal-to-metal contact can be readily established at the interface. *Derby (1990)* has indicated some of the possible chemical reactions which may occur at the interface between a pure metal and simple oxides.

On the other hand, if the oxide film is chemically stable, as for aluminium-based materials, then achieving a metallic bond can be difficult. The presence of a tenacious and chemically stable surface layer of aluminium oxide is the main obstacle in most welding processes for aluminium based materials. Different approaches have been developed to overcome the oxide problem associated with the diffusion bonding of such materials. A short description of these approaches and the reported results follow.

Imposing macroscopic plastic deformation

In solid-state diffusion bonding, a brittle and continuous oxide layer can be broken up by imposing substantial plastic deformation. Metal-to-metal contact is thus promoted because of local disruption of the oxide film on both faying surfaces. Early work on deformation bonding (pressure bonding) of aluminium alloys by *Cline (1966)* and recent work by *Urena et al. (1995)* both showed that about 40% deformation is required to produce bonds with reasonable strengths. *Cline* also studied the effects of joint design and surface condition on the strengths of Al-6061 bonds, in which grooves with different depths were machined on the faying surfaces to provide a low initial contact area with high local pressure. The highest tensile bond strength, of 110 MPa, was obtained with a 1.5 mm groove depth and 50% deformation.

Enhancing microplastic deformation of the surface asperities

An alternative approach to overcoming the oxide problem in solid-state diffusion bonding is to use a fairly rough surface finish, which may lead to higher bond strengths compared to polished surfaces. The rougher the surface the more the plastic deformation on the asperities, therefore more oxide fracture occurs and consequently metal-to-metal bonding is improved. *Ricks et al. (1990)* studied the effect of surface roughness on the shear strength of Al-8090 bonds. Despite a considerable scatter in results, it was concluded that higher bond strengths were achieved when a rougher surface preparation was adopted. This is probably due to the higher deformation of the surface asperities on a rough surface which leads to more rupture of the surface oxide, in comparison with a smooth surface. These results are consistent with those reported by *Tensi & Wittmann (1990)* in which the influence of surface preparation on the bond strength of Al-7475 bonds was investigated.

Enjo et al. (1978) used electrical resistance measurements of Al-Al bonds to show that faying surfaces treated by coarse emery paper produced more metallic bonds than smooth faying surfaces. The effect of the shape of asperities (asperity angle) on the interfacial contact process has been recently modelled by *Takahashi & Tanimoto (1995a),* although the effect of surface oxide layer was not considered. The model was reasonably verified by conducting some experiments on oxygen-free copper, see *Takahashi & Tanimoto (1995b).*

In contrast, *Harvey et al. (1985)* showed that polishing the silver cladding on Al-7010 improved the bond strength, compared with the bonds made using as-clad samples. The specimens were argon ion sputter cleaned before the deposition of the silver layer, therefore there was no aluminium oxide between the cladding and the base metal (see *Harvey et al. (1986)* for experimental details). This inconsistency regarding the effect of surface roughness on bond strength, is probably due to the different properties of the surface layers of silver and aluminium. The surfaces of silver coated samples are virtually oxide free, so improving the surface finish increases the metal-to-metal contact at the interface. In contrast, in the case of uncoated aluminium faying surfaces, bond strengths improve by the generation of oxide-free surfaces as a result of the local deformation of the asperities. Low temperature solid-state bonding of copper, using different surface preparations, was investigated by *Nicholas et al. (1990).* There was a

significant reduction in the bond strength as the surface roughness increased, which is consistent with the above conclusion regarding the effect of surface roughness on the bonding behaviour of materials without oxide layers.

Use of interlayers and the effect of alloying elements

Barta (1964) examined a variety of interlayers (silver, gold, nickel, aluminium, tin, zinc, iron, copper and magnesium) for low temperature diffusion bonding of Al-7075. The interlayers were in the form of electroplated, vacuum deposited, plasma sprayed, loose foils and clad Al-7072. Bonding was carried out under a very high pressure of 165 MPa in the temperature range 150-230°C. The use of most interlayers resulted in either very poor bonds or no bonding. The highest bond strength achieved, using a clad aluminium sample, was 76 MPa; improving to 110 MPa after post bond heat treatment. However, low temperature diffusion bonding may be of benefit for high precision joining where mechanical properties are not a crucial factor. *Bienvenu & Koutny (1990)* manufactured a small component for a detector, using a silver coating to sandwich a thin foil of an Al-Mg alloy (8 μm) between two thicker templates (50 μm) of the same material at 400°C.

Maddrell & Wallach (1990) studied the effects of active alloying elements such as magnesium and lithium on the morphology of the surface Al_2O_3 layer, when bonding aluminium-based alloys. According to this research, these active elements decompose and break up the aluminium oxide layer at the interface. A good correlation between bond strength and the extent of broken oxide was observed, leading to the conclusion that the greater the concentration of these elements, the greater the disruption of the oxide layer and, consequently, higher bond strengths. *Kotani et al. (1996a&b)* found that increasing the bonding temperature changed the amorphous oxide layer gradually into crystalline particles. The temperature at which the amorphous oxide layer was annihilated could be decreased by additions of magnesium to the alloy matrix.

Ricks et al. (1990) investigated the effect of some alloying elements on the bond strengths of Al-8090, using aluminium alloy interlayers containing gallium, lithium and magnesium with thicknesses of about 100 μm. The use of Al-Mg interlayers improved

the bond shear strength by up to 50% in comparison with bonds made using pure aluminium interlayers, i.e. from 100 to 150 MPa. In recent work, *Church et al. (1996)* conducted tensile tests on miniature Al-Li 8090 bonds. A scanning Auger microprobe was used to analyse the elemental composition of the fractured surfaces. Despite the presence of oxygen in all samples, bonds with high strengths contained lithium and aluminium whereas lithium was not detected on the fracture surfaces of the poor bonds. It was concluded that lithium possibly reacted with aluminium oxide to form a thermodynamically more stable oxide, therefore the bond strength was increased due to the disruption of the initial oxide layer. *Dunford & Partridge (1990, 1991 & 1992)* and *Gilmore et al. (1991)* concluded that the lithium in Al-8090 modified the aluminium oxide into discontinuous and less stable Li-Al spinels during the bonding process. TEM examination of the interface proved the absence of the continuous oxide layer in Al-8090 bonds. However, according to *Maddrell & Wallach (1990),* the native oxide layer was not substantially disrupted and the bond line remained decorated by semi-continuous layer of oxide which reduced the bond strength. Based on TEM observation, *Urena et al. (1996a)* proposed that interface oxide particles may not be the main cause responsible for pinning down the interface, but that Al_3Zr, which was detected along the grain boundaries in the parent material (Al-8090) as well as at the bond interface, suppresses the migration of the interface.

All the results, mentioned above are consistent with *Maddrell et al.'s (1989)* results showing that the presence of some alloying elements, such as Mg and Li can improve bond strength. Similar results had been reported earlier by *Dray (1985).*

Non-conventional bonding and testing methods

Enjo & Ikeuchi (1984) carried out the diffusion bonding of Al-2017 in the temperature range above the solidus line but below the liquidus line, where solid and liquid phases coexist (i.e. 580°C). In spite of the formation of a liquid phase, this method was referred to as solid-state diffusion bonding. It should be mentioned that, in contrast to transient liquid phase, solidification in this method occurs as a result of cooling, as in brazing. It was assumed that the formation of the liquid phase could aid the disruption of the oxide layer and provide intimate contact at the interface. Preferential melting at the bond

interface and the grain boundaries was directly observed at the bonding temperature. The volume fraction of the liquid phase proved a crucial factor. The maximum shear strength (270 MPa) was achieved when the volume fraction of the liquid phase was 2~3%. The tensile strength of the joint was increased to 400 MPa by a post bond heat treatment. However, when the volume of the liquid phase exceeded 3%, grain boundary cracking occurred and the bond line was associated with a large amount of porosity. No explanation was given for the fact that, despite the formation of the liquid phase at the grain boundaries, the base material could still withstand a bonding pressure of 1 MPa. Because of the high temperature used, the detrimental effects of melting on the microstructure and shape of the base material are expected to be substantial. In practical terms, the process does not seem viable as a minor miscarriage during the bonding process would destroy the part which is heated up to its solidus temperature.

Yokota et al. (1997) developed a new method based on a combination of solid-state diffusion bonding and friction welding to join Al-6061 and Al-6060/SiC MMC. In this method, a torsional force was exerted while an axial force was acting on the parts to be joined. One of the parts had a conical end in order to exclude the worn oxide film from the interface. The specimens were heated using a high frequency induction system and the axial load applied, while the torsional force was used to rotate the upper part at a constant speed of 6 rpm. The maximum tensile strength of the bonds, made applying 90 MPa axial pressure at 250°C, was 200 MPa. An important advantage of this method over diffusion bonding and friction welding is claimed to be the low bonding temperature (250-350°C) and short bonding time (~5 minutes), which reduces the plastic deformation during the bonding process. However, in contrast to diffusion bonding, the method is only applicable to parts with certain shapes (preferably with round cross section) which should be machined to provide conical ends. Also, unlike friction welding which is carried out in air, the new method requires a vacuum.

Dunford & Partridge (1987, 1990, 1991 & 1992) have reported the highest bond strengths for Al-8090, i.e. 181 to 202 MPa for lap shear tests with an overlap of 2 mm. However, the shear strengths decreased drastically (~50%) for overlaps of about 4 mm. *Tensi et al. (1989)* also carried out lap shear tests on Al-7475 with a very short overlap length of 1.5 mm; a maximum shear strength of 410 MPa was reported. However, the

reliability and practicality of the methods which are evaluated under extreme testing conditions (e.g. shear test on the joint with an overlap of less than 2 mm) are doubtful.

Cailler et al. (1991) used high speed dynamic loading equipment to study the bond strength, failure elongation and failure energy of Al-2017 diffusion bonds. The projectile speed was 30 m/s and the time duration for transmitting the load was less than 114 μs. The tensile strengths of the joints in the as-bonded condition reached 290 MPa, in comparison with 300 and 460 MPa which were the tensile strengths of the parent material in the as-bonded and in the fully aged-hardened condition, respectively. The failure elongation of the bonded samples was about one third of the parent material with the same thermal cycle. *Debbouz & Navai (1997)* adopted a similar approach to study the effect of bonding conditions on the mechanical properties of Al-2017 bonds. In both cases, it is not mentioned why the bonds were not post bond treated to achieve a fully hardened condition rather than heat treating the parent material. If that had been done, the comparison between the mechanical properties of the bonds and the parent material would be more conclusive.

Summary

It can be concluded that, despite the vast research on the solid-state diffusion bonding of aluminium alloys, this method has failed to reliably produce high strength joints. The presence of a wide scatter in bond strengths is a particularly discouraging feature of solid-state bonding. Non-conventional solid-state diffusion bonding processes rely on extreme bonding conditions or require complicated equipment in an attempt to improve reliability; therefore these approaches tend to have very restricted application.

2.4 TLP diffusion bonding of aluminium alloys

As discussed before, the formation of a liquid phase in TLP diffusion bonding could assist the disruption of an oxide layer and thus promote metallic contact. Therefore TLP diffusion bonding of aluminium-based materials has been of interest. The results of previous research on this method are discussed with respect to the type of interlayer used. Due to the importance of aluminium-based metal matrix composites, the joining of these materials is reviewed in the next section.

Zinc based interlayers

Ricks et al. (1990) investigated TLP diffusion bonding of Al-8090 sheets using a roll clad interlayer with a chemical composition of Zn–1 wt.% Cu. This method was based on a combination of roll bonding and TLP diffusion bonding. A very careful surface preparation technique including mechanical and chemical cleaning was conducted to ensure good bonding between the cladding and the substrate. The rolling conditions were also optimised to obtain the required mechanical properties. Reproducible bond shear strengths in the order of 100-150 MPa were reported together with considerable improvements in hot peel strength compared with solid state bonding. It was concluded that precipitation of zinc on the grain boundaries, on both sides of the interface, limited the bond strength. The zinc-rich areas remained unaffected after post bond heat treatment. Due to the rolling stage, this technique is only applicable for joining sections which can be roll bonded, e.g. plates.

The use of a thin zinc interlayer of 1.3 μm thickness for diffusion bonding Al-8090 (virtually without Li and Mg) and Al with 5 at.% Mg was not satisfactory, *Maddrell (1989)*. Unfortunately, because of the different surface preparation techniques and bonding conditions between this work and that of *Ricks et al*., no reliable conclusion can be drawn.

Livesey & Ridley (1990) also investigated the effect of ion beam cleaning on bond strength. The average shear strength of Al-8090 bonds using 3 μm thick zinc interlayers was 164 MPa without ion beam cleaning, although that could be increased up to 190 MPa by ion beam cleaning before sputter coating. Despite an 18% scatter in the former case, these strengths are 40 to 50 MPa higher than those obtained by *Ricks et al*. in which a thicker zinc cladding of about 50 μm had been rolled on each side of the aluminium being joined.

Silver interlayers

Dray (1985) used silver interlayers with a thickness of 0.25 μm on each faying surface when bonding Al-6061. A two stage bonding sequence was used. Initially, bonding was at a temperature about 5°C above the eutectic temperature of aluminium-silver (572 °C) for 5 minutes using a pressure of 1.25 MPa. The second stage was for 35 minutes at 450°C using a pressure of 2.5 MPa. Tensile bond strengths equivalent to the parent material were reported, although the impact strengths were one third that of the parent material. Based on rough diffusion calculations, *Dray* estimated that the formation of a liquid phase was unlikely. The combination of the heating rate and the interlayer thickness was such that silver could diffuse rapidly away from the interface during heating and so the eutectic composition could not be established when the eutectic temperature eventually was reached. TEM observations did not show any clear evidence of melting at the interface. *Dray* recommended the use of thicker interlayers and/or a faster heating rate to achieve true TLP diffusion bonding.

Urena & Dunkerton (1989) tried thicker silver interlayers (1, 12.5, and 25 μm) when bonding Al-8090. A maximum tensile strength of about 110 MPa for a 12.5 μm interlayer was reported. The presence of a high volume of voids in the case of a 1 μm interlayer, and the precipitation of thick brittle intermetallics in the case of a 25 μm interlayer, were given as the reasons for the poor mechanical properties. Despite the formation of a liquid phase at the interface, the bond strengths were lower than those reported by *Dray*.

Copper interlayers

Dray (1985) used 1 μm copper interlayers for the TLP diffusion bonding of Al-6061 and obtained tensile and impact strengths close to the strength of the parent material. The bonding cycle included 10 minutes at 555 °C followed by 30 minutes at 450 °C. The presence of a dendritic pattern at the interface was clear evidence of melting. TEM and EPMA investigations revealed copper-rich precipitation in the matrix away from the bond line and also segregation of magnesium and silicon, as Mg_2Si particles, at the interface.

Maddrell (1989) examined TLP diffusion bonding of Al-8090 (virtually without Mg and Li) and Al with 5 at.% Mg, using the same interlayer. In the former case, a thin oxide layer was apparent along most of the bond line although it was not discernible in some parts. These bonds were not shear tested, However, shear strengths as high as 170 MPa were measured for Al-5 at.% Mg despite the clearly discernible bond-line. *Maddrell* concluded that the interfacial energy between the oxide particles and the liquid phase has a key role in the final oxide distribution pattern.

Dunford et al. (1990) studied the effect of various overlap lengths on bond shear strength, using ion beam cleaning before copper deposition. The shear strength of Al-8090 bonds with an overlap length of less than 3 mm was 191± 8 MPa but it declined to about 70 MPa for overlaps greater than 4 mm (see also *Gilmore et al. 1991*). However, the surface preparation method, used for oxide removal before copper coating, restricts the application of the method.

Summary

TLP diffusion bonding, as a method for joining aluminium alloys, resulted in bonds with higher strengths than those made using solid-state diffusion bonding. However, the reported bond strengths and/or associated scatter in the strength have not been satisfactory and further work is required to improve bond quality.

2.5 Joining aluminium metal matrix composites

Great attention has recently been paid to the production and application of aluminium metal matrix composites (Al-MMCs) because of their superior mechanical properties compared with un-reinforced aluminium alloys, *Lloyd (1994)*. The most significant property of these Al-MMCs is their high elastic modulus. Elastic modulus is the limiting criterion in the design of components that fail by some sort of elastic instability, e.g. buckling, and it does not normally change significantly by alloying or hardening processes. The elastic modulus for Al/SiC composites increases almost linearly on increasing the volume fraction of SiC particles, *Peel et al. (1995)*. High stiffness, strength and also wear resistance are the main advantages of this composite. Unfortunately, despite the potentially vast applications for aluminium-based composites, relatively few attempts have been made to develop a reliable joining process. Thus, the lack of a reliable and economical joining technique has restricted the application of these materials and more investigation is required.

Ellis (1996) reviewed the joining techniques developed for Al-MMCs. Generally, fusion welding is not successful for joining Al-MMCs. Non-uniform distribution of the reinforcement particles in the weld zone and precipitation of plate-like brittle compounds, e.g. aluminium carbide in Al/SiC-MMCs, are major problems when fusion welding. Manipulation of the molten pool was difficult and even filler materials with high fluidity would not mix with the viscous molten composite. In some respects, the welding described above was more similar to brazing rather than fusion welding, as almost no reinforcement particles were observed in the weld bead. In some cases, very low corrosion resistance has been reported, e.g. where aluminium carbide forms from dissociated SiC particles and is corroded in the presence of water very rapidly, releasing acetylene gas. However, matrix-particle chemical reaction and particle segregation can be reduced with careful control of heat input and consumables when using TIG and MIG welding processes. Other fusion welding processes such as laser and electron beam welding were also not satisfactory, *Ellis (1996)*. Friction welding seems a promising technique for joining these materials providing that geometrical restrictions on components and the associated massive deformation can be tolerated.

Fewer detrimental reactions are associated with solid and liquid state diffusion bonding as they can be carried out at a lower range of temperatures than fusion welding processes. *Ellis (1992)* reported the results of solid-state diffusion bonding of Al-7075/SiC 20 vol.% at constant temperature of 500°C using silver, copper and aluminium interlayers with different thicknesses. Although the bonding temperature was lower than the eutectic temperature of the binary Al-Cu system, local melting occurred at the bond line. High particle density and an ample number of defects were observed. All bonds made using copper interlayers failed during machining. In contrast, no trace of silver and no evidence of particle enrichment were observed when using silver interlayers. As for aluminium interlayers, there was no sign of diffusion to or from the interlayer. The shear test results showed that already low shear strengths in the as-bonded condition decreased after a full heat treatment.

Urena et al. (1995) used Al-8090, Supral 100 (superplastic Al-Cu alloy) and pure silver as interlayers when solid-state diffusion bonding Al-2124/SiC. A shear strength of 70 MPa was obtained using Al-8090 interlayers with plastic deformation in the range of 20 to 30%. Strengthening of the base material adjacent to the interlayer is attributed to the presence of lithium within the interlayer. The silver and Supral interlayers resulted in much lower bond strengths. In another investigation, the bond strengths reported for Al-2014/SiC using Al-8090 and silver interlayers were 50 and 36 MPa, respectively, *Urena et al. (1996b)*. All the bond strengths reported were well below the strength of the corresponding parent material.

There are a few reports on the TLP diffusion bonding of aluminium metal matrix composites. *Niemann & Garrett (1974b)* used copper interlayers for the eutectic bonding of boron-aluminium monolayer foils. An intensive investigation on different surface preparation techniques was carried out, using an ellipsometer to measure the thickness of the oxide layer. This instrument has sufficient sensitivity to detect a monolayer of oxide on a metallic surface. A copper coating of about 20 μm thickness was subsequently deposited on both sides of each monolayer after ion beam cleaning. Bonding was carried out under 1.7 MPa pressure at a temperature slightly above the Al-Cu eutectic temperature. Although the formation of a liquid phase was isothermal (based on the interdiffusion of copper atoms in the aluminium matrix), solidification of

the liquid phase was induced in a non-isothermal manner, i.e. by decreasing the temperature just after formation of the liquid phase. Satisfactory results were reported with minimal degradation of boron filaments. As mentioned before, the use of ion-beam cleaning to remove the oxide layer substantially restricts the development of this technique on a commercial scale.

Partridge & Dunford (1991) studied the effects of particle size, distribution and symmetry on the different types of interface which can form at the bond line in composite materials. They showed that bond strength is influenced by the area fractions of the particle/particle, particle/matrix and matrix/matrix interfaces. Insertion of an interlayer, when solid-state bonding, may increase or decrease the particle/matrix area fraction depending on the particle distribution and symmetry on the faying surfaces. Details of this approach are discussed in section 4.4. A shear strength of about 100 MPa was reported for the solid-state diffusion bonding of Al-8090/SiC 20 vol.% with an overlap of 2 mm, *Dunford & Partridge (1992)*. Using 80-100 μm thick interlayers of Al-8090, increased the bond strengths up to 170 MPa. TLP diffusion bonding, using 10 μm copper interlayers, resulted in a higher shear strength of >170 MPa. No data are available for the parent material shear strength as adopting the same shear test conditions was not possible. Much lower shear strengths are expected when testing with overlap lengths more than 2 mm, see section 2.4. *Gomez de Salazar et al. (1997)* used a brazing filler material (Al-12 wt.% Si) for TLP diffusion bonding of two Al-6061/Al_2O_3 MMCs with 10 and 20 vol.% particle, and the maximum shear strengths were 87 and 65 MPa for the composites, respectively. Solid-state diffusion bonding of the same material resulted in lower bond strengths, *Escalera et al.(1997)*.

The effect of alloying elements on bond strength, such as Mg within an alloy interlayer, was studied by *Ikeuchi & Asano (1993)*. They used Al-Mg-Cu alloys, containing 0.5 to 2 wt.% Mg, as the interlayer for TLP diffusion bonding of an alumina-fibre reinforced aluminium MMC to pure aluminium. The shear test results showed that the higher the Mg content the higher the bond strength. Increasing the Mg content from 0.5 wt.% to 2 wt.% increased the tensile bond strength from 60 MPa to its maximum value of ~100 MPa. SEM observations showed a remarkable improvement in the fracture surfaces and this is consistent with the measured shear strengths.

Summary

Joining aluminium metal matrix composites, using either solid-state or fusion welding processes, was found to be even more difficult than the bonding of unreinforced aluminium alloys. This is mostly due to the detrimental effects of the bonding processes on the reinforcement particles, e.g. undesirable decomposition or segregation of the reinforcement at or about the bond line. As for aluminium alloys, the TLP diffusion bonding of aluminium MMCs resulted in higher bond strengths than when using solid-state diffusion bonding. However, the highest bond strengths, reported to date, are well below the strengths of the parent materials. Moreover, due to the superplastic behaviour of some of these composites at the bonding temperature (about 550°C when using a copper interlayer), the bonding process is associated with substantial plastic deformation.

2.6 Diffusion bonding of aluminium-based materials in air

Reports on the diffusion bonding of aluminium-based materials in air are scant. *Morley & Caruso (1980)* investigated the solid-state diffusion bonding of an aluminium silicon casting alloy (Al-390) in air and nitrogen. The samples were silver coated in order to prevent oxidation of the faying surfaces. The tensile strengths of the bonds made in nitrogen were up to 57 MPa, whereas the bonds made in air had virtually no strength.

Ricks et al. (1989) modified the surface layers of Al-8090 to induce TLP diffusion bonding in air. The base materials were roll-clad, using a zinc based alloy, to prevent the oxidation of the faying surfaces during bonding. The cladding was followed by hot and then cold rolling processes. Reproducible bonds with shear strengths of 100 to 120 MPa were reported. However, due to the pre-bonding procedure which requires substantial changes in the initial shape of the parent material, the technique has limited application. Moreover, the reported strengths are not high.

Livesey & Ridley (1990) used vapour deposited zinc interlayers for joining Al-7475, Al-8090 and Supral 220 in air. The samples were chemically treated before the coating process. The interlayer thickness varied from 1.5 to 6 μm and various bonding pressures were examined. This investigation revealed that increasing the bonding pressure from 2 to 3 MPa, increased the bonding shear strength dramatically. However, despite a relatively high average shear strength of 228 MPa for the Al-7475 bonds, using 3 μm interlayers, the scatter in results was of the order of ±27%. The Al-8090 bonds had an average shear strength of 164 MPa with a variation of ±23%. These values, surprisingly, are higher than those obtained by *Ricks et al. (1990)* who used a thicker cladding of about 50 μm zinc rolled on each side of the aluminium being joined in vacuum, see section 2.4. This improvement may be attributed to the chemical treatment that *Livesey & Ridley (1990)* adopted before coating. The TLP diffusion bonding of Supral 220 using the same method was not satisfactory.

Pilling & Ridley (1987) tried solid-state diffusion bonding Al-7475. The samples were chemically treated in NaOH and HNO_3 and bonding was carried out in air. The bonds produced had shear strengths in the range 30-150 MPa. The source of such a wide variation in shear strength was not identified in their research.

Bushby & Scott (1993) used copper interlayers for the TLP diffusion bonding of pure aluminium in air. Bonding was carried out under transient pressure with an initial value of 3 MPa which was dropped down to about 1 MPa within the bonding time of 60 minutes. Bond shear strengths up to ~50 MPa were achieved. Increasing the initial pressure up to 10 MPa resulted in bond shear strengths of 96 MPa. The use of the same procedure for bonding Al/Nicalon (SiC fibre) composite in air was not successful although a much higher initial pressure (i.e. 30 MPa) was applied. The shear strength of the bonded composite in which 66% of the central area was bonded was 34 MPa. Taking into account the unbonded area, this value was normalised to 51 MPa. In a similar approach, a Cu-Ag eutectic alloy, instead of pure copper, was used as the interlayer and the bonding temperature was decreased from 550 to 510°C, *Bushby & Scott (1995a)*. The use of the alloy interlayer resulted in similar strengths for the composite bonds, though aluminium bonds had lower shear strengths (~65 MPa).

Bushby & Scott (1995b) used an interlayer of Al-2124 for solid-state diffusion bonding Al-2124/SiC 30 vol.% composite in air. Bond shear strengths of about 110 MPa with a wide scatter of ±45% were reported. This value is about 40% of the shear strength of the composite.

Summary

TLP diffusion bonding in air resulted in low bond strengths with unreasonably high scatter. In the most successful methods, the base materials were coated before bonding (e.g. by Cu deposition or Zn roll-cladding) to prevent further oxidation of the faying surfaces during TLP diffusion bonding in air. Even using these approaches, a wide scatter of ±25% in strengths was reported. Obviously, due to the already unsatisfactory results of solid-state diffusion bonding in vacuum, conducting the process in air has not been developed.

2.7 Summary

Diffusion bonding is a promising method for joining materials for which conventional welding methods have proved unsuccessful. More than three decades of research on the diffusion bonding of aluminium-based materials has resulted in a comprehensive understanding of bond formation mechanisms and the problems associated with the stable aluminium oxide film which hinders the formation of an ideal joint at the bond line.

Solid-state diffusion bonding may result in high strength bonds if plastic deformation is large enough to provide metal-to-metal contact as a result of oxide disruption on the faying surfaces. The effects of alloying elements in either the base material or an interlayer have been studied, and show that some alloying elements such as magnesium enhance disruption of the oxide layer, leading to higher bond strengths.

Alternatively, transient liquid phase (TLP) diffusion bonding has been considered a promising method for joining materials with stable oxide films due to the presence of a liquid phase between two faying surfaces. As an example, the use of copper interlayers has proved to be successful when joining some aluminium-based alloys and composites.

Despite a vast amount of research in this field, design engineers do not consider diffusion bonding to be a reliable method for joining aluminium-based materials for commercial applications. The bond strengths reported for these materials are lower than the strengths of the corresponding parent materials. Also, a most discouraging feature of diffusion bonding is the presence of an unreasonably wide scatter in the results; this suggests that the method is an unreliable joining process for aluminium-based materials.

Achieving high strength bonds when using a complicated bonding process (such as ion beam cleaning to remove the oxide film before TLP diffusion bonding) has very limited application. Similarly, introducing a high amount of plastic deformation to improve the bond strength confines the use of such an approach to applications where massive deformations can be tolerated. The approaches which rely on the effect of alloying elements, in order to improve the bond quality, cannot be employed for a vast range of the materials which lack those particular elements.

Despite several attempts to model TLP bonding, none has considered the real conditions involved in a bonding process. For example, the effect of pressure as a crucial bonding parameter has been neglected. However, the results of analytical approaches can be used as guideline. The numerical simulations for TLP diffusion bonding were based on unjustified and questionable assumptions and, at the moment, they are neither verifiable nor can be used by other researchers.

Hence, in order to overcome the problems associated with the diffusion bonding of aluminium-based materials, six new methods have been developed during this Ph.D. research. A new analytical model and a numerical simulation for the fourth method is also proposed.

Appendix

Advantages and limitations of diffusion bonding are as follows.[*]

Advantages:

1. The process has the ability to produce high quality joints so that neither metallurgical discontinuities nor porosity exist across the interface. An ideal diffusion bond is free from flaws, oxide inclusions, voids and loss of alloying elements.

2. With properly controlled process variables, the joint would have strength and ductility equivalent to those of the parent material.

3. Joining of dissimilar materials with different thermo-physical characteristics, which is not possible by other processes, may be achieved by diffusion bonding. Metals, alloys, ceramics and powder metallurgy products have been joined by diffusion bonding.

4. Fairly high precision products can be manufactured without subsequent machining because of the solid-state nature of the process and relatively low bonding pressures required. This means that good dimensional tolerances for the products can be attained.

5. Diffusion bonding of components with intricate shapes or cross sections is possible.

6. Heavy section parts can be joined by diffusion bonding without pre-heating.

7. Apart from the dimensions of the bonding machine, there is no limitation on the number of joints which can be carried out simultaneously.

8. Excluding the heating stage, the time required for bonding is independent of the size of bonded area.

---

[*] *Welding Handbook of AWS (1976), Kazakov (1985), Houldcroft (1977) and Dray (1985)*

9. Reduction of sensitivity to corrosion has been reported in some diffusion bonded alloys e.g. titanium and zirconium.

10. Apart from the initial investment, the consumable costs of diffusion bonding are relatively low as no expensive solder, electrodes, or flux are required (although the capital costs and the costs associated with heating for relatively long times may be high).

11. Diffusion bonding is free from ultraviolet radiation and gas emission so there is no direct detrimental effect on the environment, and health and safety standards are maintained.

12. Automation is possible by computer controlling the basic variables of the diffusion bonding e.g. time, temperature, and pressure.

Limitations:

1. Great care is required in the surface preparation stage. Excessive oxidation or contamination of the faying surfaces would decrease the joint strength drastically. Diffusion bonding of materials with stable oxide layers is very difficult. Production of thoroughly flat surfaces and also precise fitting-up of the mating parts takes a longer time than with conventional welding processes.

2. The initial investment is fairly high and production of large components is limited by the size of the bonding equipment used.

3. Application of the force and heat in a vacuum or protective environment makes on-site working difficult.

4. The suitability of this process for mass production is questionable, particularly because of the long bonding times involved.

5. The lack of reliable data about joint behaviour, e.g. fatigue life or fracture toughness etc., and also inadequate methods for non-destructive testing the joint quality currently are problems, although it is expected they will be overcome in the future.

Chapter 3

3. Experimental procedure

3.1 Parent materials and interlayers

The diffusion bonding of the following aluminium-based alloys and composites was investigated in this work.

- Al-8090 with 14.5 wt.% SiC particles
- Al-359 with 20 wt.% SiC particles
- Al-6082
- UL-40 (Al-Li alloy)
- pure commercial aluminium (99%)

Their nominal compositions, in weight percent, are listed in Table 3-1.

	Si	**Fe**	**Cu**	**Mg**	**Ti**	**Li**	**Zr**	**Zn**	**Mn**	**Cr**
Al-8090/SiC	0.2	0.3	1.3	1.1	0.1	2.4	0.1	0.25	0.1	0.1
Al-359/SiC	9.0	0.2	0.2	0.4	0.2	-	-	-	-	-
Al-6082	0.7-1.3	0.5	0.1	0.6-1.2	0.1	-	-	0.2	0.4-1.0	0.25
UL-40	-	-	-	-	-	4.0	0.12	-	-	-

Table 3-1: Nominal compositions of matrix materials (wt.%, balance aluminium).

All the as-received materials were fully age-hardened and in the form of 25-40 mm thick plates with the exception of the Al-6082 alloy which was supplied as 10 mm diameter rod. The distribution of SiC particles in the matrix of the Al-8090/SiC composite was found to be non-uniform and there were patchy areas with a relatively low particle density, whereas the Al-359/SiC had a more uniform microstructure (compare figures 4-6 and 4-7).

Two forms of copper interlayer were used in this work:

- pure copper (99.9%) foils in thicknesses of 3, 7, and 12.5 μm;
- sputter coated copper with a thickness of about 0.7, 1, and 1.5 μm on each surface.

Sputter coating of the faying surfaces was carried out after grinding with silicon carbide paper of 1200 grit followed by washing in ethanol and rinsing in acetone. The system was liquid nitrogen cooled and ion beam cleaning was not conducted prior to sputter coating. Typical sputter coating conditions for deposition of about 1 μm copper are as follows.

- base pressure: 5×10^{-9} mbar (5×10^{-7} Pascal)
- argon pressure: 1.2 Pascal
- target power: 31 Watt
- target substrate distance: 36 mm
- time: 22 minutes

The thickness of the coating was measured by surface profilometer. The adhesion between the substrate and the coating was poor, so these interlayers can be considered to act in a similar way to the foil interlayers.

3.2 Bond fabrication

3.2.1 Pre-bonding procedure

As-received thick plates of Al-8090/SiC, Al-359/SiC and UL-40 were machined to produce discs of 10 mm diameter and 5 mm height. The 6082 alloy was cut into 5 mm thick discs or 25 mm long rods. The longer specimens were used as the lower pieces when bonding using an applied temperature gradient (see section 3.2.2). A small lateral hole, as close as possible to the surface to be bonded, was drilled in some of the discs and was used for inserting a thermocouple. The faying surfaces were ground using rotary silicon carbide papers from 600 grit down to 1200 grit. All the specimens and interlayers were washed thoroughly in alcohol and rinsed in acetone just before inserting into the diffusion bonder.

Special precision was required in the surface preparation stage of the samples used for bonding in air (i.e. method V and VI) in which the faying surfaces were ground to produce flat surfaces without rounded edges. A steel jig was used to hold the samples in order to produce flat surfaces, see figure 3-1.

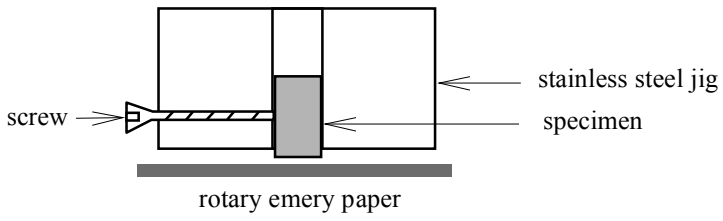

Fig. 3-1: Grinding set-up used for producing flat surfaces when bonding in air.

3.2.2 Bonding procedure

Diffusion bonding was carried out in the diffusion bonder which is shown schematically in figure 3-2. The specimen was placed on the lower platen of the bonder so that it was surrounded by the water-cooled copper coil of the R.F. induction unit with a maximum output power of 2 kW (see below for details of the specimen set-up in the new bonding methods). An initial load then was applied, just sufficient to keep the specimen in the desired orientation. The main load was applied by an electric motor via a transmission system and was measured using the load cell under the lower platen. After connecting the thermocouple to the control unit extension, the chamber was evacuated. A diffusion vacuum pump, backed up by a rotary pump, was used to evacuate the chamber down to 10^{-4} mbar.

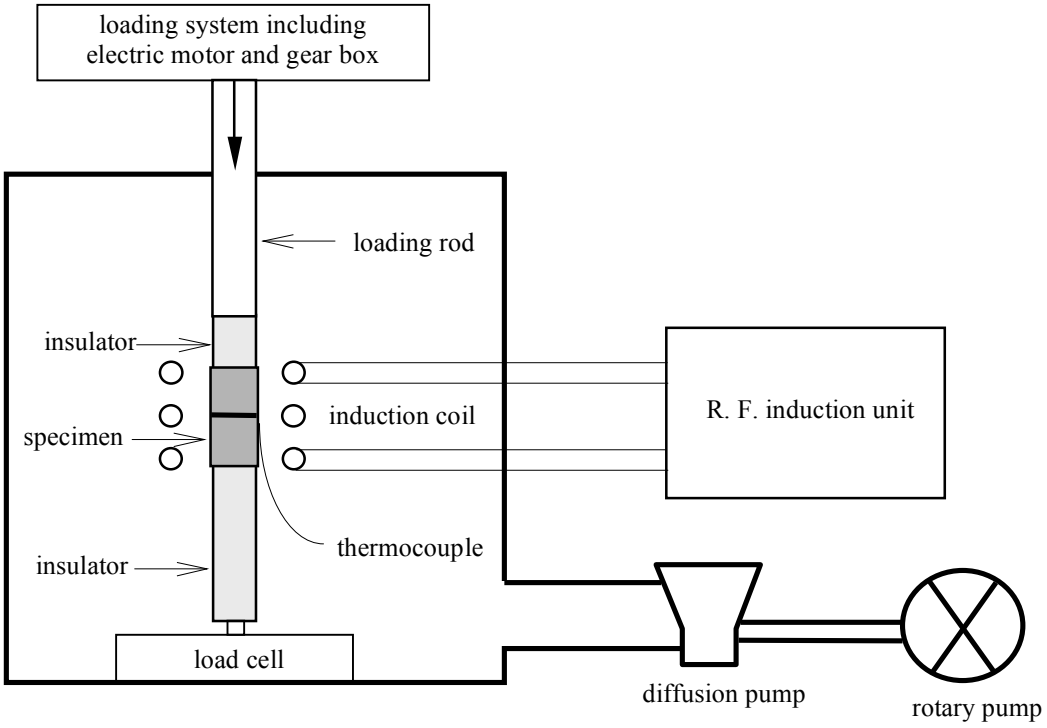

Fig. 3-2: Schematic diagram of diffusion bonder including specimen set-up in conventional TLP diffusion bonding method.

Temperature and load were controlled using an electrical interface system between the hardware components (electric motor, load cell and R.F. induction unit) and a computer. The bonding conditions, e.g. temperature, pressure and time, were input to the computer in three distinct stages corresponding to heat-up, bonding and cooling. Therefore the computer controlled the bonding sequence automatically, see figure 3-3.

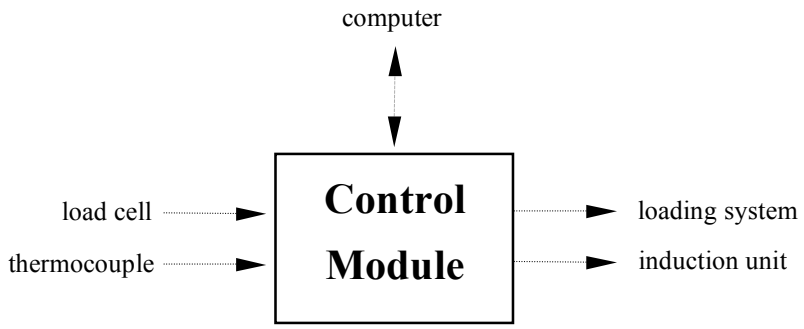

Fig. 3-3: Mechanism of pressure and temperature control in diffusion bonder.

New methods for TLP diffusion bonding aluminium alloys and composites

Six new methods for TLP diffusion bonding of aluminium-based materials were developed. The first three methods were based on applying isostatic bonding pressure, as compared to uniaxial pressure in conventional TLP diffusion bonding. These methods were developed for joining aluminium-based alloys and composites which are superplastic at the bonding temperature, and so which would suffer from massive plastic deformation due to their very low yield strengths (normally less than 1 MPa at 550°C) if bonded using conventional TLP diffusion bonding. In the fourth method, a temperature gradient was imposed across the bond line in order to increase the bond strength. The fifth method was developed for TLP diffusion bonding in air, rather than in vacuum as in the previous methods. This method relies on a fast heating stage in order to minimise the oxidation of the faying surface in ambient air. Finally, based on a combination of the fourth and fifth methods, a sixth method was developed to introduce a temperature gradient when TLP diffusion bonding in air.

Method I: *Isostatic TLP diffusion bonding*

This method is a single-stage bonding process in which the assembled specimen, including an interlayer, is inserted in a steel ring. Lateral constraint of the sample by the steel ring prevents plastic deformation, and the bonding pressure can be increased considerably from 0.1-0.2 MPa up to 5 MPa without macroscopic deformation.

The R. F. induction coil was used to heat up the steel ring which conducted heat to the specimen, rather than by heating the specimen directly as in conventional TLP diffusion bonding. For the preliminary experiments, adequate contact for heat conduction from the ring to the specimen was produced by hammering the specimen inside the tube. As the hammering stage was found to be destructive to the interlayer, a modified method for isostatic TLP bonding was designed to eliminate this stage. The jig used in the final design included two steel platens that conducted the heat through the top and the bottom of specimen, therefore lateral contact of the tube and specimen was no longer necessary. The details of this arrangement are illustrated in figure 3-4.

Method II*:* *Low pressure conventional TLP diffusion bonding followed by isostatic solid-state diffusion bonding in air*

This method is a double stage bonding process. In the first stage of this method, the specimen including an interlayer was inserted into the diffusion bonder without using the steel ring used in method I. A low bonding pressure of about 0.1 to 0.2 MPa was used to avoid plastic deformation of the pieces being joined at the bonding temperature of 550 to 560°C. In the second stage of this process, the already bonded sample was inserted in the steel ring and positioned in the diffusion bonder as in the previous method (method I). Further bonding was carried out in air at the same temperature but using a higher bonding pressure of 1 to 5 MPa.

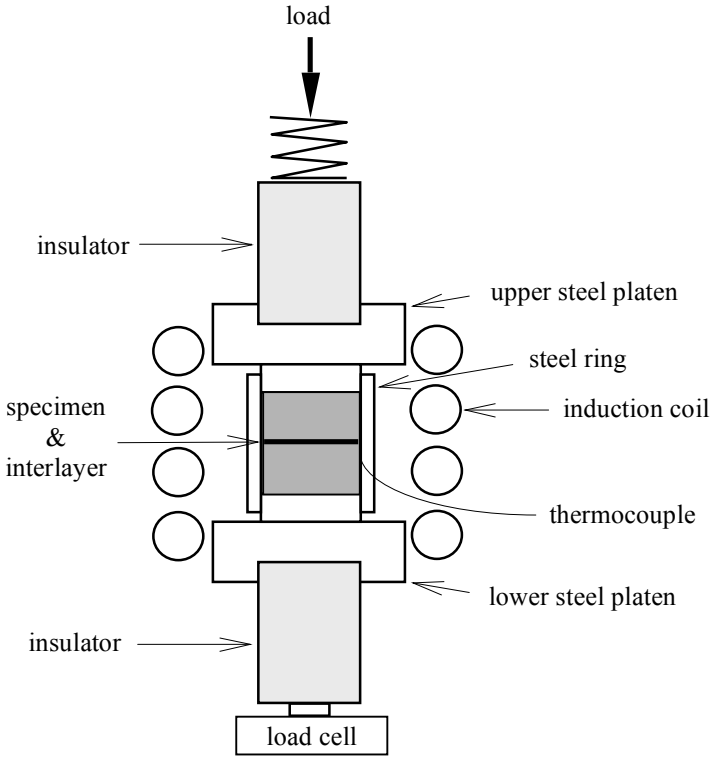

Fig. 3-4: Specimen set-up in isostatic TLP diffusion bonding (method I).

Method III: *Low pressure conventional TLP diffusion bonding followed by hot isostatic pressing (HIP) without encapsulation*

The first stage was exactly the same as in method II but in the second stage the bonded samples were inserted in a hot isostatic pressing (HIP) furnace without encapsulation (canning). The temperature was raised up to 560°C and pure argon was injected into the chamber to increase the pressure up to 5 MPa. The samples were furnace cooled after one hour and the pressure was reduced.

Method IV: *Temperature gradient TLP diffusion bonding*

The specimen set up in this method is similar to conventional TLP diffusion bonding except that the top of the specimen was placed in contact with a heat sink to induce a temperature gradient (20 to 70 °C/cm - see section 5.4.1 for details) across the interface. The lower specimen piece was longer than the upper one to improve the coupling effect of the induction heating system to the lower part of the sample. A second thermocouple was inserted in the upper piece to measure the temperature gradient. The details of the specimen set-up for method IV are shown in figure 3-5.

Method V: *High heating rate TLP diffusion bonding in air*

The design of the bonding set-up in this method was a crucial factor. The final design is shown schematically in figure 3-6. The insulation rods were machined precisely to produce parallel ends. The load was applied by an electric motor via a transmission system including a steel rod with a round tip. The point contact between the rod and the centre of the upper insulator prevents any undesirable eccentric loading. The R.F. induction coil was kept as close as possible to the specimen in order to increase the coupling effect and consequently to achieve the highest possible heating rate.

The heating rate was 20°C per second and it took less than 30 seconds to reach the bonding temperature, i.e. 550°C. The bonding time was 5 or 10 minutes including the heating stage. The bonding pressure was varied from 5 to 7 MPa (maximum yield strength of the material at the bonding temperature).

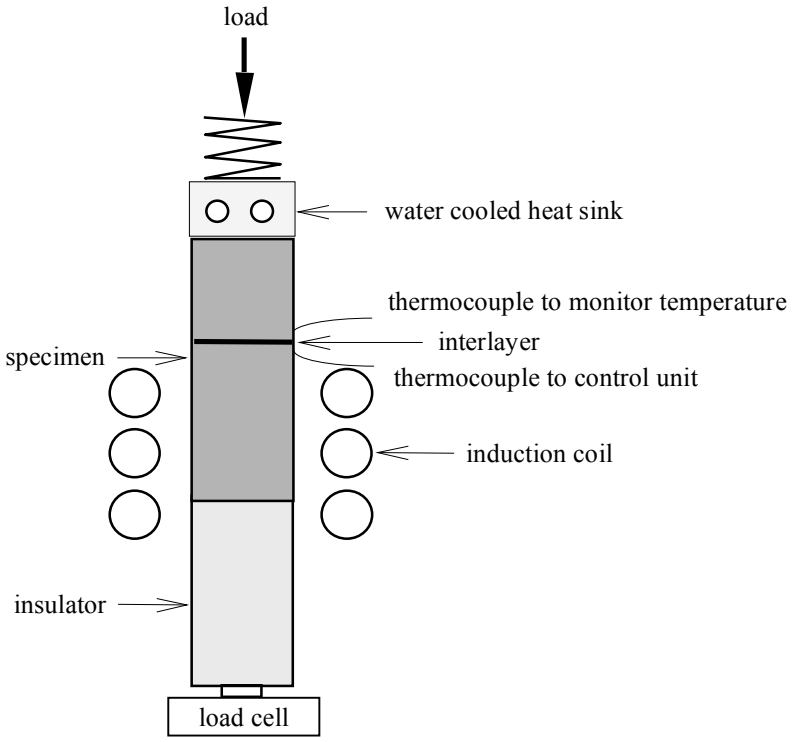

Fig. 3-5: Specimen set-up in temperature gradient TLP diffusion bonding (method IV).

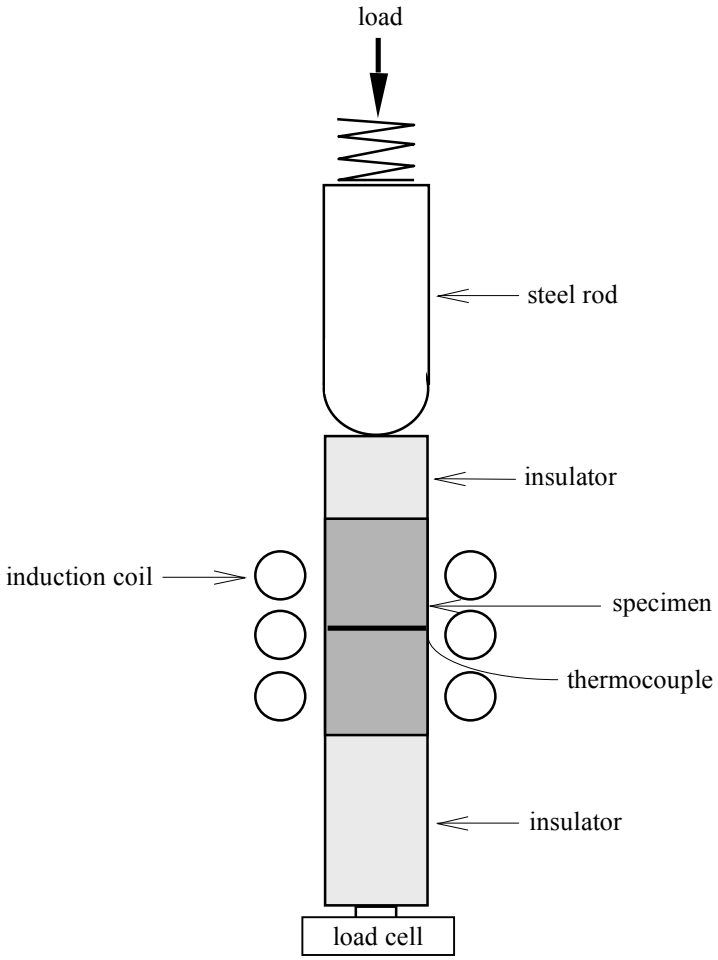

Fig. 3-6: Schematic set-up in high heating rate TLP diffusion bonding in air (method V).

Method VI: *Temperature gradient TLP diffusion bonding in air*

The preliminary experiments on method VI were carried out using the same set-up as for method IV (temperature gradient TLP diffusion bonding). Despite having used the highest input power of the heat source, the heating rate was less than those attained in method V (high heating rate TLP diffusion bonding in air). This was obviously due to substantial heat flux from the parts being joined into the heat sink. Therefore a new bonding set-up had to be designed in order to keep the heating rate sufficiently high when temperature gradient TLP diffusion bonding in air.

The new bonding set-up for method VI is based on a combination of the bonding set-ups used in methods IV and V, and is schematically shown in figure 3-7. In this new set-up, specimen positioning and the location of the induction coil are the same as those in method IV, but the water cooled heat sink is replaced with a thin slice of insulator or aluminium with a thickness which controls heat conduction to the steel rod with a round tip (similar to that used in method V). Basically, the steel bar acts as the loading bar and the heat sink at the same time. By reducing the heat flux with this set-up, the heating rates were increased, although precise control of the heating rate was found to be difficult (see Chapter 7 for more details). The temperature of the heat sink was not constant and the design of the heat sink should be modified in future work.

Specimen preparation methods and the loading procedure used in this method were the same as those used in method V.

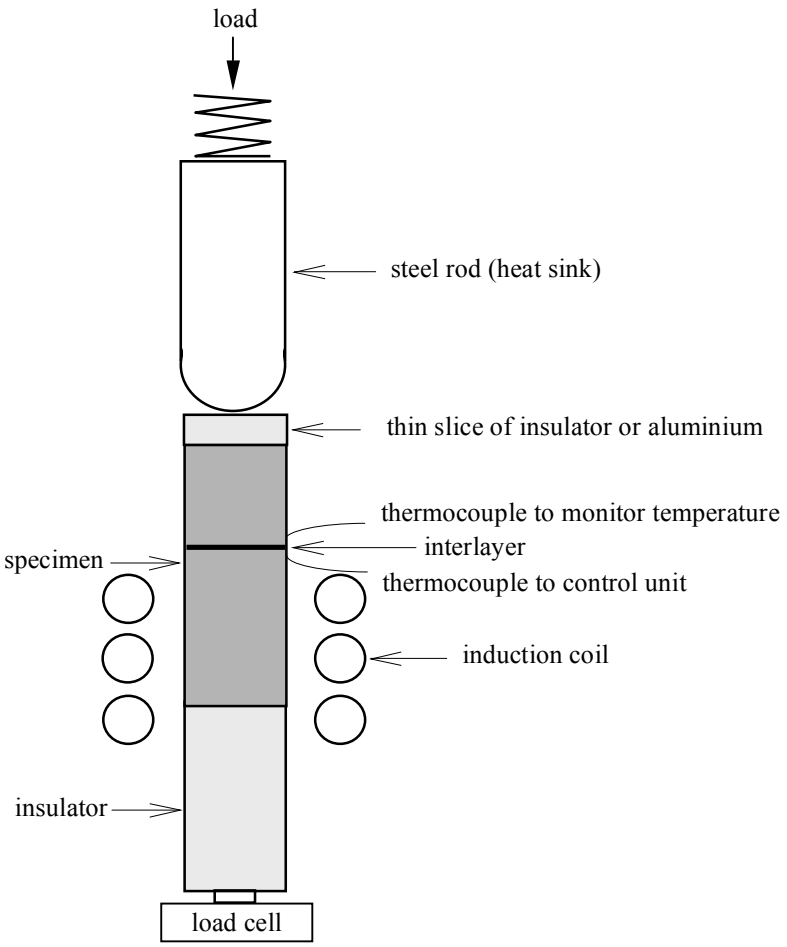

Fig. 3-7: Specimen set-up in temperature gradient TLP diffusion bonding in air (method VI).

For the sake of simplicity, the main bonding parameters and the bonding method used in each experiment will be abbreviated as shown in figure 3-8. As an example;

[T 550:560 / P 0.2:5 / t 5:60 / M III]

means that the first stage of method III was carried out at 550 °C under 0.2 MPa pressure for a duration of 5 minutes and then bonding was followed by hot isostatic pressing (hipping) at 560°C under 5 MPa pressure for 60 minutes.

3.2.3 Post bond heat treatment

Where appropriate, post-bond heat treatments were carried out to restore the mechanical properties of the bonds. Bonded specimens and control samples of parent material were soaked at 530-545°C for 20-30 minutes and quenched in water, followed by artificial ageing at 165-185°C for 6-8 hours.

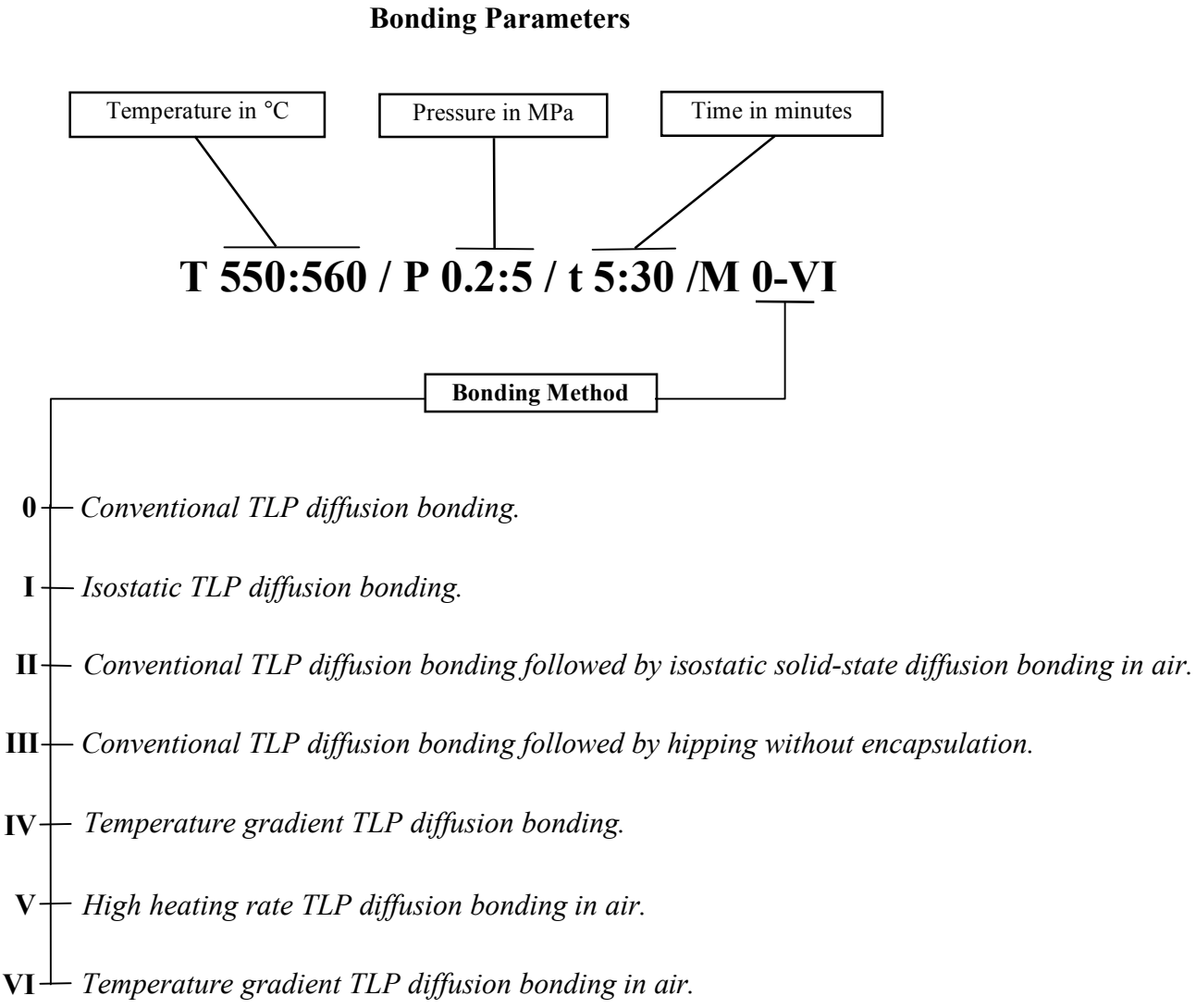

Fig. 3-8: Abbreviations used to refer to bonding conditions and methods.

3.3 Bond testing and evaluation

3.3.1 Mechanical testing

Shear testing, as the most commonly used form of mechanical testing in diffusion bonding, was used to evaluate bond strength. The experimental arrangement used for shear testing is shown schematically in figure 3-9. The grips of the rig were constructed from hardened steel which were constrained by a brass sleeve to prevent their lateral movement. The tensile force acting on the grips causes the specimen to experience an almost pure shear stress without compressive restraint perpendicular to the bond line. In contrast to a constrained lap shear test, no "dog-leg failure" can occur using this method. A screw tensile machine, with a full load capacity of 50 kN, was used for shear testing. The cross head speed was 0.5 mm/min. All samples, except Al-8090/SiC bonds, were machined to 7 mm in diameter before shear testing in order to eliminate any edge effect (see section 4.3.1 for details). In some samples, the bond line was not discernible, so these samples were polished and then etched in *Keller's* solution (for chemical composition, see the next section) before shear testing; this was done to reveal the bond line in order to ensure proper positioning of the sample in the testing tool. Bonds for each set of experiments were shear tested together with parent material given the same thermal history as the bonds.

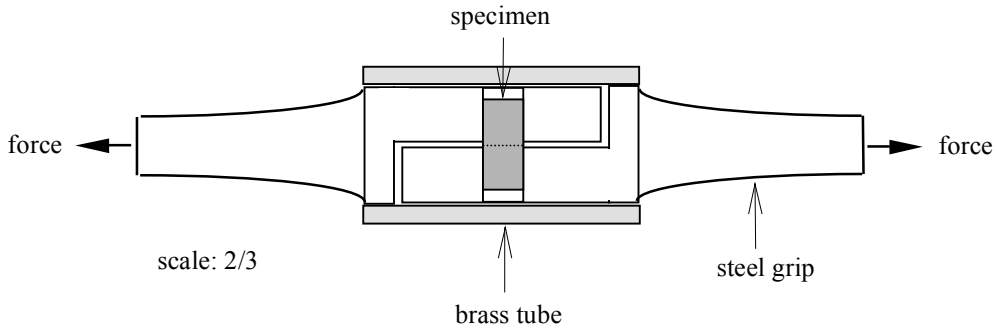

Fig. 3-9: Shear test arrangement (bond line is shown by a dashed line).

Hardness testing (micro-Vickers method with a load of 10 or 25 grams) was carried out on some of the samples to measure hardness profiles across bond lines. All the samples were ground using 1200 emery paper and polished to a ¼ micron diamond paste finish before hardness testing.

3.3.2 Metallographic examination

Light microscopy

Specimens were cut perpendicular to the bond line by hand saw and were mounted in bakelite. The mounted specimens were ground using silicon carbide papers from 600 grit down to 1200 grit followed by 6 and 1 μm diamond paste polishing. *Keller's* reagent (2.5% NHO_3, 1.5% HCl and 0.5% HF) was used as the etchant.

Scanning Electron Microscopy (SEM) and Energy Dispersive Spectroscopy (EDS)

SEM (JEOL 5800 LV) was used to study the shear fracture surfaces as it has a much greater depth of field than light microscopy. The bond region was analysed chemically by EDS. The analyses included the spot analysis of individual elements and the results are reported in weight percentage.

Transmission Electron Microscopy (TEM) of Al/SiC composite

TEM can be used to investigate the oxide morphology and to characterise the precipitates along a bond line. However, a detailed analysis of the bond line can be achieved by TEM examination only if a reliable method for foil thinning is found. Unfortunately, the use of an electrojet polishing technique was not satisfactory as the solution corroded the matrix preferentially, without reacting with the reinforcement, which eventually left a mesh-like structure! A combination of electropolishing and ion beam machining also was not satisfactory, although this technique was used for the thinning of diffusion bonds in un-reinforced aluminium alloys by *Maddrell (1989).*

The most successful method for TEM sample preparation was based on a combination of dimpling and ion bean machining. A high precision rotary cut-off machine was used to cut a bonded sample into slices of 300 μm thickness and then each slice was mounted on a flat base, using thermoplastic resin. These were then ground to produce 60 to 50 μm thickness foils. Three standard TEM discs were punched out of each foil, keeping the bond line at the centre of each discs. The dimpling technique was used to thin the area around the bond line. Finally ion beam machining was carried out until an orifice was formed in the middle of the discs. The ion beam conditions were as follows:

- accelerating voltage: 5 kV
- beam current: 0.5 mA
- double ion guns at angle: 10° to 15°
- time: 1 to 3 hours

The TEM sampling technique, used in this work, is shown in figure 3-10. A Philips 400T transmission electron microscope was used for bright field, dark field and diffraction contrast imaging.

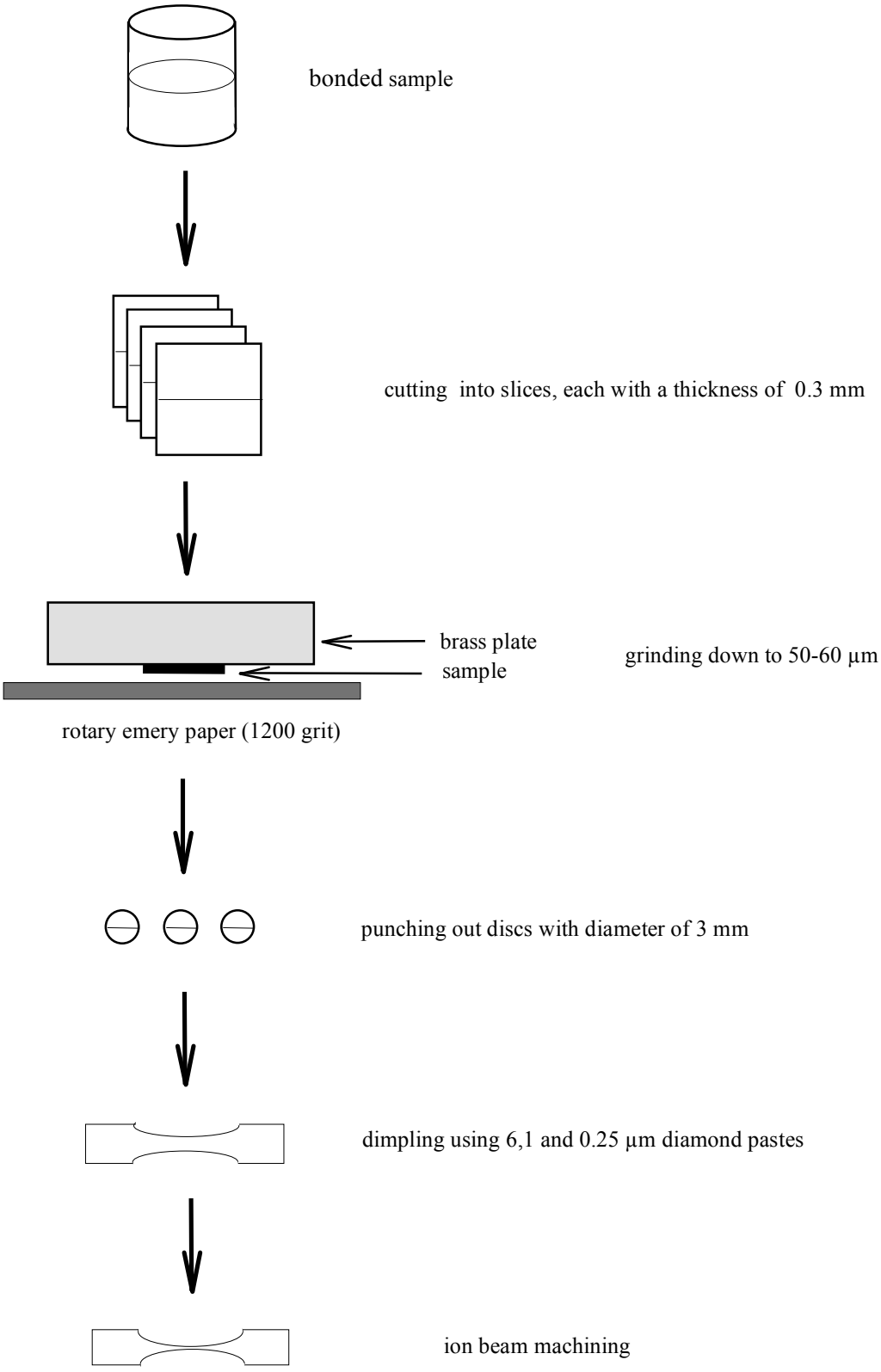

Fig. 3-10: TEM sampling procedure (not to scale).

Chapter 4

4. Methods I, II and III: New methods for TLP diffusion bonding aluminium-based composites

4.1 Introduction

The development of various metal matrix composites (MMCs) may be regarded as a major advance in materials science and technology during the last two decades, *Lloyd (1994)*. Aluminium metal matrix composites (Al-MMCs) are of considerable interest because of their superior mechanical properties compared to un-reinforced aluminium alloys (especially their high stiffness, strength and wear resistance) which can provide significant weight and performance benefits in transportation industries, *Peel et al. (1995)*. Following the recent development of low cost manufacturing processes, Al-MMCs with particle reinforcement are now available commercially. However, despite substantial improvements in the range and properties of such MMCs, their application, which is potentially vast, has been somewhat restricted by the lack of reliable and economic joining methods, *Ellis et al. (1994)*.

Although fusion welding of un-reinforced aluminium alloys is well established, the high temperature nature of the process normally causes unfavourable reactions between the reinforcement and the matrix in Al-MMCs, see section 2.5 for details. Hence an alternative approach is to use diffusion bonding which has proved successful for joining aluminium-based alloys providing that the tenacious and chemically stable surface layer of aluminium oxide is either removed or disrupted.

In solid-state diffusion bonding, the brittle and continuous oxide layer can be broken up by imposing substantial plastic deformation. Metal-to-metal contact is thus promoted because of local disruption of the oxide film on both faying surfaces. In a recent investigation of the solid-state diffusion bonding of Al-MMCs plastic deformation in excess of 40% was required to produce satisfactory bonds, *Urena et al. (1995)*. The alternative approach of removing the oxide layer in vacuum by ion beam cleaning prior to bonding is technically more complicated and this restricts its commercial application. It is evident that it has not been possible to date to produce reproducible and high-strength bonds in Al-MMCs using solid-state diffusion bonding, *Ellis et al. (1994)*.

In transient liquid phase (TLP) diffusion bonding, the formation of a liquid phase at the interface between the parts being joined can assist in the disruption of the oxide layer and so promotes metallic bonding. Consequently, the required bonding pressure in this process is quite low compared with solid-state diffusion bonding. The bonding temperature is normally chosen to be slightly above the eutectic temperature in order to ensure the eutectic reaction occurs, even though such a temperature may be relatively high (i.e. close to the solidus of the parent material) when bonding aluminium-based alloys and composites.

The use of copper interlayers has proved to be successful for joining some conventional aluminium alloys, and bonds with shear strengths comparable to that of the parent material have been reported, *Dray (1985)*. However, there is a potential difficulty in applying even the low pressure required during bonding since most Al-MMCs are very soft at TLP diffusion bonding temperatures (i.e. 550 °C when using a copper interlayer) and excessive plastic deformation can occur during the bonding process. Hence most of the previous work has been either carried out on thin plates or has used a constant deformation arrangement in order to avoid excessive distortion of the parts being joined. In the latter case, the bonding pressure is transient (decreasing as the temperature increases) and its variation depends not only on the size and shape of the sample, but also on the heating rate, the initial pressure applied and the thickness of the interlayer. Therefore, the results reported from such investigations tend to be valid only for the particular arrangement and material used. In addition, the effect of varying bonding pressure cannot be investigated readily using a method employing constant deformation.

Three new methods for TLP diffusion bonding of aluminium MMCs have been developed in this work. These methods are based on applying isostatic bonding pressure (rather than conventional uniaxial compression) in order to improve bond strength and also minimise plastic deformation of these materials in the bonding process.

4.2 The aim of using isostatic pressure for TLP diffusion bonding of aluminium MMCs

The aim in developing new methods for TLP diffusion bonding of Al-MMCs was to overcome the following problems:

a) to improve bond strength since the highest bond strengths reported using TLP diffusion bonding are much lower than the shear strength of the parent material;

b) to reduce the extent of plastic deformation when diffusion bonding aluminium-based materials, since this would not be tolerated in a number of potential applications.

c) to minimise the scatter in bond strength since high scatter has been a major problem with diffusion bonding, degrading the reliability of the process.

The use of isostatic compression, in place of conventional uniaxial compression, has the following advantages:

i) the possibility of applying a uniform and constant bonding pressure across the interface which should improve bond strength;

ii) the ability to vary more extensively bonding parameters such as pressure, temperature and time in order to optimise bonding conditions and hence bond strengths;

iii) the virtual elimination of plastic deformation which under an isostatic stress-state is both negligible and also almost independent of the applied pressure, temperature, shape, and dimensional variations. This leads to the possibility of high precision joining of intricate parts with minimal deformation.

The three new approaches for TLP diffusion bonding, all based on the application of isostatic pressure, are summarised in figure 4-1. The first variant of TLP diffusion

bonding, method I, is a single stage process in which the process starts and finishes under a constant isostatic pressure. The second method (method II) consists of two stages. In the first stage, TLP diffusion bonding is carried out in vacuum under very low pressure to avoid excessive plastic deformation. The bonding time is also kept as short as possible to minimise any deformation arising from creep, and this also has the advantage of minimising any reaction between reinforcement and matrix in Al-MMCs. The second stage uses solid-state diffusion bonding under a relatively high isostatic pressure to increase bond strength. This stage is carried out in air. The third method (method III) is similar to method II except that isostatic pressing is replaced by hipping (hot isostatic pressing) without encapsulation. The technical details of, and results from, these methods are described below.

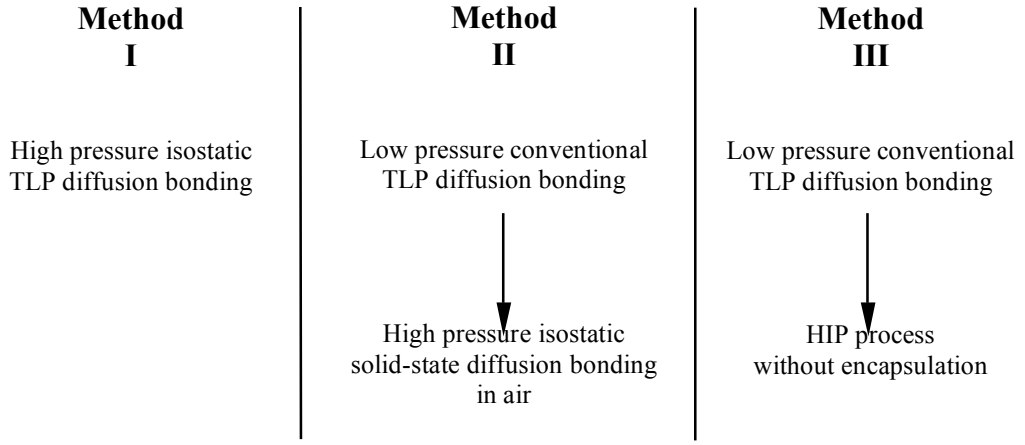

Fig. 4-1: Three approaches for TLP diffusion bonding based on applying isostatic pressure used in the present work.

4.3 Results and discussion

About 110 bonding trials were carried out and the use of isostatic compression in methods I and II resulted in a remarkable improvement in the bond strengths of Al-8090/SiC and Al-359/SiC composites compared with those obtained using conventional TLP diffusion bonding.

4.3.1 Methods I and II

- **Mechanical properties**

The shear test results for Al-8090/SiC bonds are summarised in figure 4-2 which includes maximum, average and minimum shear strengths for each of the methods. Note that at least three samples were produced and shear tested for each of the bonding methods. The highest bond strength achieved, using a 3 μm thickness copper interlayer and the bonding conditions of [T 560 / P 1 / t 60 / M I], was 221 MPa which is 85% of the shear strength of the parent material given the same T6 heat treatment. The highest bond strength obtained using method II and the same interlayer was estimated to be 219 MPa (84% of the shear strength of the parent material) – see below. These values are the highest bond strengths reported for this composite to date. They also are higher than the maximum achievable bond strength predicted in the model of *Partridge & Dunford (1991)*. In that model, the maximum bond shear strength of a TLP diffusion bonded joint in Al-8090/SiC composite is predicted to be lower than 190 MPa. This inconsistency between the predictions of the model and the experimental results of this work is discussed in section 4.4. In comparison, the shear strengths of bonds, made using conventional TLP diffusion bonding with bonding pressures of 0.1 to 0.2 MPa, were very low (maximum 105 MPa), see figure 4-2. The use of higher bonding pressures (above 0.2 MPa) for conventional TLP diffusion bonding was not possible because of the associated massive plastic deformation of the material at the bonding temperature (560 °C).

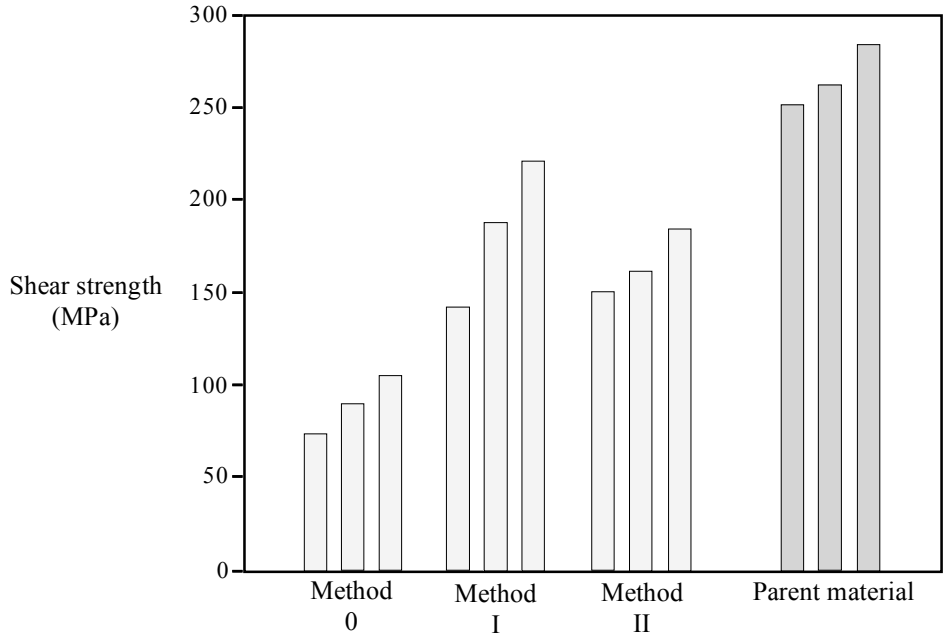

Fig. 4-2: Maximum, average and minimum shear strengths of Al-8090/SiC bonds, made using a 3 μm thickness copper interlayer and different bonding methods, compared with those of the parent material (bonding condition in the text).

The above estimate for bond strength using method II was made for the following reason. The actual measured bond strength using the bonding conditions of [T 560:560 / P 0.2:1 / t 5:60 / M II] was 184 MPa (71% of the shear strength of the parent material, see figure 4-2). However, as rotary grinding in the surface preparation stage tended to result in rounded edges, complete contact between the interlayer and the faying surfaces could not be established across the entire faying surfaces. Surface profilometry showed that when two such ground pieces were put together, a peripheral crevice with a depth of up to 1 mm could be formed. The unbonded areas on the outer edge of a fracture surface of a Al-8090/SiC composite, bonded using method II, are shown in figure 4-3.

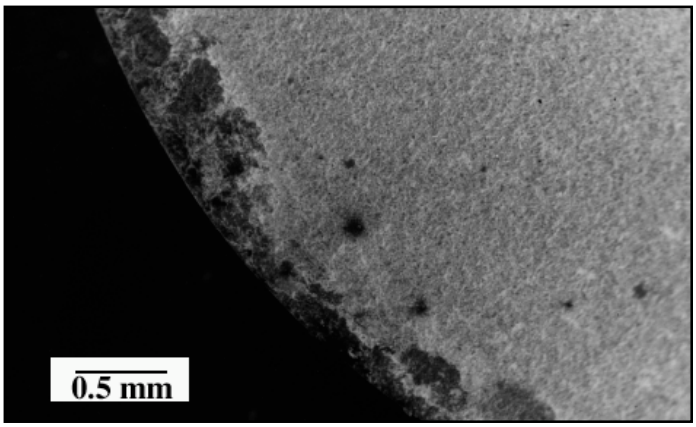

Fig. 4-3: SEM micrograph showing the edge effect in a Al-8090/SiC composite bonded by method II; unbonded peripheral areas on the outer edge of a fracture surface are seen.

Recalculation of the bond strength excluding the unbonded peripheral areas (as estimated from observation of the fracture surface, figure 4-3) gives a shear strength of 219 MPa. This correlates well with the shear test results (i.e. 221 MPa) achieved using method I in which there was no edge effect. Consequently, the higher as-measured bond strengths achieved by method I, compared to method II, are not unexpected as in the former case the entire bonding process was carried out under isostatic pressure with a high bonding pressure, thus ensuring that the edges were brought into complete contact. In contrast, the bonding pressure in method II was very low at the onset of the process

when the liquid phase was present and this resulted in an unbonded–peripheral area. Increasing the bonding pressure in the second stage of method II (isostatic solid-state diffusion bonding in air) cannot eliminate the edge effect as not only is the liquid phase no longer present at the interface but also oxidation occurs on the exposed unbonded peripheral area at the interface.

In order to eliminate any further edge effects associated with the use of method II, the Al-359/SiC specimens were machined after bonding but before shear testing. The highest bond strength of Al-359/SiC composite achieved using this method was 242 MPa (92% of the shear strength of the parent material given the same heat treatment). This is the highest bond strength for this aluminium-based composites that has been reported to date. In the course of the bonding, some technical problems occurred (e.g. temperature and/or pressure instability, variation in heating rate or surface contamination etc.) which resulted in "defective" samples. However all the bonded samples, including these "defective" samples, were shear tested and the minimum bond strength found was 212 MPa (i.e. 80% of the shear strength of the parent material) – see figure 4-4. Hence it is evident that, as well as increasing the average bond strength, the minimum value measured and the overall scatter in the results would both be improved by better control of bonding parameters and by using better surface preparation techniques.

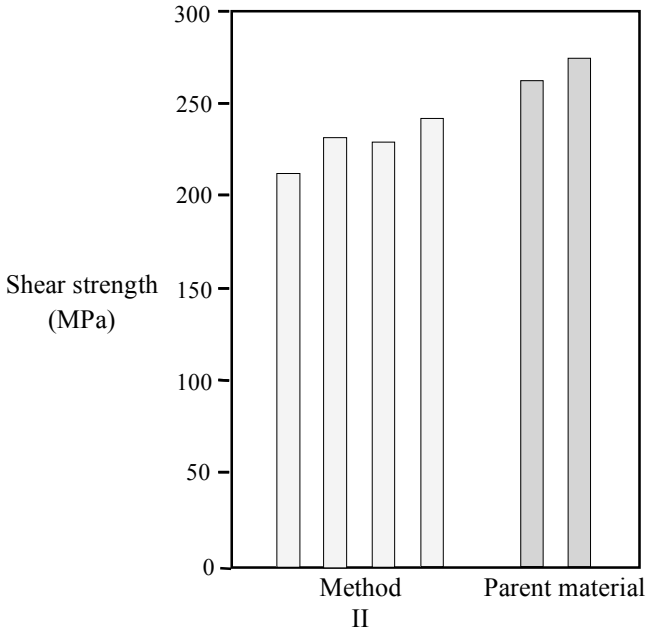

Fig. 4-4: Shear test results of Al-359/SiC bonds, made using a 7 µm thickness copper interlayer and method II, compared with the maximum and minimum shear strengths of the parent material (bonding condition: [T 560:560 / P 0.2:2 / t 5:60 / M II]).

The effect of bonding time on the strength of Al-8090/SiC bonds was also investigated. Although only a limited number of specimens were tested, it seems that increasing the bonding time from 15 to 30 minutes under high isostatic pressure (5 MPa) does not improve bond strength. The effect of bonding time when using lower bonding pressure was not studied. The effects of bonding pressure, interlayer thickness and bonding time on the bond strengths of the 8090 Al-SiC are summarised in figure 4-5.

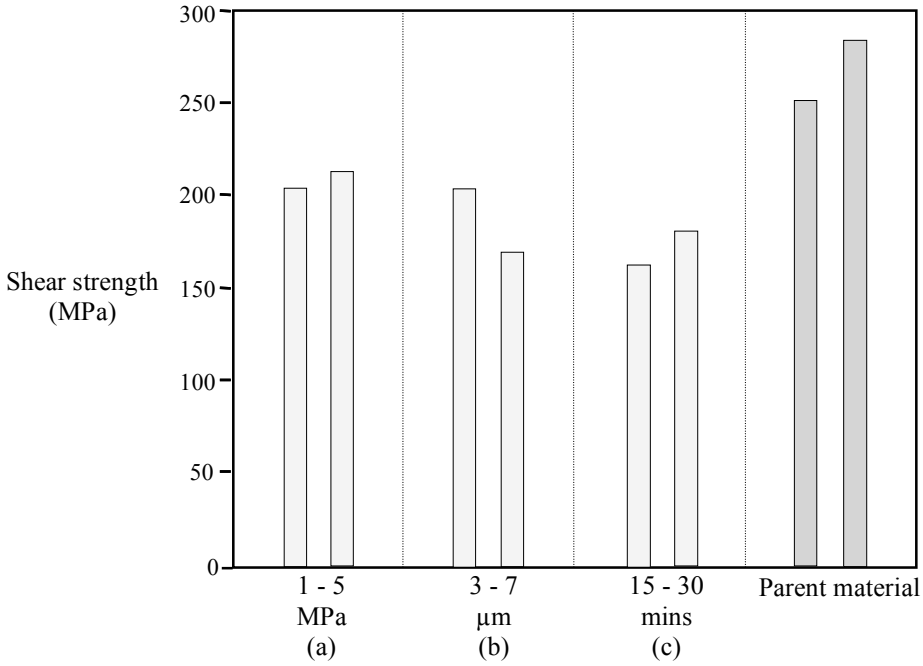

a) bonding pressure;
b) copper interlayer thickness;
c) bonding time.

Figure 4-5: The effects of bonding parameters on the average shear strengths of Al-8090/SiC bonds, made using method I, compared with the maximum and minimum shear strengths of the parent material.

- **Microstructural observations and effects of interlayer thickness**

A typical microstructure of the Al-359/SiC bond after low pressure TLP diffusion bonding and before isostatic pressing is shown in figure 4-6a, in which the presence of some large voids indicates a lack of complete bonding along the bond line. In contrast, no voids are seen on the bond line after isostatic pressing using method II, figure 4-6b. These microstructures are quite consistent with the shear test results, confirming the effect of isostatic pressing in improving bond strength (see figure 4-2). Further investigation of the effect of bonding pressure on bond strength revealed that there was little benefit in increasing the isostatic pressure above 1 MPa. Note the massive agglomeration of the SiC reinforcement at the bond line, a consequence of using 7 μm thick copper foils.

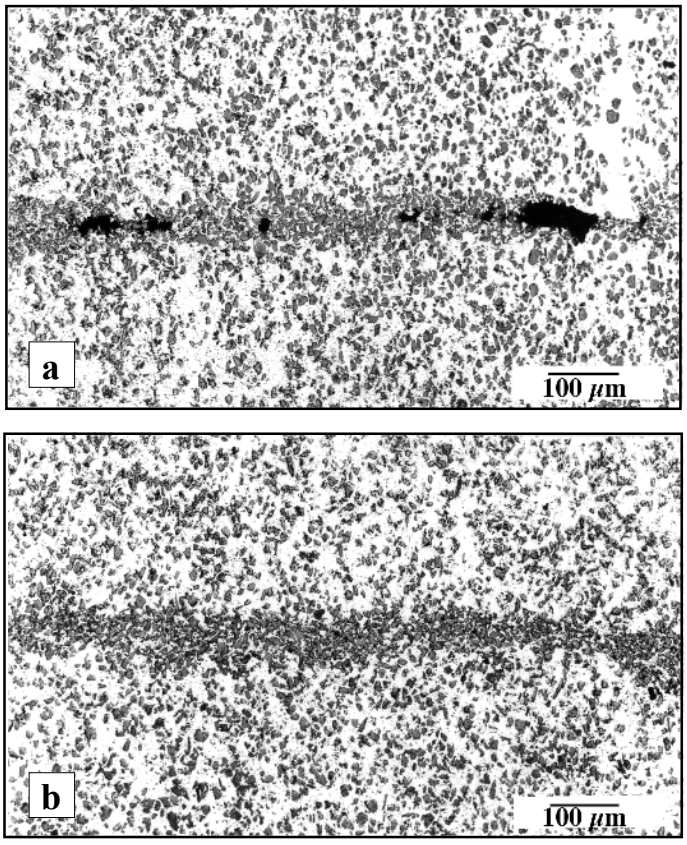

a) low pressure TLP diffusion bonding (note voids along the bond line);
b) as (a) but followed by isostatic pressing in air which has eliminated the voids.

Fig. 4-6: Microstructure of a Al-359/SiC bond made using a 7 μm thickness copper interlayer.

The effect of interlayer thickness on bond strength, microstructure and fracture surface appearance was investigated. Using copper interlayers of 1 and 3 μm thicknesses and constant bonding condition of [T 560 / P 0.2 / t 30 / M 0], Al-8090/SiC composite bonds were produced for shear testing. The highest bond strength of 105 MPa was obtained using a 3 μm thick copper foil. This is 40% of the shear strength of the parent material given the same heat treatment. The shear strengths of the bonds made using interlayers of 1 μm thickness were relatively low and no evidence of melting was observed. Therefore, the 1 μm copper interlayer was not used in subsequent trials.

A typical microstructure of a Al-8090/SiC bond, made using method I and a 3 μm thick copper interlayer, with a bonding time of 30 minutes, is shown in figure 4-7a. The bond line is hardly discernible. EDS analysis showed that there was no increase in copper at the bond line and no evidence of intermetallic formation was observed. In contrast, the use of the thicker 12.5 μm copper interlayers caused unfavourable massive movement and agglomeration of the SiC particles across the bond line as shown in figure 4-7b.

All the Al-359/SiC bonds were made using 7 μm thickness interlayers and the same effect of agglomeration of the SiC particles was observed, figure 4-6. The use of thinner interlayers should result in less displacement of the reinforcement and might therefore result in higher bond strengths, figure 4-5. TEM investigation revealed that a 3 μm copper interlayer is enough to disrupt the oxide layer on Al-8090/SiC composite and to promote metal-to-metal contact, figure 4-8. However, a minimum thickness of interlayer is required at the interface for liquid phase formation and this thickness should be optimised for each application.

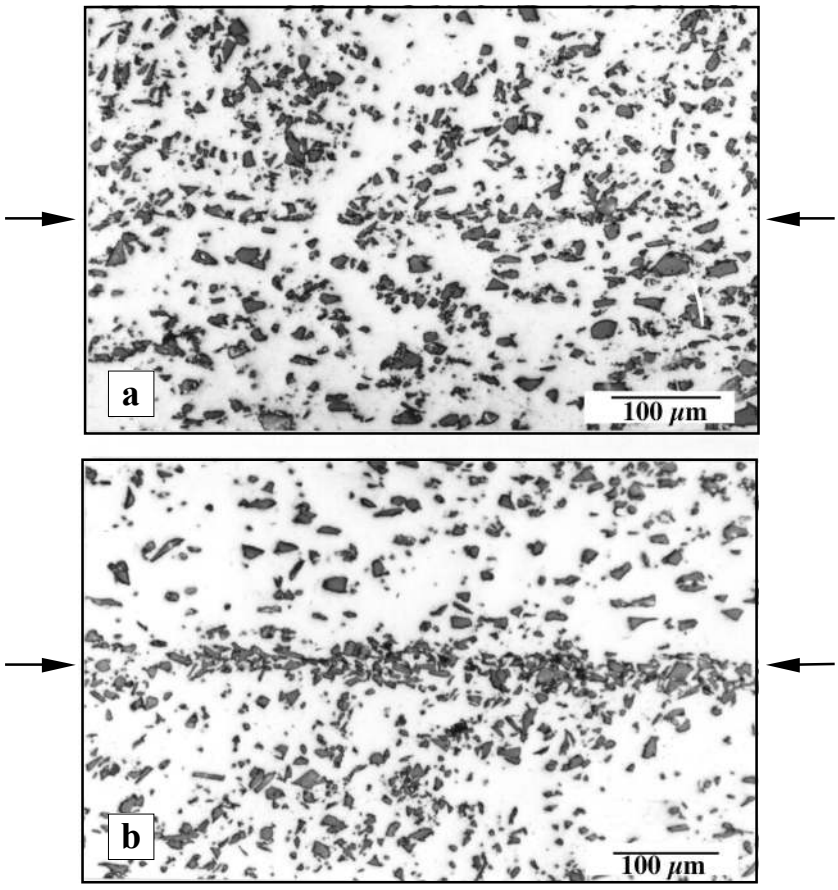

a) 3 μm interlayer;
b) 12.5 μm interlayer.

Fig. 4-7: Effect of interlayer thickness on the distribution of SiC particles at the bond lines of Al-8090/SiC composites bonded using method I (arrows show bond line).

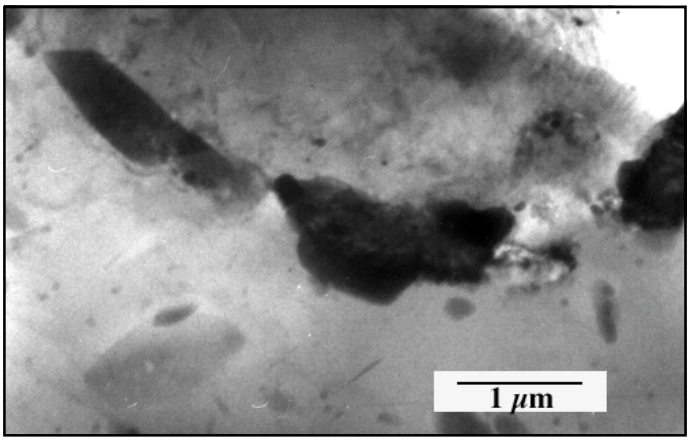

Figure 4-8: TEM micrograph of bond line (Al-8090/SiC) showing metal-to-metal contact between the disrupted oxides (method I).

The fracture surfaces of the parent materials and of both bonded composites were examined by SEM. In the case of Al-8090/SiC, the fracture surfaces of the parent material and the bond with highest strength, made using a 3 μm copper interlayer, looked similar implying that the fracture process was similar for both, figures 4-9a,b. In contrast, in the case of Al-359/SiC, the corresponding fracture surfaces were not identical when 7 μm copper interlayers were used, figures 4-9c,d. This is not surprising as massive agglomeration of the reinforcement at the interface would be expected to alter the fracture mode (compare figure 4-6 with figure 4-7a).

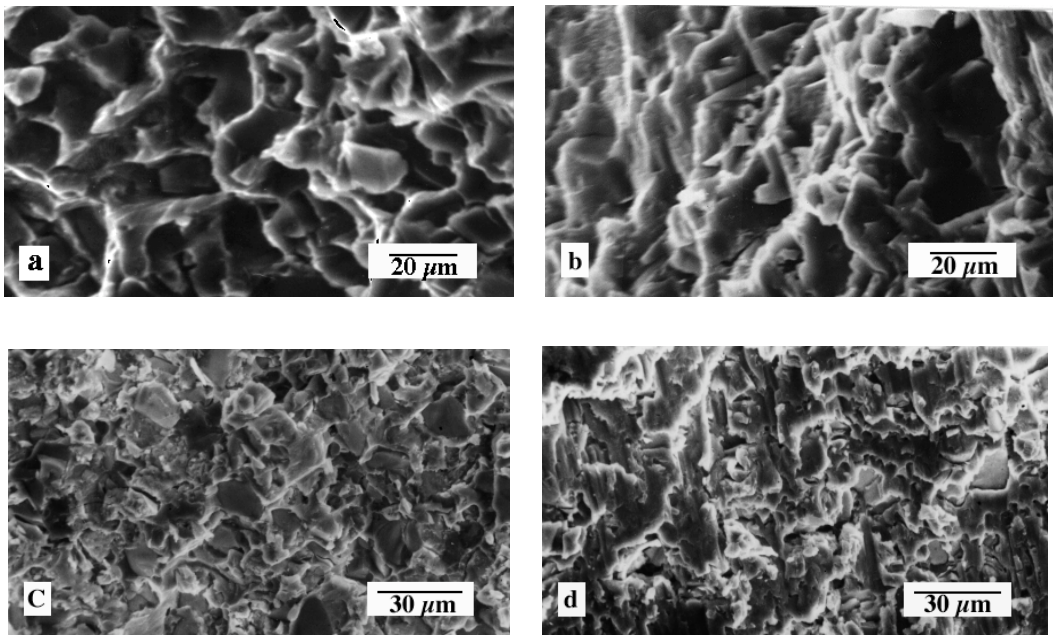

a) Al-8090/SiC bond made using a 3 μm copper interlayer (method I);
b) Al-8090/SiC parent material;
c) Al-359/SiC bond made using a 7 μm copper interlayer (method II);
d) Al-359/SiC parent material.

Figure 4-9: SEM micrographs of fracture surfaces.

4.3.2 Bonds in Al-Li alloy (UL-40)

The interfacial reaction between the copper interlayer and the UL-40 was very different from that of the other materials used in this work. This may be attributed to the presence of a lithium-rich oxide and/or hydroxide on the surface, which keeps the stable surface layer intact. Using conventional TLP bonding and copper interlayers with thicknesses of 1, 3 and 7 μm, low bonding strengths in as-bonded condition were obtained (about 30% of shear strength of the parent material in the solution treated condition). There was no substantial evidence of melting (pressure drop or expulsion of liquid phase) during the bonding process. Figure 4-10a shows the microstructure at the edge of a UL-40 bond where long range diffusion of copper has occurred, as seen on both sides of the bond line. Some intermetallics within the copper diffused zone were also seen in a band parallel to the bond line, figure 4-10b. The distance between this band and the bond line (copper rich zone) is almost twice its distance from the diffusion boundary showing that these intermetallics are probably $CuAl_2$. The rapid diffusion of copper which probably occurred during heating to the bonding temperature could explain the lack of melting. The effect of imposing a temperature gradient on the microstructure of UL-40 bonds is discussed in section 5.4.1.

The bond strength was improved remarkably by using method I and by increasing the interlayer thickness to 12.5 μm. The highest bond strength achieved was 155 MPa which is 65% of the shear strength of the parent material. However, using two layers of 12.5 μm interlayer resulted in lower strengths probably because of formation of Cu-Al-Li intermetallics at the interface. Further investigation is required in order to understand the nature of the various interfacial reactions in TLP diffusion bonding of aluminium alloys with high lithium content.

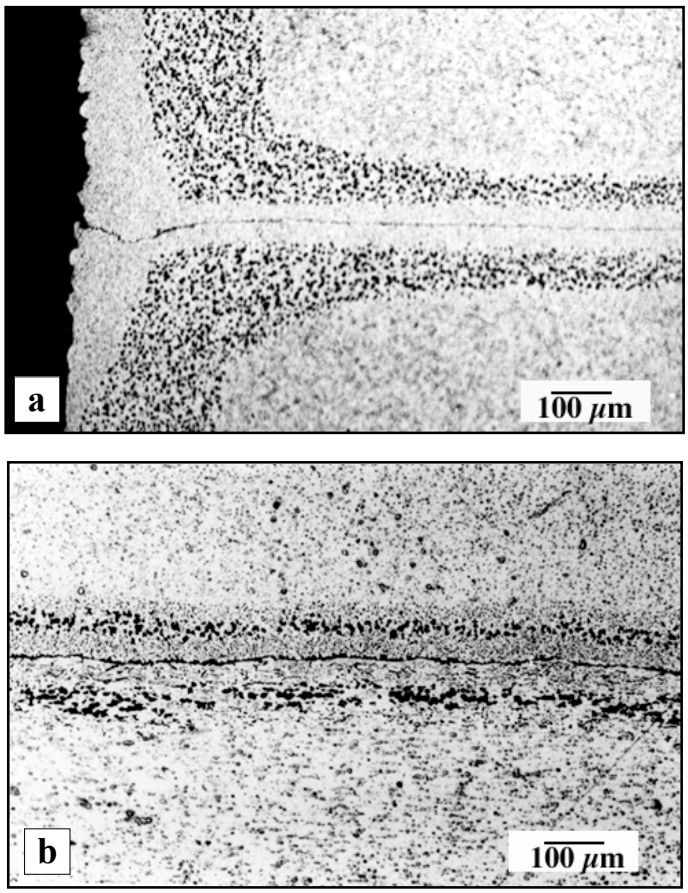

a) outside edge of specimen (10 minutes at 550 °C, 7 µm copper interlayer);
b) middle of specimen (4 minutes at 550 °C, 12.5 µm copper interlayer).

Fig. 4-10: Bond lines (UL-40) showing extent of copper diffusion zones and precipitation of intermetallics (dark band) within the diffusion zones.

4.3.3 Method III

Following the low pressure TLP diffusion bonding, in the first stage of method II, the partially bonded sample has to be inserted in a steel jig to avoid plastic deformation during subsequent high-pressure isostatic pressing . In contrast, in method III, the second stage of the bonding process for the partially bonded sample is replaced by a hipping process.

Simple finite element analysis, using Abacus and Patran packages, was carried out to investigate and compare the plastic deformation around the interfacial voids during the second stages of both methods II and III, and also in conventional solid-state bonding (i.e. without any lateral constraint). Figure 4-11 shows schematically a bonded sample with some voids at the interface. The results of the finite element analyses, when bonding pure aluminium, are shown in figure 4-12. The analyses were carried out for a quarter of the model in figure 4-11 as a consequence of symmetry.

In the case of solid-state bonding without lateral constraint, figure 4-12a, some void shrinkage and massive lateral deformation has occurred. However the patterns of void deformation in figures 4-12b and 4-12c are fairly similar, suggesting that the second stage of the method II can be replaced be a hipping process. Theoretically, the stress state and the field of strain in both cases should be exactly the same when the shear strength of the material is negligible in comparison with the applied force, i.e. when the material behaves like a liquid. The present difference in the patterns, 12b and 12c, is due to the shear strength of pure aluminium at the bonding temperature which has been considered in the model.

The importance of hipping used in method III is for two reasons. First, there is no need to constrain the material and, therefore, parts with complicated shapes can be processed without a loss of dimensional accuracy. Second, in contrast to conventional HIP bonding, encapsulation is not necessary as the bond line is already sealed in the first stage of the method and this should facilitate use of this approach.

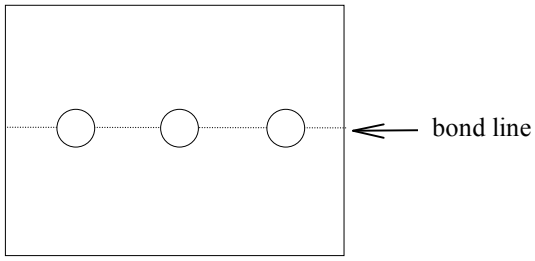

Fig. 4-11: A simple model of a partially bonded sample including some voids in the interface.

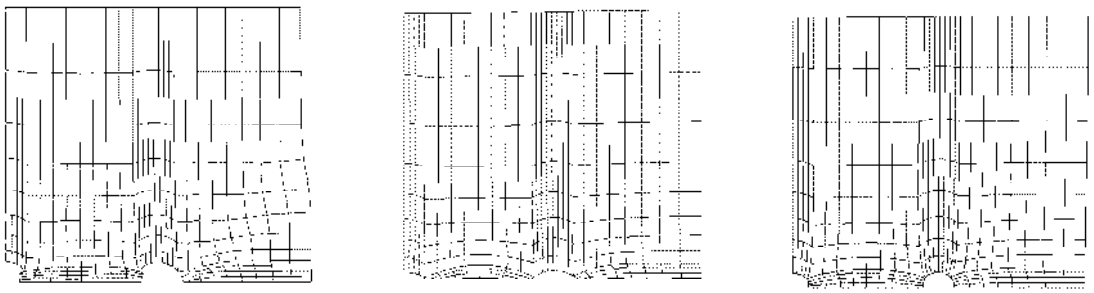

a) conventional solid-state bonding;
b) isostatic solid-state diffusion bonding (Second stage of method II);
c) hot isostatic pressing (second stage of method III).

Fig. 4-12: The results of finite element analyses showing void deformation at the interfaces of pure aluminium bonds.

The results of preliminary bonding trials on Al-359/SiC composite and un-reinforced 6082 alloy, using hipping in the second stage of method III, were quite promising. The highest bond strength achieved for 6082 bonds, using a 7 μm thickness copper interlayer and the bonding conditions of [T 560:560 / P 0.2:5 / t 15:60 / M III], was 200 MPa (89% of the shear strength of parent material). No evidence of oxidation or gas leakage into the bond line was observed, showing that a 7 μm thickness interlayer was enough to seal the joint for subsequent hipping without the need of encapsulation.

Bonding of the Al-359/SiC composite was not so successful. The slow cooling rate in the hipping chamber caused sufficient softening that the hipped samples deformed excessively during machining. Microscopic observation of the fracture surfaces showed also that sealing was not complete in the case of the composite and so some gas was forced into the bond line during the hipping stage. The lack of sealing may be attributed to insufficient melting in the first stage of bonding.

The results obtained using method III have shown that isostatic pressing after low pressure TLP diffusion bonding can be replaced by HIP process without encapsulation (canning). Method III can, therefore, be used for joining intricate parts with minimal deformation and high precision. Figure 4-13 shows a component which consists of three pieces of an aluminium alloy bonded using method III. The fabrication of such a part by other techniques such as machining or conventional diffusion bonding is almost impossible and the use of conventional "HIP Bonding" would require complicated encapsulation techniques. This demonstrates the particular advantage of using method III.

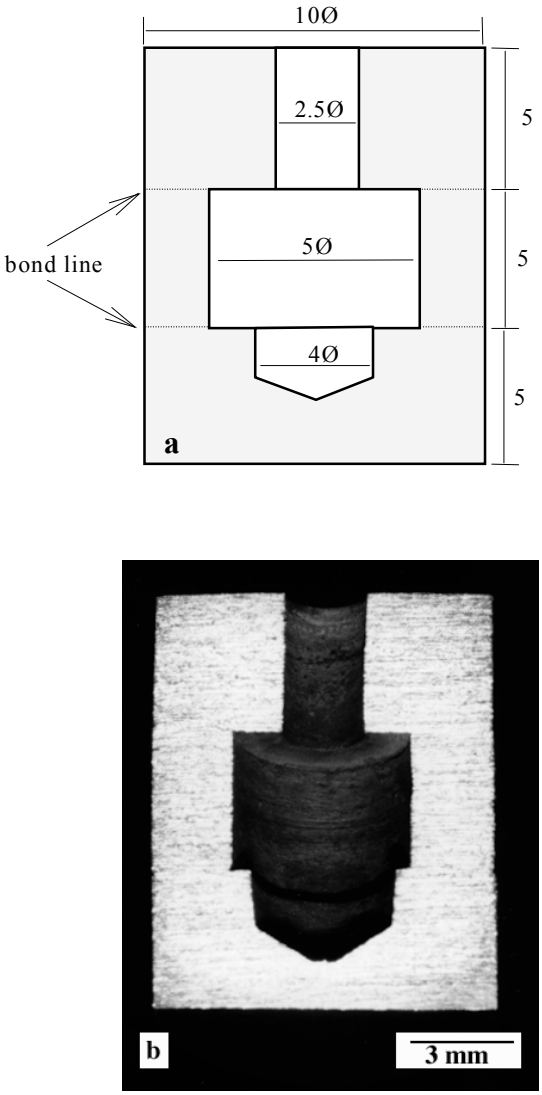

a) schematic cross section (dimensions in millimetres);
b) fabricated component (cross section).

Fig. 4-13: A component consisting of three pieces of an aluminium alloy fabricated using method III.

4.4 Case study: The role of reinforcement particles when diffusion bonding Al-MMCs

Solid-state diffusion bonding

The bond line of an MMC-MMC joint generally consists of three different interfaces: matrix/matrix, matrix/particle and particle/particle. Obviously, the area fractions of these interfaces depend on the volume fraction and distribution of the reinforcement on each of the two faying surfaces. *Partridge & Dunford (1991)* proposed a model which shows that insertion of a matrix interlayer into a MMC-MMC bond interface may increase or reduce the area fraction of the matrix/particle interface. According to this model, the presence of either particle/particle or matrix/particle interfaces leads to a lower shear strength of the bonded composite, compared to that of the bonded matrix alloy (i.e. with 100% matrix/matrix interface). This is explained as follows: firstly, almost no bond strength arises from a particle/particle interface and, secondly, the strength of a matrix/particle bond is assumed to always be lower than that of a matrix/matrix bond.

Experimental results of method I showed that joints in Al-809/SiC composite with shear strengths as high as 221 MPa can be achieved (see section 4.3.1). This value is greater than the upper bound value for the shear strength of a TLP diffusion-bonded Al-8090/SiC composite as predicted by the model of *Partridge & Dunford* mentioned above (i.e. 190 MPa). This inconsistency between the theoretical predicted value and experimental result is considered below.

Basically the model assumes microscopically planar faying surfaces which form a flat interface when the two surfaces are brought together during the diffusion bonding process. However, SEM examination of a polished Al-8090/SiC composite revealed that the reinforcement particles stick out of the polished surfaces, see figure 4-14. This is simply due to the faster abrasion of the relatively soft aluminium matrix, compared

with that of the hard SiC particles, during prior surface preparation. Figure 4-15 shows the results of profilometry carried out on the surfaces of an Al-8090/SiC composite and an un-reinforced aluminium alloy, both polished in exactly the same way. As expected, due to the protruding SiC particles, the surface roughness of the composite is much higher than that of the alloy.

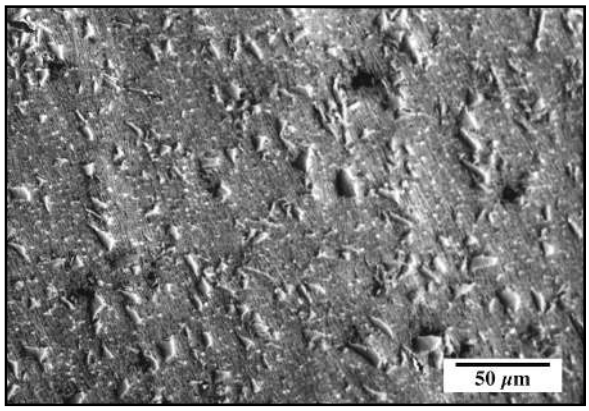

Fig. 4-14: SEM micrograph of Al-8090/SiC composite in the as-polished condition.

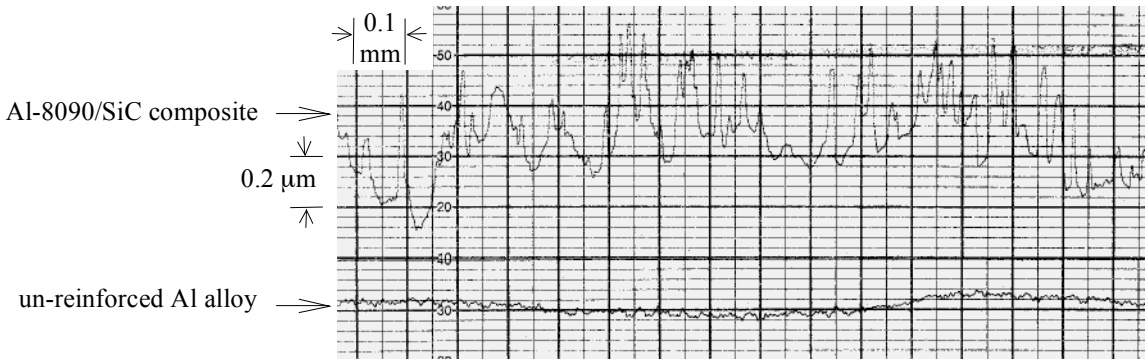

Fig. 4-15: Surface roughness of an Al-MMC in comparison with an un-reinforced Al alloy.

In light of the above observations, it would be reasonable to assume that during solid-state diffusion bonding of the composite, some of the SiC particles on each faying surface can easily penetrate into the aluminium matrix on the other surface (bearing in mind that aluminium matrix alloys are much softer than SiC particles, particularly at the bonding temperature). The depth of penetration depends on the shape of a particle and

can reach up to 0.6 μm for the composite used in this work. Figure 4-16a shows the distribution of particles at the interface of an Al-MMC joint for an ideally planar interface as assumed by *Partridge & Dunford*. According to their model, none of the particles on the faying surfaces cross the bond interface. In contrast, and consistent with the protrusion of the reinforcement, the bond line of a joint made of non-planar faying surfaces is associated with interlocked reinforcement particles along the bond interface, see figure 4-16b.

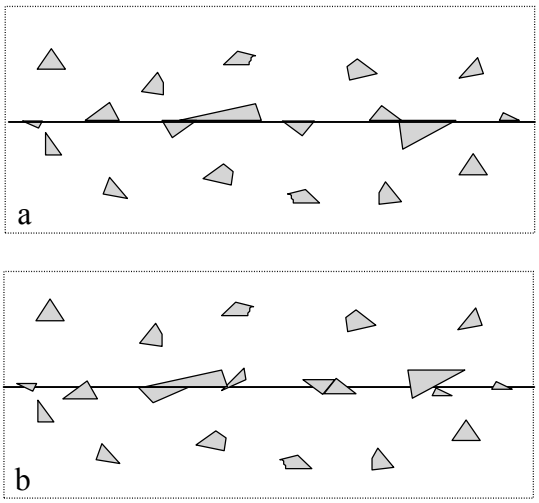

a) ideally planar faying surfaces (*Partridge & Dunford, 1991);*
b) non-planar faying surfaces including protruding reinforcements.

Fig. 4-16: Schematic diagram of reinforcement distribution at bond interfaces of an Al-MMC diffusion bonded joint with different surface condition.

Transient liquid phase diffusion bonding

As mentioned before, the bond line of a TLP diffusion-bonded composite is associated with agglomerated reinforcement particles, see figure 4-6. Due to the formation of the liquid phase and its subsequent solidification when TLP diffusion bonding an Al MMC, the reinforcement particles soaked in the liquid are displaced from their original locations, and eventually segregate around the bond line. The segregation of the particles depends on the amount of liquid phase (which is a function of the thickness of the interlayer and the bonding temperature for a particular binary system) and the size of the particles. *Zhai & North (1997)* studied the effect of particle size (Al_2O_3) on the

segregated layer in a dissimilar joint of Al-6061/Al_2O_3 and alumina. They concluded that the width of the segregated layer increases as the particle size decreases. This is due to the fact that the smaller particles are more easily pushed forward by the advancing liquid/solid interface, whereas the larger particles are left behind the moving boundary.

Due to the presence of the liquid phase around the reinforcement particles in the bond region, the formation of particle/particle interfaces is doubtful as a liquid film would be expected to exist between colliding particles. Because of this fact and also due to the massive penetration of the particles at the bond line, generalising the above model for a TLP diffusion bond is even less realistic than for a solid-state diffusion bond.

Summary

Despite substantial differences in the mechanisms responsible for particle distributions at bond lines, when solid-state or TLP diffusion bonding an MMC, it can be concluded that in both processes the reinforcement particles form a non-planar interface compared to the bond line in an un-reinforced alloy. The assumption of a microscopically planar interface, as shown in figure 4-16a, is not justifiable in either case. The formation of a non-planar interface can be of benefit in increasing the bond strength. In addition, the formation and solidification of the liquid phase around each particle in the bond region, when TLP diffusion bonding an MMC, is not taken into account in the model proposed by *Partridge & Dunford.*

This may explain the existing inconsistency between the theoretical predicted values and the experimental results achieved in this work. The proposed model seems to be too simple to accurately predict bond strengths as it ignores the presence of a non-planar interface in composite joints due to the protruding particles and also the formation of liquid around the reinforcement particles when TLP diffusion bonding. A more comprehensive investigation is required to achieve a reasonable correlation between the area fractions of different interfaces and the bond strength of a composite joint.

4.5 Summary

Three versions of TLP diffusion bonding, based on using isostatic compression, were developed in the course of this work.

The use of method I (isostatic TLP diffusion bonding) for joining aluminium-based composites proved successful for producing high strength bonds. In the case of Al-8090/SiC composite, bonds with shear strengths of up to 221 MPa (85% of the shear strength of the parent material) were produced using 3 μm thickness copper interlayers and applying 1 MPa bonding pressure. This is the highest bond strength for this composite that has been reported to date. Increasing the bonding time above 15 minutes, when the bonding pressure was high (5 MPa), improved the bond strength only slightly.

Method II, which was used for joining Al-359/SiC composite, consisted of low pressure TLP diffusion bonding followed by isostatic pressing in air. The highest bond strength for the Al-359/SiC bonds, using a 7 μm thickness copper interlayer, was 242 MPa which is 92% of the shear strength of parent material. This value is the highest bond strength for any aluminium-based composite that has been reported to date.

The results of preliminary bonding trials using method III, low pressure TLP diffusion bonding followed by hipping without encapsulation, are very promising. The highest bond strength for un-reinforced Al-6082 (Al-Mg-Si alloy) achieved was 200 MPa (89% of the shear strength of parent material). This technique can be used to fabricate intricate components with minimal deformation. In contrast to conventional "HIP bonding", the liquid formed in the first stage of method III can seal the bond and so the complexity associated with encapsulation is avoided. However, there was some evidence of gas leakage into the composite bonds made using method III, showing that sealing was not complete and that possibly a thicker interlayer should have been used to ensure sufficient melting. Further investigations are in progress.

The aluminium-lithium alloy (UL-40) showed quite different bonding characteristics, probably because of the high percentage of lithium (4 wt.%) which forms a very stable surface layer. Copper interlayers with different thicknesses were tried and the maximum bond strength achieved, using method I and an interlayer of 12.5 μm thickness, was 155 MPa (65% of the shear strength of parent material). Further improvement in bond strength requires a comprehensive investigation into the nature of the interfacial reactions during TLP diffusion bonding of this alloy.

The shear test results and examination of the microstructures showed that the thickness of the interlayer has a key role in TLP diffusion bonding of Al-MMCs. Low bond strengths resulted from the use of a 1 μm thickness copper interlayer. On the other hand, the use of a thick interlayer (e.g. 12.5 μm) caused unfavourable agglomeration of the reinforcement particles about the bond line. Thicknesses of between 3 and 7 μm resulted in excellent strengths but the thickness of the interlayer should be optimised for each alloy.

Chapter 5

5. Method IV: Temperature gradient TLP diffusion bonding

5.1 Introduction

Transient liquid phase (TLP) diffusion bonding is a promising method for joining materials with stable oxide films. The presence of a liquid phase between two faying surfaces can accelerate the joining process by disrupting any oxide and increasing the diffusion rate at the interface. However, during isothermal solidification in TLP diffusion bonding, the insoluble oxide particles and impurities, trapped within the liquid phase, are pushed forward by the advancing solid/liquid boundaries. Eventually, these particles agglomerate at the bond line and so can prevent metal-to-metal contact from being fully established.

Accordingly, regardless of the type of diffusion bonding process, whether solid-state or TLP, the bond lines are more or less planar and generally include impurities and discontinuities which inhibit the formation of an ideal metallic bond. Therefore, the strengths of such joints are expected to be somewhat less than the strengths of the corresponding parent materials. In addition, the random distribution of oxide particles at normally flat interfaces causes a wide scatter in the strengths of the bonds. In this chapter a new TLP diffusion bonding method is described. This new method produces joints with non-planar bond lines so leading to excellent reliability and shear strengths as high as those of the parent material.

5.2 Theoretical aspects of temperature gradient TLP diffusion bonding

Geologists have been studying the concept of frozen sea waters for many decades. *Whitman (1926)* investigated certain characteristics of salt-water ice, including the elimination of salt from floating sea ice during the warm season which had been reported by Arctic travellers. He showed that liquid droplets of brine, entrapped in sea ice, migrate from the colder part of the ice to the hotter part, provided the temperature of the ice is not below the eutectic temperature. It was concluded that the salt diffuses out of the ice as brine droplets due to the temperature gradient.

Three decades later, *Pfann (1955)* produced *p-n* semiconductive junctions by moving a thin layer of molten Al-Si alloy through crystals of silicon and germanium, under a temperature gradient. This process, called temperature gradient zone melting (TGZM), includes a molten zone travelling up from the bottom to the top surface of a crystal, where it solidifies by decreasing the temperature below the eutectic temperature. *Pfann* also showed that imposing a temperature gradient during conventional zone refining (i.e. when a local hot zone is moved along a bar) can be of benefit by increasing the travel rate without increasing the concentration variation.

Conventional TLP diffusion bonding relies on the formation of a liquid phase at the bond line during an isothermal bonding cycle, as a result of interdiffusion between an interlayer and the base material. In contrast to *Pfann's* method for producing *p-n* junctions, this liquid phase eventually solidifies at constant temperature as a consequence of continued diffusion of solute from the liquid phase into the adjacent solid phase. Accordingly, the kinetics of a TLP process would, at first sight, appear to depend mostly on the overall diffusivity of the solute in the solid parent material from the liquid phase. Until now, this has been the generally accepted explanation for TLP diffusion bonding. Thus, if the diffusion coefficient in the solid is assumed to be zero, the solidification stage theoretically would never occur because the solid/liquid

boundaries would be locked due to a lack of diffusion in both the liquid (once homogenisation has been achieved) and also the solid phase.

However, during isothermal solidification in TLP diffusion bonding, it should be possible to build up a composition gradient across the liquid phase by simply imposing a temperature gradient, ΔT, across the reaction zone, see figure 5-1.

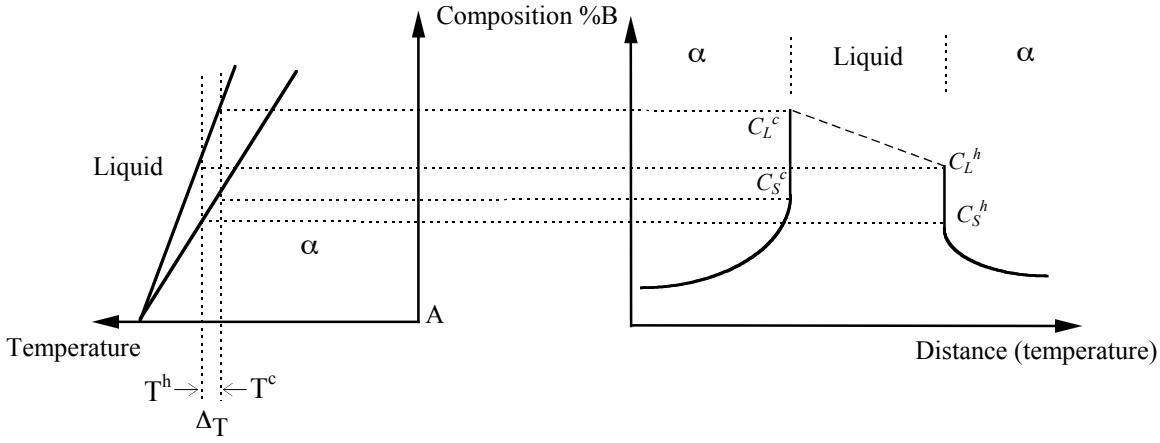

Fig. 5-1: Graphical representation of the composition profile within a transient liquid phase when a temperature gradient is imposed across the reaction zone.

Having established a composition gradient within the liquid, the liquid phase can act as a rapid diffusion path for the solute (B atoms) to migrate from the left-hand interface, with higher equilibrium solute concentration (lower temperature T^c), toward the right-hand interface, with a lower equilibrium solute concentration (higher temperature T^h). A consequence of this solute diffusion is that the concentration of the solute in the left-hand interface becomes less and so its equilibrium solidification temperature rises above the isothermal bonding temperature. Hence, as solute diffuses into the liquid, solidification occurs at the left interface which accordingly advances to the right leaving a solid with a composition of C_S. At the same time, the solute concentration in the vicinity of the right interface increases and so the solid/liquid equilibrium temperature at which solid and liquid coexist decreases (as expected from the phase diagram);

consequently, melting occurs. The net result is that the right-hand interface retreats to the right with the left-hand interface following, i.e. the interfaces move from the colder side to the hotter side. As solute is included in the solid which forms at the left-hand interface, the liquid will become steadily depleted in solute so that after a finite time all the liquid will solidify.

This new method of temperature gradient TLP diffusion bonding, developed in this work, has some similarities with conventional TLP diffusion bonding and temperature gradient zone melting. However, it should be emphasised that, in this method, solidification of the liquid phase occurs isothermally (in contrast to temperature gradient zone melting) and, meantime, unlike conventional TLP diffusion bonding, the isothermal solidification does not require diffusion of solute in the solid phase. An important result from this new approach is that bonding times are likely to be considerably shorter than those predicted using models which are based on solid-state diffusion. An additional feature of imposing a temperature gradient during TLP diffusion bonding is to produce a non-planar bond line, rather purifying the base material or introducing solute atoms, as in zone refining. Accordingly, a new experimental set-up and analytical model had to be developed in this work.

5.3 Numerical simulation of temperature gradient TLP diffusion bonding

To date, only a few models of the kinetics of a moving boundary in transient liquid phase processes have been proposed (see section 2.2). Using these analytical and numerical models, a long completion time for isothermal solidification is predicted. In the most recent work by *Zhou et. al. (1995)*, the completion time for the diffusion bonding of a nickel single crystal, using a Ni-19 at.% P interlayer, has been reported to be 36 hours when bonding at a temperature of 1150°C. In polycrystalline materials, relatively fast solute diffusion through the grain boundaries expedites the process and consequently the bonding times are expected to be much shorter, e.g. about 20 hours when bonding a nickel polycrystal under the same conditions as above. Nevertheless, these are very long bonding times.

A simple mass balance calculation proves that completion of the TLP process under a temperature gradient is possible even if the diffusivity of the solute in the solid phase is assumed to be nil. This represents a condition for which existing conventional models of TLP diffusion bonding would suggest that bonding could not be achieved. To verify this idea, an explicit finite difference analysis of the new method, using *Fick's* diffusion equations and Mathematica software, was carried out in the current work. The first and second derivatives of the concentration profiles, near to the moving boundaries, were approximated by employing *Crank's (1975 & 1984)* approach (see the appendix at the end of this chapter). Assuming a temperature gradient across the liquid phase domain and zero diffusivity in the solid phase, the new method was simulated. The graphical results of the modelling, where isothermal solidification has started to occur at the left hand interface, is shown in figure 5-2. The solid phase has a composition of C_s^c which decreases as the interface moves further to the right.

In a similar simulation in which the temperature gradient was omitted, the solid/liquid boundaries were stationary. An analytical solution for the new method is given in Chapter 6.

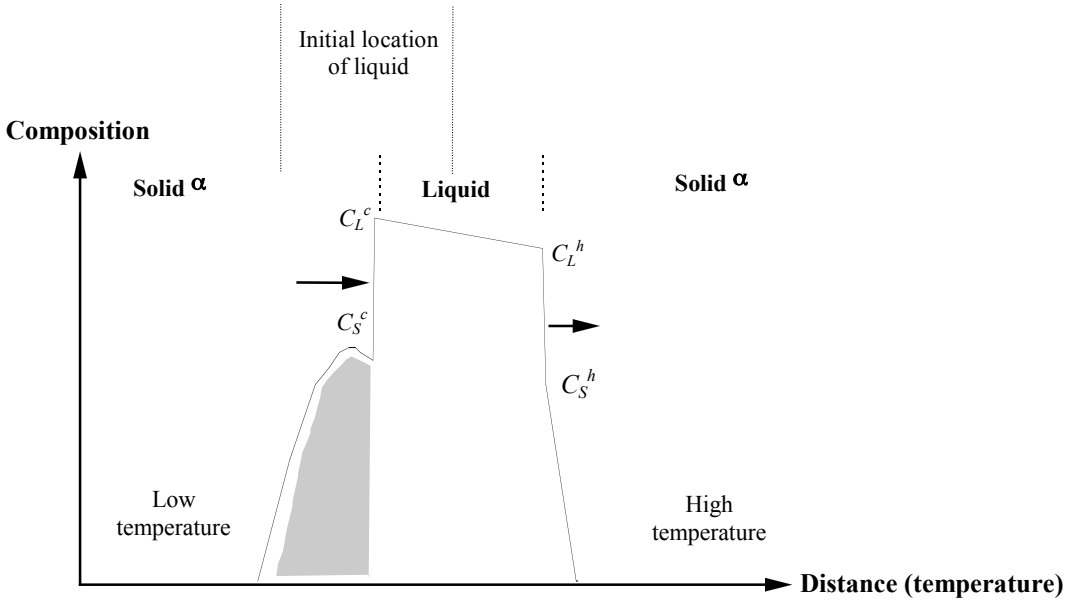

Fig. 5-2: The graphical result of a finite difference model shows that solidification occurs at the left-hand interface in a TLP process with zero diffusivity in the solid. Arrows show the direction of movement of the solid/liquid interfaces.

5.4 Results and discussion

To study the effect of a temperature gradient on the microstructures and strengths of the bonds, more than 10 different set-ups were designed and up to 150 bonding trials were carried out. In addition to the effects of bonding temperature and magnitude of temperature gradient, the effects of bonding pressure, bonding time were also studied in order to optimise the bonding conditions. Most of the samples were evaluated by metallographic examination, and then a few bonds, with appropriate microstructures, were shear tested. A summary of the results is presented below.

5.4.1 Microstructure examination

The magnitude of the temperature gradient has a significant effect on the resulting microstructure of the bond line. The higher the temperature gradient, the more the interface departs from being planar, which is the normal form of the interface when conventional TLP diffusion bonding is carried out. Having designed and optimised the heat sink, the magnitude of temperature gradient was varied by changing the temperature of the lower piece (see figure 3-5) from 540 to 560 °C (assuming that the temperature of the upper piece, in contact with the heat sink, remained reasonably constant). Bond lines with various geometries were produced by TLP diffusion bonding aluminium alloys using copper interlayers and different temperature gradients in the range of ~20 to ~70 °C/cm. Figure 5-3 shows schematically the relationship between the magnitude of the temperature gradient and the resulting bond line morphology. Imposing a minor temperature gradient changes the planar interface into a sinusoidal structure. A further increase in the temperature gradient leads to cellular and eventually fully dendritic growth across the bond line.

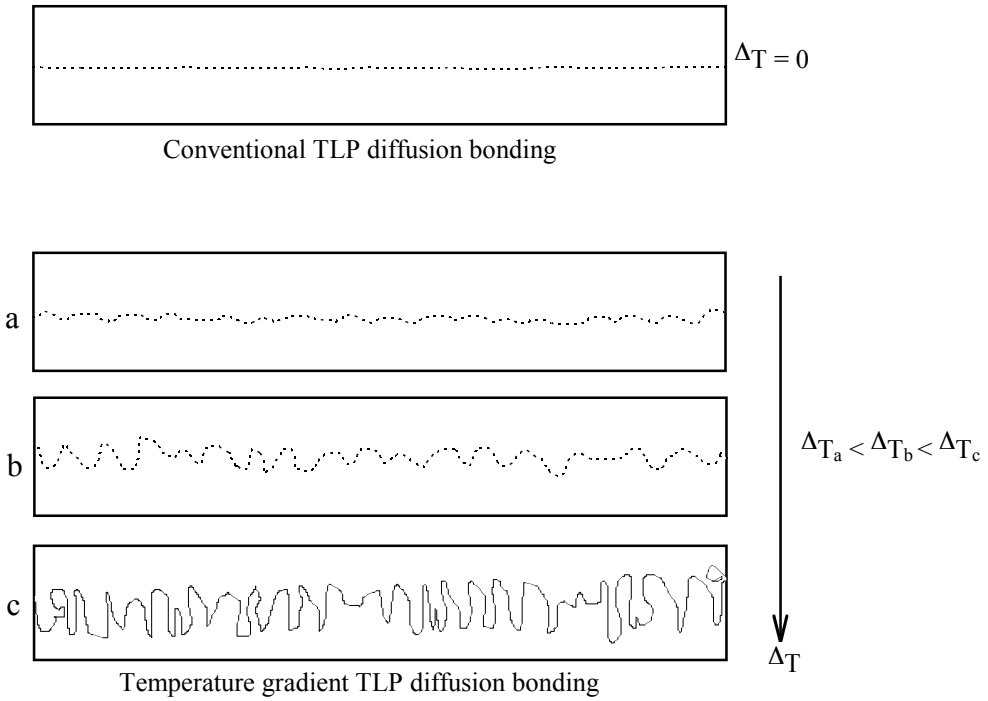

Fig. 5-3: Effect of imposed temperature gradient ΔT on the bond line microstructure in TLP diffusion bonding: a) sinusoidal, b) cellular and c) dendritic structures compared with the planar bond line of a conventional TLP diffusion bond.

Cross sections of actual bonds in Al-6082 made using different temperature gradients are shown in figure 5-4. Formation of the dendritic structure (obtained using a high temperature gradient) was always associated with void formation between the dendrites.

Using the new method, the Al-359/SiC composite was bonded to the Al-6082 alloy to produce a dissimilar joint. The interfaces in temperature gradient TLP diffusion bonding move from the cold side towards the hot side, so the alloy was inserted into the induction coil while the composite was outside the coil and in touch with the heat sink. This geometry was chosen in order to enhance the penetration of the reinforcement particles (SiC) into the alloy matrix. The bond line microstructure of a dissimilar bond, made using the new method and a 7 μm copper interlayer, is shown in figure 5-5. The formation of a sinusoidal interface resulted in impingement of the SiC reinforcement into the Al-6082 alloy matrix, and this is expected to increase the shear strength of the joint up to the shear strength of the parent alloy (see below).

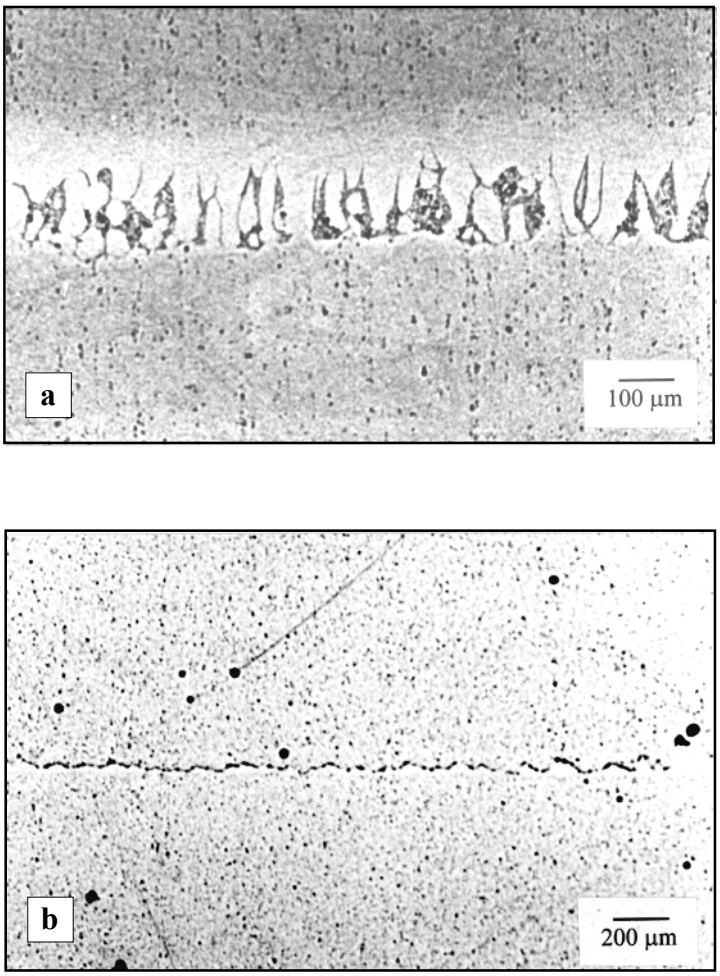

a) high temperature gradient and formation of dendritic structure;
b) low temperature gradient and formation of sinusoidal bond line.

Fig. 5-4: Optical micrographs from cross section of Al-6082 bonds.

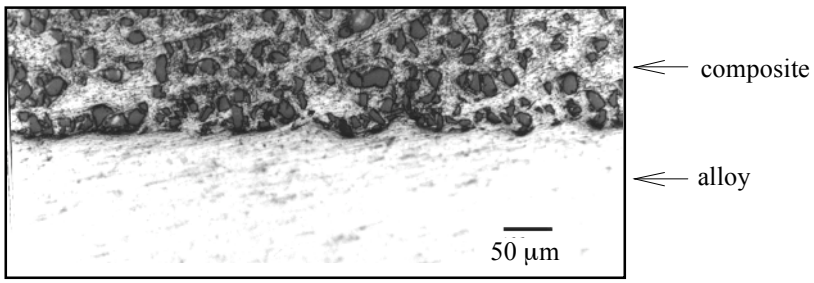

Fig. 5-5: Cross section of dissimilar joint of Al-6082 alloy and Al-359/SiC composite, made using 7 µm copper interlayer under a temperature gradient.

As mentioned before in Chapter 4, the interfacial reaction between the copper interlayer and the UL-40 using TLP diffusion bonding was found to be very different from that of other aluminium alloys. This is attributed to the presence of a stable lithium-rich oxide and/or hydroxide on the surface, which keeps the stable surface layer intact. Consequently, a planar and fairly thick bond line forms when TLP diffusion bonding this alloy, see figure 4-10. Therefore it was of interest to use the new method to investigate whether it would break up the normally continuous bond line of this alloy. A few experiments have been carried out so far and the results are very promising. Imposing a temperature gradient has a dramatic effect on the microstructure of the UL-40 bond line, showing that the stable interface is disrupted, see figure 5-6. Although no assessment of mechanical properties has been carried out on the UL-40 bonds, it is expected that the use of the new method may lead to higher bond strengths than the previous reported values.

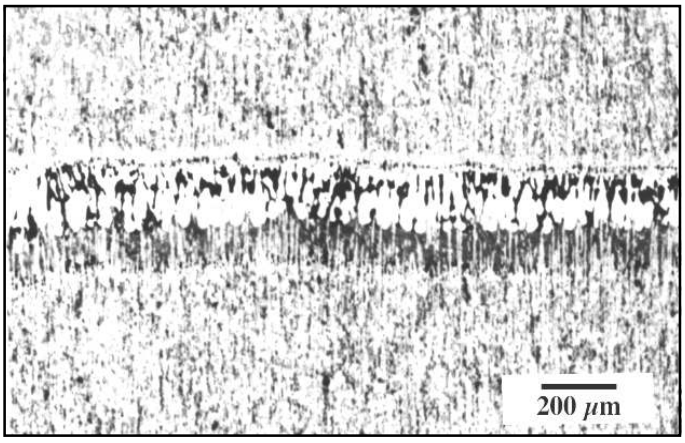

Fig. 5-6: Cross section of a UL-40 bond made under temperature gradient using a 12 μm copper interlayer (method IV).

5.4.2 Shear test results

Metallographic observations showed that, for the particular heat sink and induction system used in this work, the temperature of the lower piece should not exceed 542±1°C when temperature gradient TLP diffusion bonding Al-6082. The use of higher temperatures led to the formation of undesirable interdendritic voids and large unbonded areas at the interface. Using a constant bonding temperature of 542°C in all experiments, the effect of bonding pressure, bonding time and interlayer thickness on bond strength was investigated. Figure 5-7 shows the results of shear tests carried out on the bonds produced using method IV and different bonding parameters. A temperature gradient between 20 to 60°C/cm was used, although the samples made using 0.5 MPa pressure were part of the preliminary attempts to optimise the bonding conditions when the temperature gradient was imposed only after the initial heating stage. The control of temperature was found to be difficult and, therefore, this method was not continued.

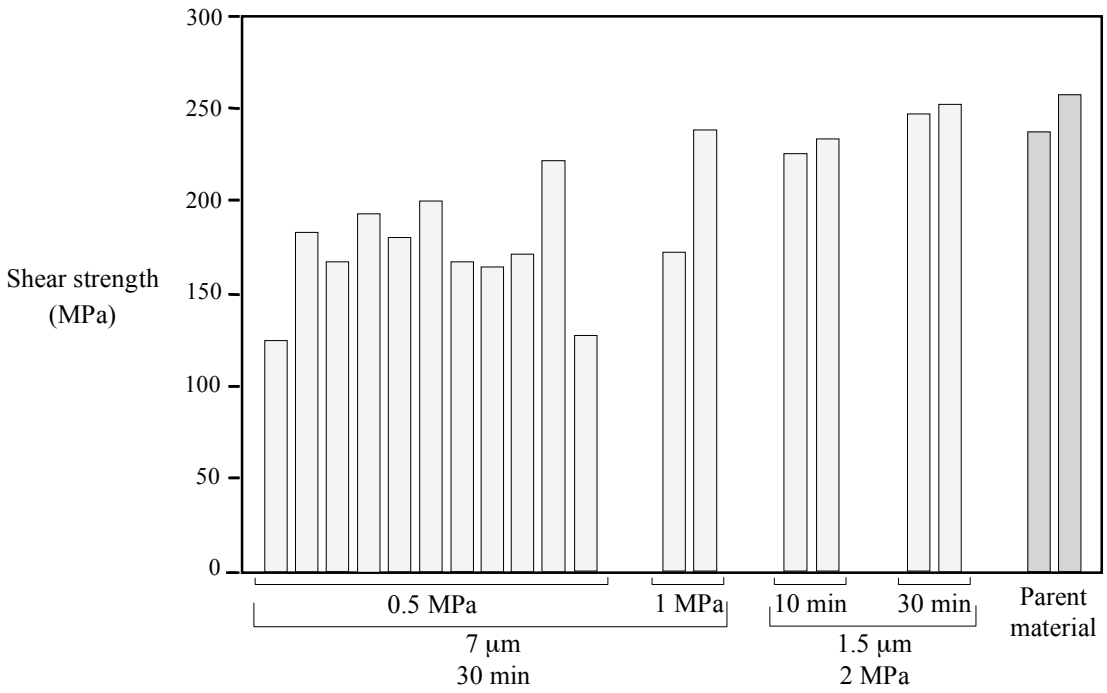

Fig. 5-7: Shear test results of Al-6082 joints produced using temperature gradient diffusion bonding (method IV) and different bonding conditions, compared with the maximum and minimum shear strengths of the parent material subjected to the same thermal cycle.

In light of the above results it can be deduced that the bonds with higher strengths and lower scatter were made when using thinner interlayers. Also, increased bonding pressure and time were beneficial in increasing bond strength.

Having optimised the magnitude of the temperature gradient (~30 °C/cm) and the interlayer thickness for the Al-Mg-Si alloy, Al-6082, samples were produced and shear tested in the fully aged condition. The results are shown in figure 5-8 in which the shear strengths of Al-6082 bonds are compared with that of the parent material subjected to the same thermal cycle. Bonds with shear strengths as good as that of the parent material can be achieved reliably when using a sputter coated copper interlayer with a thickness of 1.5 μm, and applying 1 MPa bonding pressure. Figure 5-9 shows the cross section of a sheared sample which withstood an applied shear stress of 251 MPa; the maximum and minimum shear strengths of the parent material subjected to the same thermal cycle were 237 and 252 MPa respectively.

It is assumed that the evolution of the interface from planar to a sinusoidal/cellular structure improves the bond strength due to the increased non-planar surface area of the interface. To verify this assumption, the fracture surfaces of the Al-6082 bonds, made using conventional TLP diffusion bonding and the new method, were examined by SEM. A substantial difference in the topography of the fracture surfaces due to the imposed temperature gradient was observed, and this is consistent with the optical micrographs in figure 5-4. The apparent fracture surface area has increased dramatically due to the development of a sinusoidal interface when a moderate temperature gradient is imposed during the bonding process. This effect can be clearly observed by comparing the SEM micrographs in figure 5-10. However, as mentioned before, imposing a higher temperature gradient leads to the formation of a dendritic structure, associated with unfavourable massive interfacial voids. It is obvious that where voids exist, the bond strengths would be low due to the presence of large unbonded areas between the dendrites. Therefore, accurate control of the bonding conditions is required to achieve maximum bond strength by the formation of a sinusoidal interface rather than a dendritic structure.

Only a few dissimilar bonds of Al-359/SiC and the Al-6082 were made using the new method, and shear tested. The maximum shear strength, achieved using a 3 μm copper interlayer with a bonding pressure of 1 MPa, was 202 MPa. Meanwhile, the shear strengths of the composite and the alloy, having the same heat treatment, were 233 and 206 MPa respectively. These results confirm the potential of the approach for the joining of dissimilar materials.

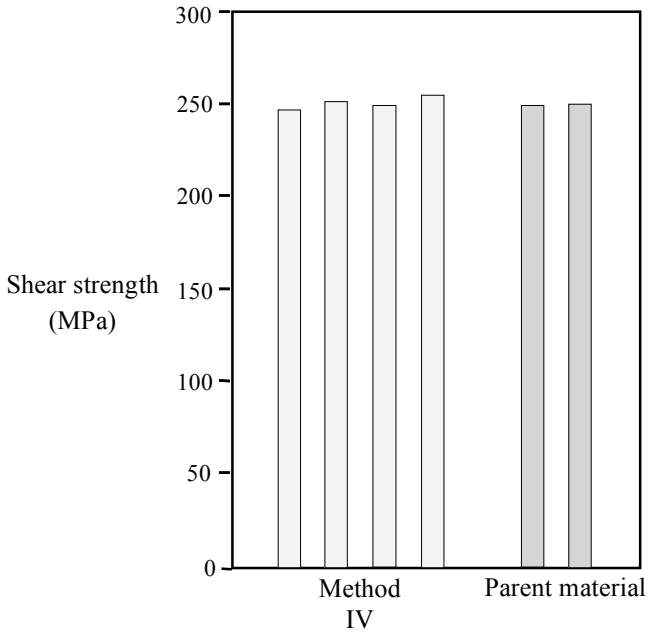

Fig. 5-8: Shear test results of the Al-6082 bonds produced using method IV, compared with the maximum and minimum shear strengths of the parent material subjected to the same thermal cycle (bonding conditions in the text).

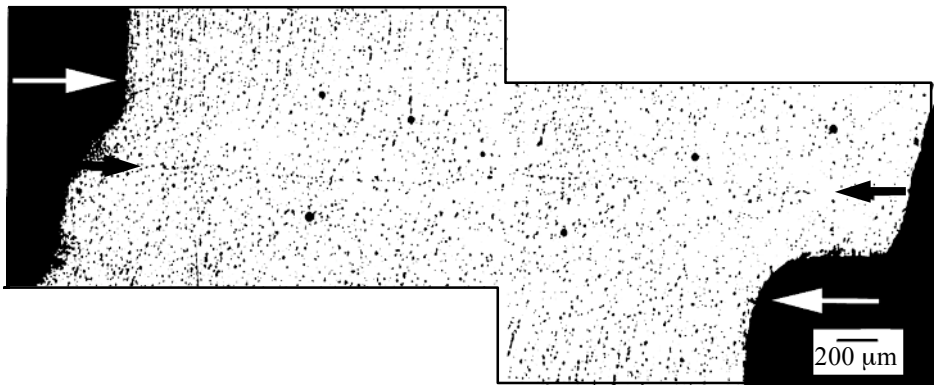

Fig. 5-9: Cross section of an Al-6082 bond with sinusoidal interface (shown by black arrows), made using a low temperature gradient, which withstood 251 MPa in a shear test. White arrows show the direction of the applied shear force and the extent of lateral plastic deformation.

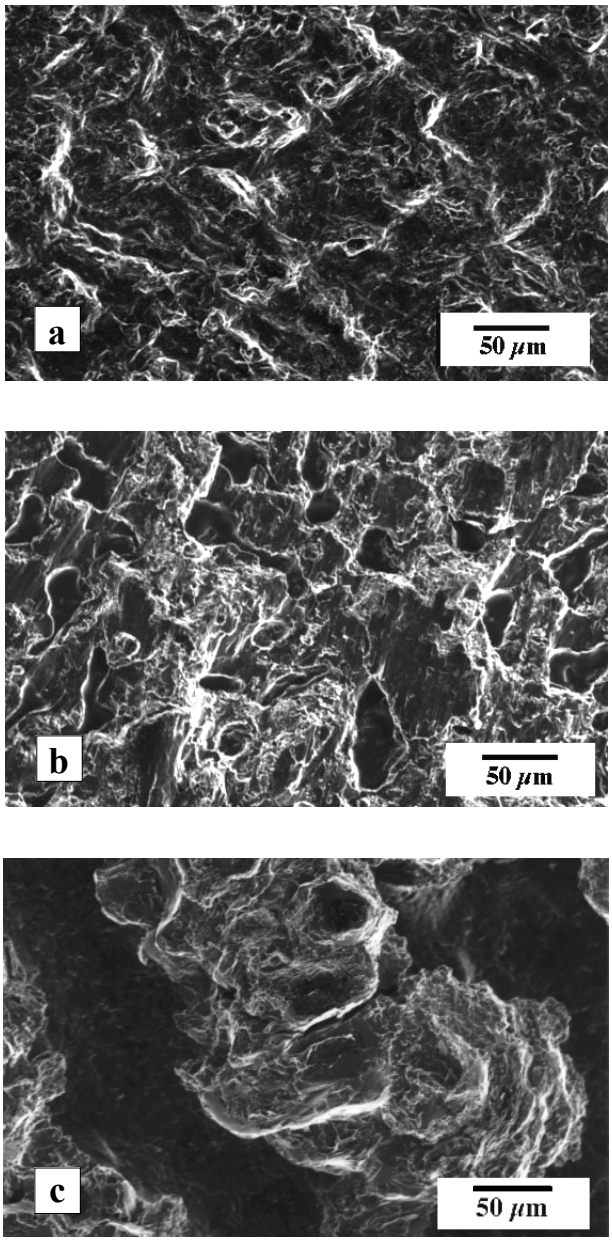

a) conventional TLP diffusion bonding (without temperature gradient);
b) moderate temperature gradient and formation of rougher fracture surface (with shear strength as high as that of parent material);
c) intensive temperature gradient and formation of interdendritic voids.

Fig. 5-10: SEM micrographs showing the effect of a temperature gradient on the topography of fracture surfaces of Al-6082 bonds.

5.4.3 Chemical analysis and hardness testing results

As explained in section 2.2, the liquid phase in conventional TLP diffusion bonding solidifies symmetrically as a result of solute diffusion from the liquid phase into the both adjacent solids. This leads to a bell shape solute distribution and consequently to a smooth change in the hardness profile across the bond region (*Bushby & Scott 1995a., Tuah-poku et al. 1988* and *Osawa 1995*). However, in temperature gradient TLP diffusion bonding, solidification occurs only at the colder solid/liquid interface at which solute is deposited as it moves towards the hotter interface. The results of chemical analysis (EDS) and microhardness tests on a dendritic bond line of Al-6082, made under a high temperature gradient, are shown in figure 5-11.

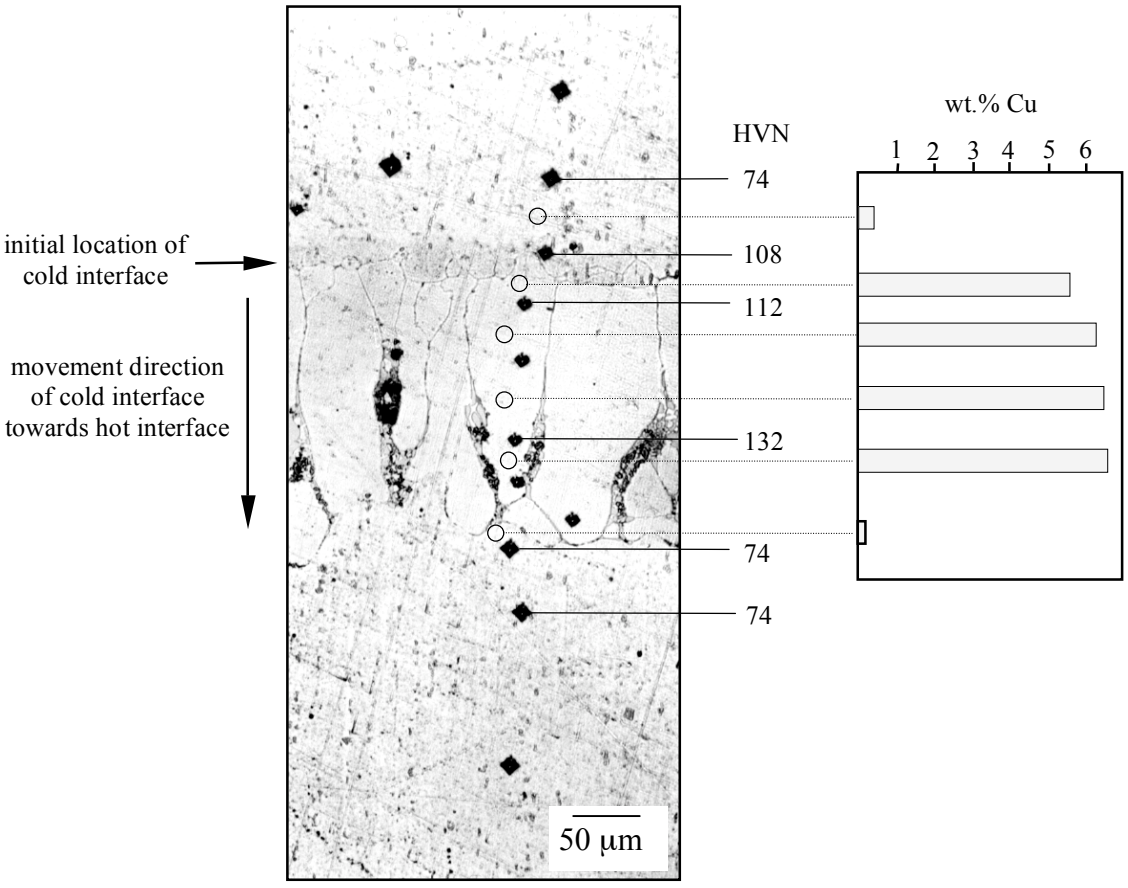

Fig. 5-11: Results of EDS chemical analysis and microhardness testing on a dendritic bond line of an Al-6082 bonds, made using method IV and copper interlayer.

There is a sharp increase in copper concentration when moving from the solid parent material (top) towards the root of the dendrite where the solidification started (i.e. the initial location of the colder interface). The concentration remains more or less constant within the dendritic structure (with an average of 6 wt.% Cu) and suddenly drops to 0.2 wt.% Cu just under the tip of the dendritic zone. Bearing in mind that the initial nominal concentration of copper is 0.1 wt.%, these results show that in this method, in contrast to conventional TLP diffusion bonding, no substantial diffusion of copper into the bulk material has occurred during the solidification stage. In addition, the microstructure shows that solidification occurred isothermally, otherwise there would have been a substantial amount of eutectic phase (Al-33 wt.% Cu) at the bond interface (see figure 6-9a which illustrates the microstructure of a bond made under non-isothermal conditions). These observations are consistent with the assumptions made in the analytical modelling of this method, see Chapter 6.

The hardness profile across the bonded region follows almost the same pattern as the copper concentration. The hardness is much higher within the solidification zone compared to the bulk of the alloy. This suggests that the presence of copper increased the hardness within the solidification zone. The variation in the hardness around the bond line decreased after a post-bond heat treatment (see figure 7-6), as would be expected from diffusion of copper into the parent material.

As mentioned before, the formation of a dendritic structure is not favourable for bonding because of the presence of interdendritic voids at the interface. However, the above analysis helps to demonstrate the nature of the bonding process. In light of the above results, it can be concluded that the solute concentration profile does not follow the same pattern associated with a conventional TLP diffusion bond. This confirms that the solidification mechanisms in these two processes are basically different (as was explained in section 5.2).

5.5 Summary

The use of temperature gradient TLP diffusion bonding, as a novel method for joining aluminium-based materials, proved successful. Using this approach, bonds with shear strengths as high as those of the parent materials were produced reliably. Also, the formation of the conventional planar bond line, which is associated particularly with materials with stable oxide layers (e.g. aluminium-based alloys), can be avoided. This is advantageous since planar bond lines generally are associated with not only relatively poor mechanical properties but also a high scatter in the results. It is assumed that the evolution of the interface from planar to a sinusoidal/cellular structure improves the bond strength because of the increased surface area of the interface. More metal-to-metal contact is established at the bond line, compared to a planar interface, and this results in high strength bonds.

The kinetics of this new method rely on the diffusion of solute in the liquid phase. Therefore, optimisation of this technique can also be used to decrease bonding times compared with those needed for conventional TLP diffusion bonding. Assuming that diffusion in the liquid phase is 10^2 to 10^4 times faster than bulk diffusion in a solid phase, then the bonding times, using this method, are anticipated to be much shorter than for conventional TLP diffusion bonding. This is examined further in Chapter 6.

Finally, it is believed that temperature gradient TLP diffusion bonding is applicable to a wide range of aluminium-based alloys and composites. It also likely to be of benefit when joining other materials and metallic alloys, particularly those with stable oxide films.

Appendix

A simple numerical simulation, using an explicit finite difference method and *Fick's* equations, was developed to analyse the method of temperature gradient TLP diffusion bonding (method IV). In this simulation, the first and second order differential equations, at the nodes close to the moving solid/liquid boundary, were estimated using *Crank's (1984 & 1975)* approximations as shown by the equations below. Figure 5-12 shows the fixed grid used in the simulation in which $p\delta x$ is the fractional distance between the grid lines and the moving boundary ($0 < p < 1$). The method was implemented in a computer program written for Mathematica software.

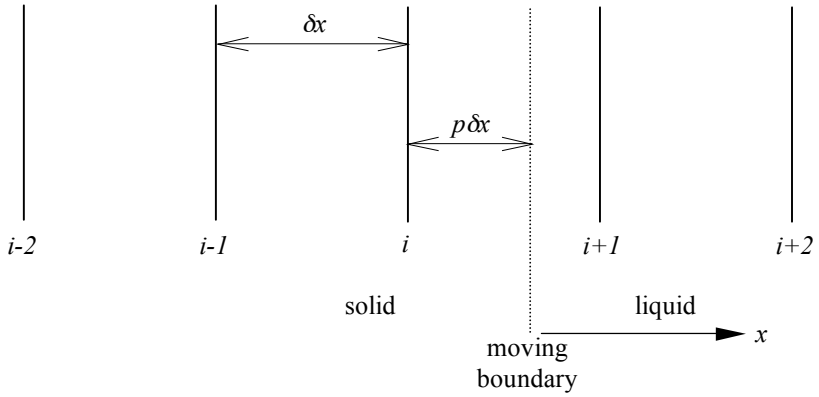

Fig. 5-12: The fixed grid used for finite difference analysis of method IV.

For the node i near the moving boundary:

$$\left.\begin{aligned}\frac{\delta^2 C_i}{\delta x^2} &= \frac{2}{(\delta x)^2}\left(\frac{C_{i-1}}{p+1} - \frac{C_i}{p} + \frac{C_{LS}}{p(p+1)}\right)\\ \frac{\delta C_i}{\delta x} &= \frac{1}{\delta x}\left(\frac{pC_{i-1}}{p+1} - \frac{(p+1)C_i}{p} + \frac{(2p+1)C_{LS}}{p(p+1)}\right)\end{aligned}\right\} \text{ for } p < 0.5$$

$$\left.\begin{aligned}\frac{\delta^2 C_i}{\delta x^2} &= \frac{2}{(\delta x)^2}\left(\frac{C_{LS}}{(1-p)(2-p)} - \frac{C_{i+1}}{1-p} + \frac{C_{i+2}}{2-p}\right)\\ \frac{\delta C_i}{\delta x} &= \frac{1}{\delta x}\left(\frac{(2p-3)C_{LS}}{(1-p)(2-p)} + \frac{(2-p)C_{i+1}}{1-p} - \frac{(1-p)C_{i+2}}{2-p}\right)\end{aligned}\right\} \text{ for } p > 0.5$$

C_{LS} is equilibrium concentration(s) of solute at solid/liquid boundary.

Chapter 6

6. Analytical modelling of temperature gradient TLP diffusion bonding (method IV)

The use of temperature gradient TLP diffusion bonding resulted in reliable bonds with shear strengths as high as those of the parent material (see section 5.4.2). An analytical solution is proposed in this chapter which is capable of predicting precise bonding times and bond line displacements when TLP diffusion bonding under a temperature gradient. Based on a mass conservation approach, a simpler solution for predicting the bond line displacement is also obtained. This latter solution is combined with the precise solution to obtain a approximate solution for predicting the bonding time.

The results of both sets of solutions are compared to each other for different bonding parameters. This comparison shows that the approximate solution is in agreement with the precise solution for a range of reasonable bonding parameters and material properties.

The bond line displacement and bonding time predicted by the model for an ideal Al-Cu binary system are compared with the results of an experiment which was carried out on pure aluminium and copper. The theoretical values predicted by the model are in agreement with the experimental results. Finally, the possible application of this model to conventional TLP diffusion bonding is discussed.

6.1 Background

Due to the following two main reasons, none of the existing previous models or numerical simulations made for either TLP diffusion bonding, *(Tuah-poku et al. 1988 and Zhou et al. 1995)* or temperature gradient zone melting, *(Pfann 1955)* can be adopted for modelling the new method of temperature gradient TLP diffusion bonding.

• Conventional TLP diffusion bonding relies on the diffusion of solute in the base material to make isothermal solidification possible. In contrast, in temperature gradient TLP diffusion bonding, diffusion within the liquid phase plays the main role in the solidification process, and diffusion in the solid phase can be ignored due to the much higher diffusion rate in the liquid phase.

• In temperature gradient zone melting, the liquid zone travels along the base material and eventually solidifies, far from its initial location, when the temperature is decreased below the eutectic temperature. The migration rate of the liquid layer and its effect on the distribution of solute have been investigated in various models *(Tiller 1963)*. However, in temperature gradient TLP diffusion bonding, solidification of the liquid is isothermal and occurs in the vicinity of the initial location of the interface. In fact, microscopical observations show that the final position of the interface is very close to its initial location.

Therefore a new approach was required to provide an analytical solution for the new method of temperature gradient TLP diffusion bonding in order to calculate bonding times and the displacements of the moving boundaries. It subsequently became evident that the new approach could be used to model conventional TLP diffusion bonding by making a small and simple assumption.

6.2 Precise analytical solution

The model proposed in this work is based on three basic assumptions.

1. All phases are in equilibrium with each other according to the corresponding equilibrium phase diagram.

2. As the diffusion rate of the solute in a solid usually is at least 100 times slower than in the liquid phase, it is reasonable to ignore the minor contribution of solid-state diffusion when considering the kinetics of the whole process.

3. As the bonding temperature and the induced temperature gradient have to be chosen to avoid melting of the base material, it can be concluded that the maximum width of the solidification zone (i.e. migration distance of the liquid zone before solidification) is much less than the distance where the temperature of the pure base material hypothetically approaches its melting point (denoted by X_m), see figure 6-2.

Figure 6-1 shows a part of a simple binary phase diagram where the liquidus and the solidus are assumed to be straight lines. The initial composition of the homogenised liquid phase at the bonding temperature is C_{L0}*.

For the sake of clarity in the mass balance approach, all terms associated with the phase diagram in which concentrations are defined as mass/volume, have been distinguished using the superscript symbol *. The use of appropriate units for concentration e.g. kg/m^3 is essential in order to achieve an exact solution when using *Fick's* diffusion laws.

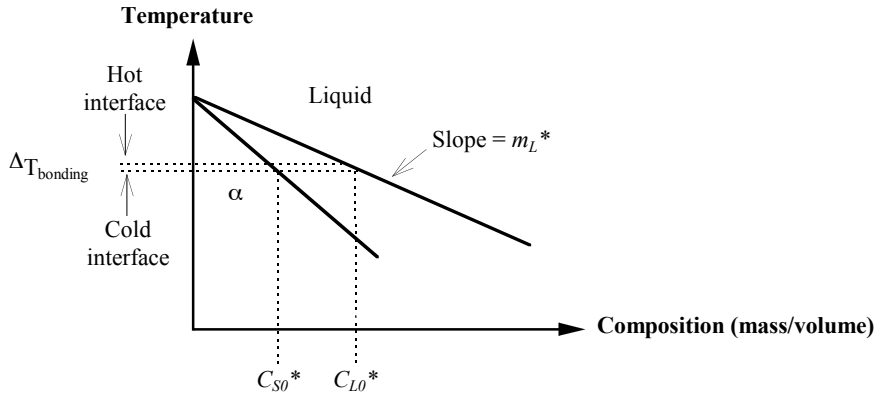

Fig. 6-1: Schematic phase diagram showing the basic parameters used in the analytical calculations.

Figure 6-2 shows the concentration profile just before the solidification stage in temperature gradient TLP diffusion bonding, and is consistent with the binary system shown in figure 6-1 when a temperature gradient of G (°C/metre) is imposed across the bond zone. The maximum width of the liquid zone depends on the composition and the thickness of the interlayer, the heating rate and the bonding pressure.

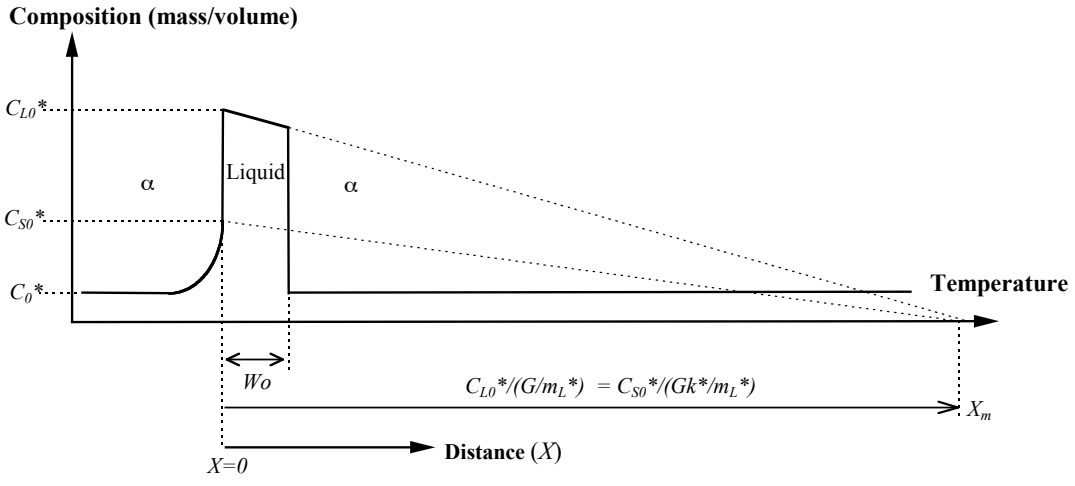

Fig. 6-2: Concentration profile at the beginning of solidification stage in a TLP diffusion bonding with a temperature gradient G across the interface.

The effect of bonding pressure on the width of the liquid phase has been ignored in previous work. As would be expected, experimental observations show that the higher the bonding pressure the narrower the liquid zone. The proposed calculation based on the initial thickness of the interlayer can provide a rough estimate of the width W_0 of the liquid zone, which then may be corrected by a applying a suitable compensation factor for the effect of bonding pressure.

The initial locations of the cold and hot interfaces are $X=0$ and $X=W_0$, respectively. The induced temperature gradient causes a concentration gradient in the liquid phase according to the corresponding phase diagram (the concentration of the liquid in equilibrium with a solid changes with temperature as is evident from the gradient of the liquidus and solidus lines in figure 6-1). Due to this concentration gradient in the liquid phase, this phase acts as a rapid diffusion path for the solute atoms and allows them to move away from the cold interface toward the hot interface. Applying a mass balance for a small displacement dX of the cold interface, according to *Fick's* first law, leads to the following differential equation:

$$(C_L^* - C_S^*)\frac{dX}{dt} = -D\frac{dC_L^*}{dX} \tag{6-1}$$

where C_L^* and C_S^* are the equilibrium compositions of the liquid and solid adjacent to the interface, D is the diffusion coefficient of solute in the liquid phase and t is the time. Assuming a linear temperature gradient, $dT/dX=G$, across the bonding zone, then according to the phase diagram in figure 6-1, the concentration gradient within the liquid phase at equilibrium is:

$$\frac{dC_L^*}{dX} = \left(\frac{dC_L^*}{dT}\right)\left(\frac{dT}{dX}\right) = \frac{1}{m_L^*}G \tag{6-2}$$

Therefore, the concentration C_L^* at each point within the liquid phase can be expressed by a linear polynomial function of its distance X from the initial location X=0 of the cold interface:

$$C_L^* = C_{L0}^* + \left(\frac{G}{m_L^*}\right)X \tag{6-3}$$

Substitution of equation 6-3 into equation 6-1 and subsequent integration yields:

$$\left(\frac{G}{2m_L*}\right)X^2 + C_{L0}*X = -\left(\frac{DG}{(1-k*)m_L*}\right)\ t + constant \tag{6-4}$$

where $k*$ is the partition coefficient i.e. C_S^*/C_L^*. With initial conditions of $X=0$ at $t=0$, the integration constant comes out to be zero and the following equation gives the instantaneous location of the cold interface as a function of time:

$$\left(\frac{G}{2m_L*}\right)X^2 + C_{L0}*X + \left(\frac{DG}{(1-k*)m_L*}\right)\ t = 0 \tag{6-5}$$

At the same time, the increased concentration of solute in front of the hot interface lowers the melting point and the interface retreats to the left. Repeating the mass balance approach for the hot interface, a differential equation similar to equation 6-1 can be obtained:

$$(C_L* - C_0*)\frac{dX}{dt} = -D\frac{dC_L*}{dX} \tag{6-6}$$

where C_0* is the initial concentration of the solute in the base material. Substitution of equation 6-3 in equation 6-6, integrating and then applying the initial condition of $X=W_0$ at $t=0$ gives an expression for the location of the hot interface as a function of time:

$$\left(\frac{G}{2m_L*}\right)X^2 + X(C_{L0}* - C_0*) + \left(\frac{DG}{m_L*}\right)\ t - (C_{L0}* - C_0*)W_0 - \frac{GW_0^2}{2m_L*} = 0 \tag{6-7}$$

As can be seen from equations 6-5 and 6-7, the transient locations of the interfaces are independent of each other. Also, the slope of the concentration profile in the liquid phase, G/m_L*, determines the velocities of both moving boundaries for the given materials and the bonding conditions used. Solidification of the liquid phase will be terminated when the left-hand interface reaches the right-hand interface at a distance of X_b (bond line displacement) within a time duration of t_b (bonding time). Simultaneous

solving of equations 6-5 and 6-7, using Mathematica software, yields the bonding time as the following polynomial function:

$$t_b = \frac{(k^*-1)}{2DG^2k^{*2}}[W_0{}^2G^2k^* + 2C_{L0}{}^*W_0Gk^*m_L{}^* - 2C_0{}^*W_0Gk^*m_L{}^* + 2C_0{}^{*2}\ m_L{}^{*2} - 2C_{L0}{}^*C_0{}^*k^*m_L{}^{*2} - 2C_0{}^*m_L{}^*(W_0{}^2G^2k^* + 2C_{L0}{}^*W_0Gk^*m_L{}^* - 2C_0{}^*W_0Gk^*m_L{}^* + C_0{}^{*2}\ m_L{}^{*2} - 2C_{L0}{}^*C_0{}^*k^*m_L{}^{*2} + C_{L0}{}^{*2}\ k^{*2}\ m_L{}^{*2})^{\frac{1}{2}}] \quad (6\text{-}8)$$

and the final location of the interface relative to the initial position of the cold interface (i.e. bond line displacement) is:

$$X_b = \frac{(C_0{}^* - C_{L0}{}^*k^*)m_L{}^* - \left((-C_0{}^* + C_{L0}{}^*k^*)^2 m_L{}^{*2} + W_0Gk^*(W_0G + 2C_{L0}{}^*m_L{}^* - 2C_0{}^*m_L{}^*)^{\frac{1}{2}}\right)}{Gk^*} \quad (6\text{-}9)$$

It should be mentioned that equations 6-8 and 6-9 are exact solutions for the moving boundary problem in a transient liquid phase problem including a temperature gradient across the liquid zone, in which the diffusion of solute within the solid phase is assumed to be zero. As mentioned before, this is a valid assumption as the diffusion rate in a liquid is much faster than in a solid phase (i.e. about 100 times) and therefore the net effect of this assumption will not cause any significant errors in the calculations.

While the above equations provide precise determination of both the bonding time and displacement, the equations are not simple to use and so an alternative approach was sought. This is described in the next section.

6.3 Geometrical approach: conservation of mass

A geometrical approach based on the mass balance of the solute was adopted to achieve simpler formulae for bonding time and displacement. Figure 6-3 shows the concentration profiles before and after isothermal solidification where the shaded areas refer to the amount of solute involved in the joining process.

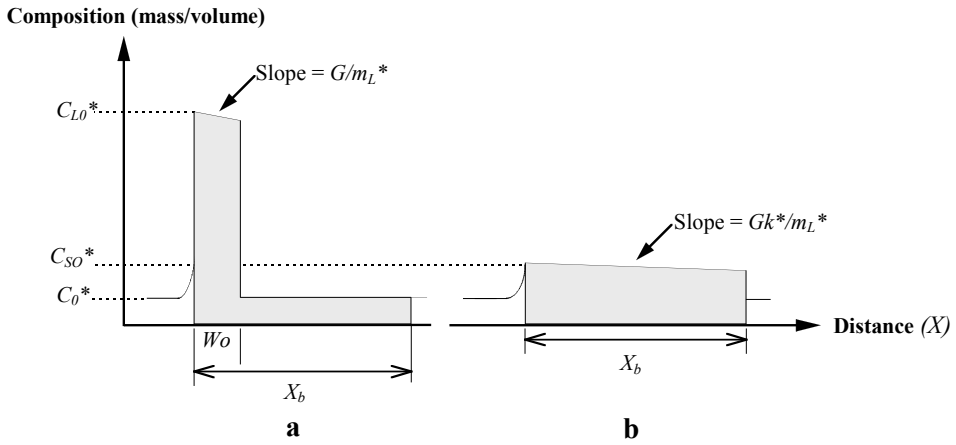

Fig. 6-3: Concentration profile just before (a) and after (b) isothermal solidification where the surface areas of the shaded zones are equal according to the mass balance of diffusing solute.

The surface areas of the shaded zones in figure 6-3 are equal . Therefore:

$$W_0\left(C_{L0}^* + \frac{W_0 G}{2m_L^*}\right) + C_0^*\left(X_b - W_0\right) = X_b\left(C_{S0}^* + \frac{X_b G k^*}{2m_L^*}\right) \tag{6-10}$$

Note that G/m_L* is negative according to figure 6-1. Rearranging equation 6-10 gives:

$$W_0\left(\frac{C_{L0}^*}{G/m_L^*} + \frac{W_0}{2}\right) + \left(\frac{C_0^*\left(X_b - W_0\right)}{G/m_L^*}\right) = X_b\, k^*\left(\frac{C_{L0}^*}{G/m_L^*} + \frac{X_b}{2}\right) \tag{6-11}$$

It should be mentioned that $C_{L0}*/(G/m_L*)$ has a physical interpretation and represents the distance X_m of the cold interface from the point where, theoretically, the melting of the pure base material occurs for a particular temperature gradient G. The geometrical interpretation of $C_{L0}^{*}/(G/m_L*)$ is also shown in figure 6-2 by the extrapolation of the dotted lines to point X_m on the right-hand side of the figure. As, in practice, the bonding temperature and the induced temperature gradient are chosen to avoid melting of the base material, it can be concluded that the maximum width of the solidification zone is much less than the distance at which the temperature of the base material hypothetically approaches its melting point (denoted by X_m). For example, typical experimental values for W_0 and X_b are 5 and 20 μm, respectively, compared with a few centimetres for X_m (see section 6.5). Thus, it is reasonable to omit $X_b/2$ and $W_0/2$ from equation 6-11 without introducing an appreciable error. Hence:

$$X_b = \frac{W_0}{k*}\left(\frac{C_{S0}* - k*C_0*}{C_{S0}* - C_0*}\right) \tag{6-12}$$

Equation 6-12 shows that the final location of the bond line is a function of the initial concentration of the liquid phase $C_{L0}*$ and the initial concentration of the solute within the base material C_0*. However, mass/volume is not an appropriate way to describe concentration when referring to phase diagrams, and equation 6-12 should be rewritten in terms of weight percentages:

$$X_b = \frac{W_0}{k}\left(\frac{\rho_L C_{S0} - \rho_S k C_0}{\rho_S (C_{S0} - C_0)}\right) \tag{6-13}$$

where C_{S0}, C_0 and k are concentration terms and the partition coefficient which correspond to a conventional phase diagram based on weight percentages. The terms, ρ_L and ρ_S are the densities of the liquid and the solid phases respectively. Equations 6-12 and 6-13 are identical given the following relationships:

$$k^* = k\frac{\rho_S}{\rho_L} \qquad (6\text{-}14)$$

$$\begin{aligned} C_{S0}^* &= C_{S0}\cdot\rho_S \\ C_0^* &= C_o\cdot\rho_S \\ C_{L0}^* &= C_L\cdot\rho_L \end{aligned} \qquad (6\text{-}15)$$

It is worth mentioning that using atomic or weight percentage (rather than mass per unit volume) as the concentration unit in the basic diffusion equations, which has been done in some of the previous analyses, can lead to major errors in the calculations unless the partial molar volumes of each constituting element in all phases, or the densities of the phases involved, are sufficiently similar. For instance, for the case in which the densities are close enough, X_b is given by:

$$X_b = \frac{W_0}{k}\left(\frac{C_{S0}-kC_0}{C_{S0}-C_0}\right) \qquad (6\text{-}16)$$

In equations 6-13 and 6-16, the width of the reaction zone X_b approaches infinity as the initial concentration C_0 reaches the equilibrium concentration of the solid phase C_{S0} in equilibrium with the liquid phase C_{L0}. This simply means that solidification in this particular case will not be terminated as the movement of the boundaries is not associated with the depletion of solute in the liquid phase. Although not exactly the same, this is very similar to zone refining in which the width of the molten region remains constant as the hot liquid zone is moved down a solid bar.

It is evident that the geometrical approach (conversation of mass) results in equations 6-13 and 6-16 which are considerably simpler than the precise analytical solution given by equation 6-9 for the bond line displacement.

6.4 Combination of analytical and mass conservation approaches

It can be shown, using numerical values, that predictions of the maximum width of the bonding zone (bond line displacement) using the mass balance approach (equation 6-12) are very close to those obtained using the precise solution (equation 6-9). Figure 6-4 shows that the values calculated for the bond line displacement, using equations 6-9 and 6-12, are in excellent agreement.

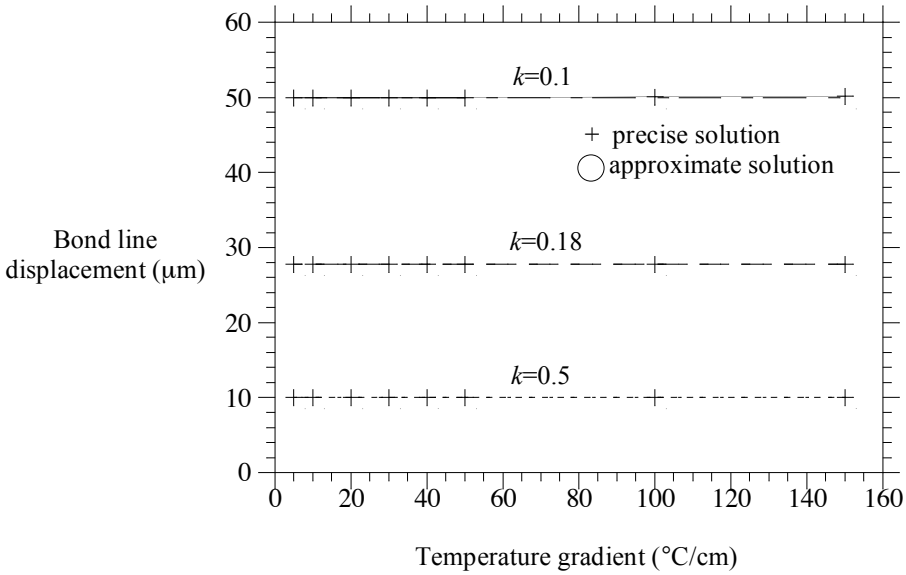

Fig. 6-4: Bond line displacement versus temperature gradient, calculated using the precise solution (equation 6-9) and the approximate solution based on the mass balance approach (equation 6-12).

Numerical values used in calculations:
$\rho_L = \rho_S$;
k = 0.1, 0.18 and 0.5;
C_{L0} = 33 wt.%;
C_0 = 0;
W_0 = 5 μm;
D = 3.26×10^{-5} cm^2/s *(Voller & Sundarraj 1993)*;
m_L = – 3.4 °C/wt.%.

As is shown in figure 6-4, the bond line displacement is independent of the magnitude of the imposed temperature gradient and, as is expected, the lower the partition coefficient k the greater the bond line displacement. However, it should be mentioned that when the partition coefficient is extremely low or high (i.e. $k<0.01$ or $k>0.99$) then the predicted values, using the precise and approximate solutions, are not equal, see figure 6-5.

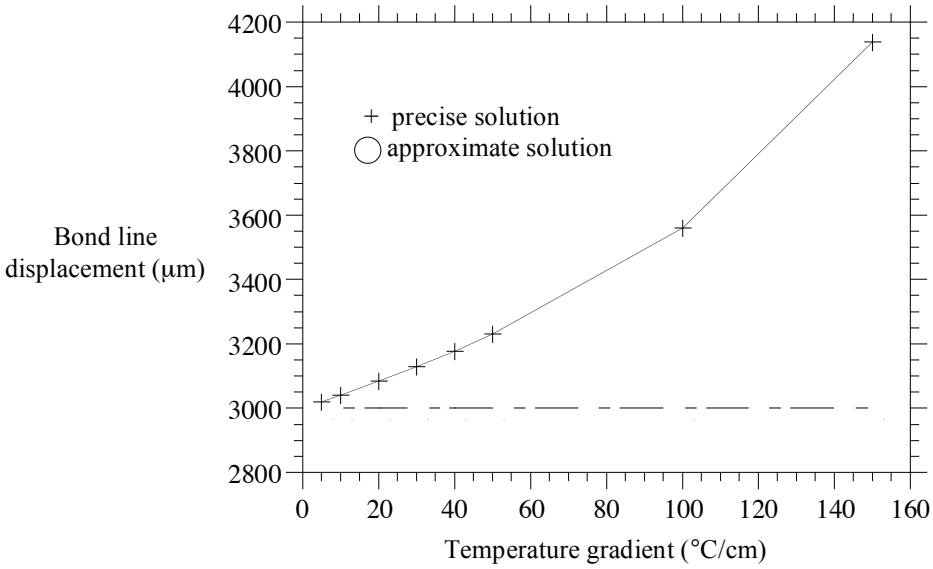

Fig. 6-5: Bond line displacement versus temperature gradient, calculated using the exact and approximate solutions for $k = 0.01$. Other parameters are as used in figure 6-4.

However, in these extreme conditions, isothermal solidification of the liquid phase would never occur and a different material would have to be used as an interlayer for TLP diffusion bonding for that particular base material. Thus, the validity of the approximate solution, in predicting bond line displacements when TLP diffusion bonding under a temperature gradient, remains intact; this justifies the assumptions made in the mass balance approach.

The results of the mass balance and precise approaches were combined and simplified to achieve a simpler equation for predicting the solidification time in TLP diffusion bonding under temperature gradient (method IV). This new approach now follows.

Substitution of X_b (bond line displacement), calculated from equation 6-12, in equation 6-5 yields the bonding time:

$$t_b = -\frac{{W_0}^2 \Omega^{*2} (1-k^*)}{2k^{*2} D} - \frac{C_{L0}^* W_0 \Omega^* (1-k^*) m_L^*}{DGk^*} \tag{6-17}$$

where Ω^* is:

$$\Omega^* = \left(\frac{C_{S0}^* - k^* C_0^*}{C_{S0}^* - C_0^*} \right) \tag{6-18}$$

Equation 6-17 can be rewritten as:

$$t_b = -\frac{W_0 (1-k^*) C_{L0}^* m_L^*}{DGk^*} \left(\frac{\Omega^*}{2k} \frac{W_0}{\frac{C_{L0}^* m_L^*}{G}} + 1 \right) \Omega^* \tag{6-19}$$

In the same way as was explained for equation 6-11, W_0 is very small compared to $C_{L0}^* m_L^*/G$ and so the left-hand term in the bracket can be omitted. This approximation is valid except when C_0^* is bigger than $0.9 C_{S0}^*$. However, in such a case, the TLP diffusion bonding of a material with such a high initial solute concentration would not be practical using that particular interlayer as isothermal solidification would never occur. Therefore equation 6-19 can be rewritten as:

$$t_b = -\frac{W_0 (1-k^*) C_{L0}^* m_L^*}{DGk^*} \left(\frac{C_{S0}^* - k^* C_0^*}{C_{S0}^* - C_0^*} \right) \tag{6-20}$$

Also, in the same way as was used when estimating X_b and using equations 6-14 and 6-15, t_b can be rewritten in terms of weight percentages:

$$t_b = -\frac{W_0 (1-k\rho_S/\rho_L) C_{L0} m_L}{DGk} \left(\frac{\rho_L C_{S0} - k\rho_S C_0}{\rho_S (C_{S0} - C_0)} \right) \tag{6-21}$$

Equation 6-21 gives the bonding time where C_{S0} , C_0 and k are concentration terms and partition coefficient corresponding to a conventional phase diagram based on weight

percentages. However, since in most cases the densities of liquid and solid phases are quite similar to each other, equation 6-21 can be further simplified:

$$t_b = -\frac{W_0(1-k)C_{L0}m_L}{DGk}\left(\frac{C_{S0}-kC_0}{C_{S0}-C_0}\right) \tag{6-22}$$

As is evident from figure 6-6, the slope of the liquidus line can be calculated in terms of ΔT_0 (freezing range of the initial liquid), k and C_{L0}. Hence:

$$m_L = -\frac{\Delta T_0 k}{C_{L0}(1-k)} \tag{6-23}$$

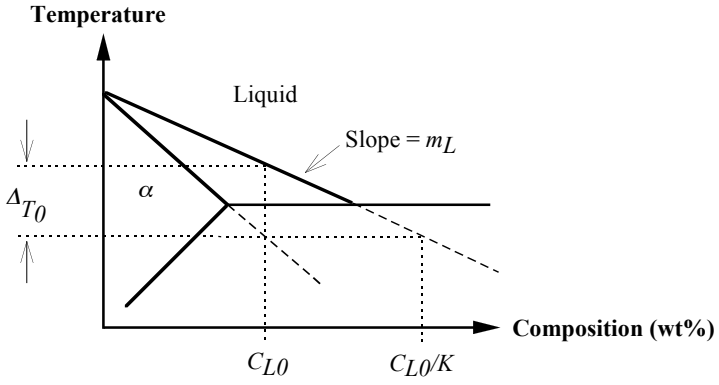

Fig. 6-6: Schematic phase diagram showing the geometrical concept of ΔT_0.

Equation 6-23 can be substituted into equation 6-22:

$$t_b = \frac{W_0\Delta T_0}{DG}\left(\frac{C_{S0}-kC_0}{C_{S0}-C_0}\right) \tag{6-24}$$

Equations 6-16 and 6-24 give the bond line displacement and bonding time when the densities of the liquid and solid phases are assumed to be similar.

Further simplification can be made for a base material with zero or low initial concentration of the solute (i.e. C_0=0). In this case, the bond line displacements and bonding times can be calculated using the following simple equations, which are the main equations which can be used to make predictions:

$$X_b = \frac{W_0}{k} \tag{6-25}$$

$$t_b = \frac{W_0 \Delta T_0}{DG} \tag{6-26}$$

The bonding times versus temperature gradient, predicted using equation 6-26 and equation 6-8 (precise solution), are shown in figure 6-7 for three different values of the partition coefficient *k*.

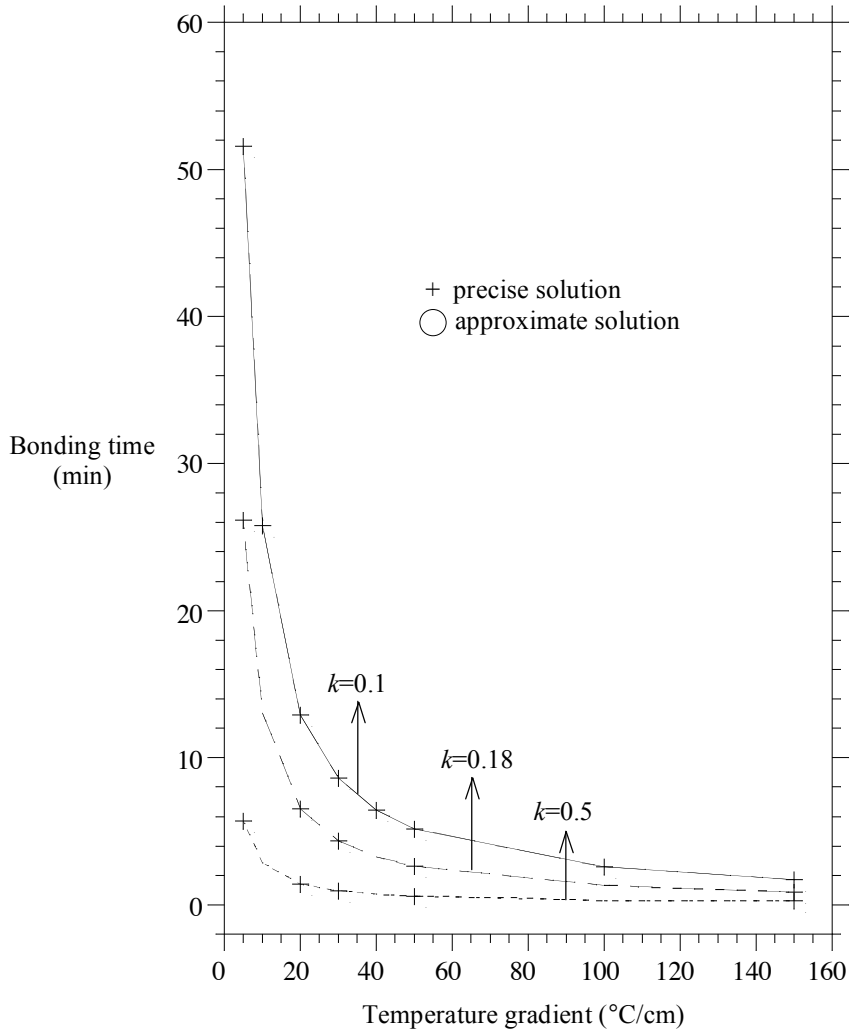

Fig. 6-7: Bonding time in TLP diffusion bonding under temperature gradient, calculated using the precise and approximate solutions (see figure 6-4 for numerical values used in the calculations).

Summary

Using figures 6-4 and 6-7, several points are immediately obvious:

• As the bonding temperature is normally chosen to be as close as possible to the lowest melting temperature to avoid the disadvantages associated with a high temperature process, the bonding time for a particular base material and interlayer can only be varied by changing the induced temperature gradient, G. This means that the higher the temperature gradient, the shorter the bonding time.

• As in conventional TLP diffusion bonding, the solidification time decreases as the partition coefficient increases. However, increasing the magnitude of the temperature gradient reduces the influence of the partition coefficient on the bonding time. The bonding times, for binary systems with different partition coefficients, become shorter and approach each other as the temperature gradient increases.

• The approach proposed in this work may also be applicable to conventional TLP diffusion bonding when, nominally, a temperature gradient is not imposed. The presence of even a very small temperature gradient across the interface will accelerate the isothermal solidification substantially. This is a new approach for modelling conventional TLP diffusion bonding and it may explain the existing inconsistency between predictions from previous models and experimental results.

• The displacement of the interface is merely a function of the initial width of the liquid phase and the partition coefficient. Both the interface displacement and the bonding time are linear functions of the initial width of the liquid phase.

The displacements of the interface and the bonding times in an Al-Cu binary system, for various widths of the liquid phase, were calculated and results are shown in figure 6-8. The effect of the magnitude of the temperature gradient on bonding time for this binary system is shown in figure 6-7 (i.e. $k = 0.18$). The calculated values have been used for experimental verification of the proposed modelling, as is described in the next section.

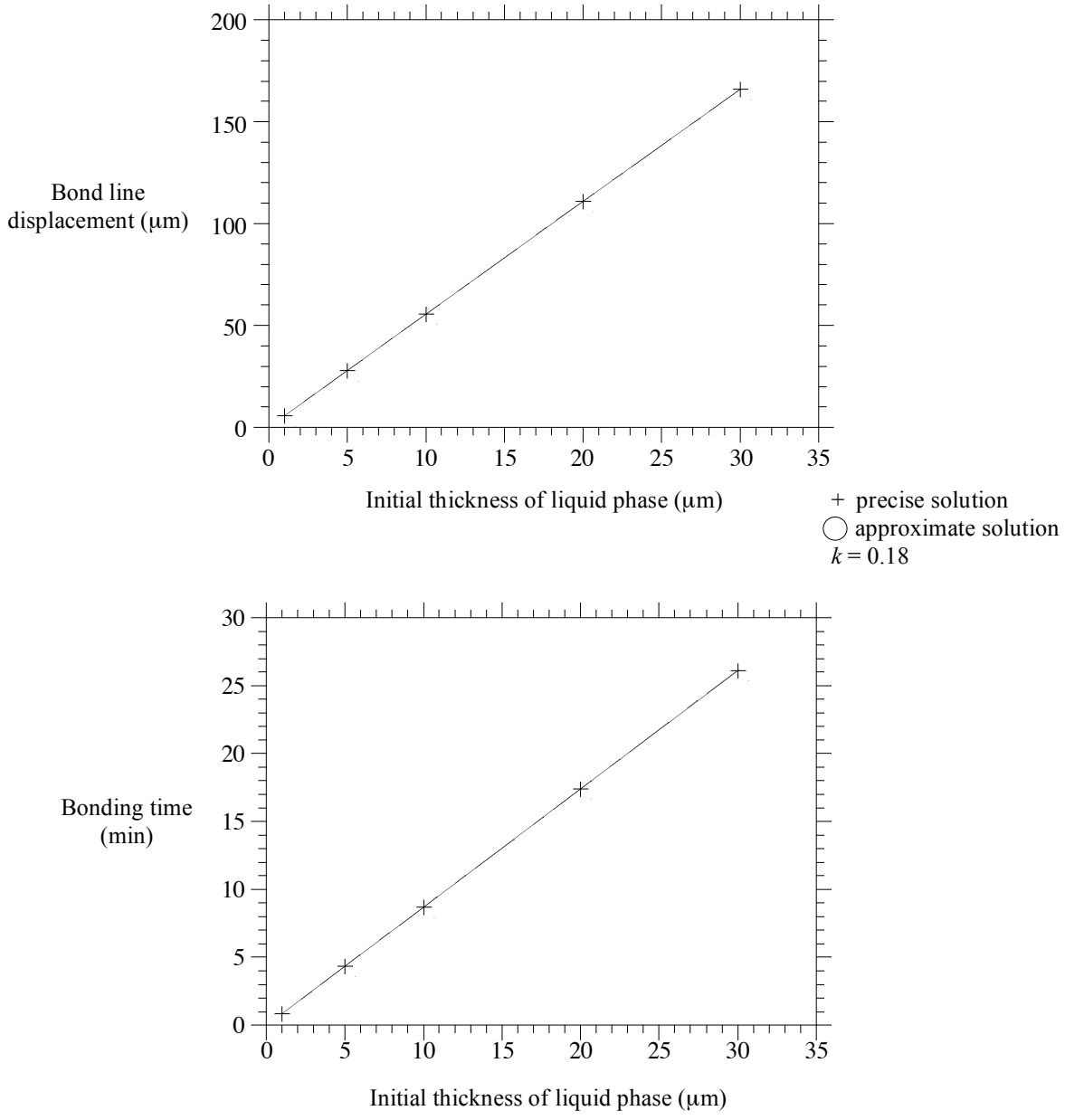

Fig. 6-8: Interface displacement and bonding time versus the initial width of eutectic phase in Al-Cu binary system; calculated using the model proposed for TLP diffusion bonding, under a temperature gradient of 30°C/cm. The other parameters are the same as those in figure 6-4.

6.5 Experimental verification of modelling

In order to verify the proposed analytical model for temperature gradient TLP diffusion bonding, preliminary experiments on bonding pure aluminium, using copper interlayers, have been carried out. The maximum width of the Al-Cu eutectic phase W_0, calculated from the phase diagram and relative densities, can be up to about 7 times thicker than the interlayer. Although TLP diffusion bonding is considered to be a low pressure bonding method, a preliminary investigation in the current work showed that the bond strength decreases drastically when the bonding pressure is below a certain amount, probably as a consequence of poor surface contact. Hence, the use of a minimal applied bonding pressure is essential in order to achieve high bond strengths. On the other hand, the bonding pressure has a drastic effect on the actual width of the liquid zone, reducing the width considerably, and this has not been allowed for in previous studies of TLP diffusion bonding.

The actual width of the liquid layer in a conventional TLP diffusion bonding was measured experimentally and then this result was substituted in equation 6-25 to calculate the displacement of the bond line in a bond made using the new method. Finally, the calculated displacement was compared with that measured experimentally. The accuracy of the model in predicting the bond time is also evaluated.

6.5.1 Experimental procedure and results

Even when using constant pressure loading equipment, the bonding pressure drops suddenly in the course of bonding when melting occurs, and it takes a few seconds for the loading system to return the pressure to its set value. This pressure variation on liquid formation was used to measure the width of the liquid eutectic phase when bonding pure aluminium using a 12.5 μm thick copper interlayer. By turning off the heating system as soon as the pressure drop commenced, it was possible to freeze the liquid phase before it could be squeezed out by subsequent restoration of the pressure.

In another experiment, the heating system was turned off just after the pressure returned to its set value. In the both cases, the solidification stage was aborted by cooling the samples.

Figure 6-9a shows the width of the Al-Cu eutectic phase (together with composition analysed by EDS) just after melting and for which no evidence of liquid leakage was observed. In comparison, figure 6-9b shows the width of the liquid phase in a sample with a few seconds longer heating time compared to the previous one. In this latter case, a massive portion of the liquid was expelled due to restoration of the applied pressure. The average thicknesses of the liquid phase were estimated to be 60 and 5 μm respectively.

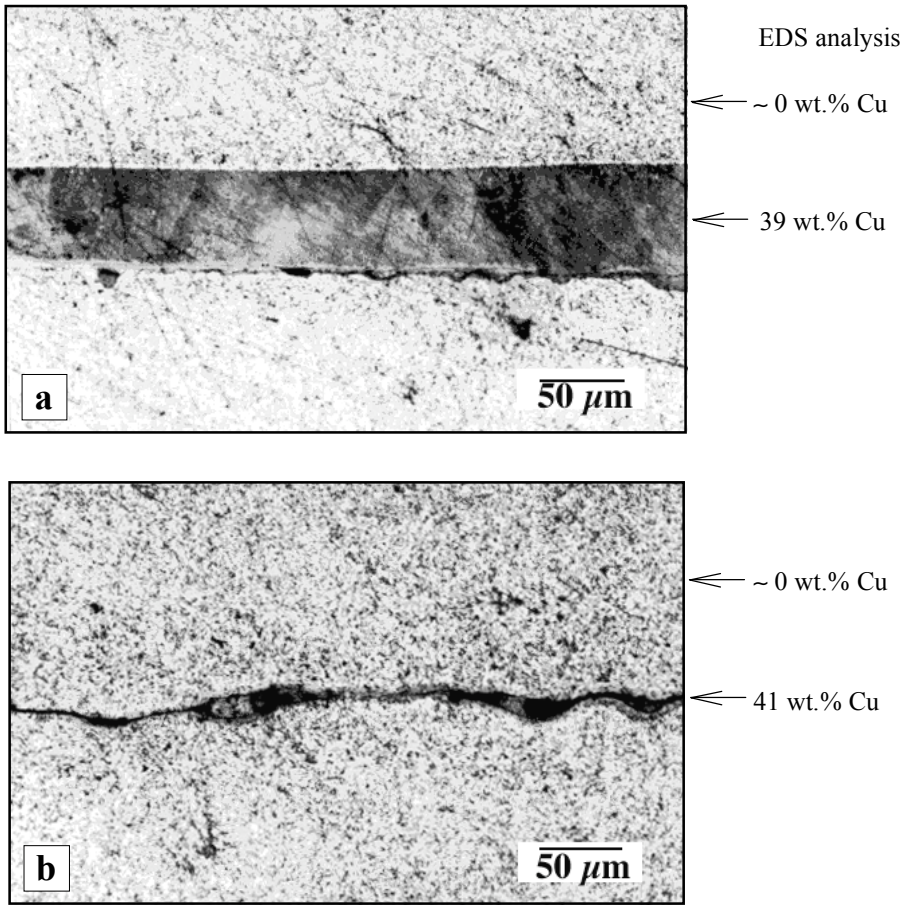

a) formation of a wide band of eutectic phase at the interface when the bonding process was aborted before expulsion of the liquid phase from the interface;

b) width of eutectic phase after expulsion of the liquid phase.

Fig. 6-9: Effect of bonding pressure of 1 MPa on the width of eutectic phase in TLP diffusion bonding of pure aluminium, using 12.5 μm thick copper interlayer. Bonding temperature was 550°C.

Therefore, as expected, there is a significant reduction in the width of the liquid phase due to the applied bonding pressure and this should be taken into account when evaluating the results of any proposed analytical solution.

As shown in the previous section, the displacement of the bond line and bonding time in temperature gradient TLP diffusion bonding can be estimated according the following simplified equations:

$$X_b = \frac{W_0}{k}\left(\frac{C_{S0} - kC_0}{C_{S0} - C_0}\right) \tag{6-16}$$

$$t_b = -\frac{W_0(1-k)C_{L0}m_L}{DGk}\left(\frac{C_{S0} - kC_0}{C_{S0} - C_0}\right) \tag{6-22}$$

where W_0 is the width of liquid phase before the solidification stage (5 μm after expulsion of some of the liquid eutectic layer) and k is the partition coefficient, i.e. ~0.18 for Al-Cu binary alloys. The calculated values are shown in figure 6-10.

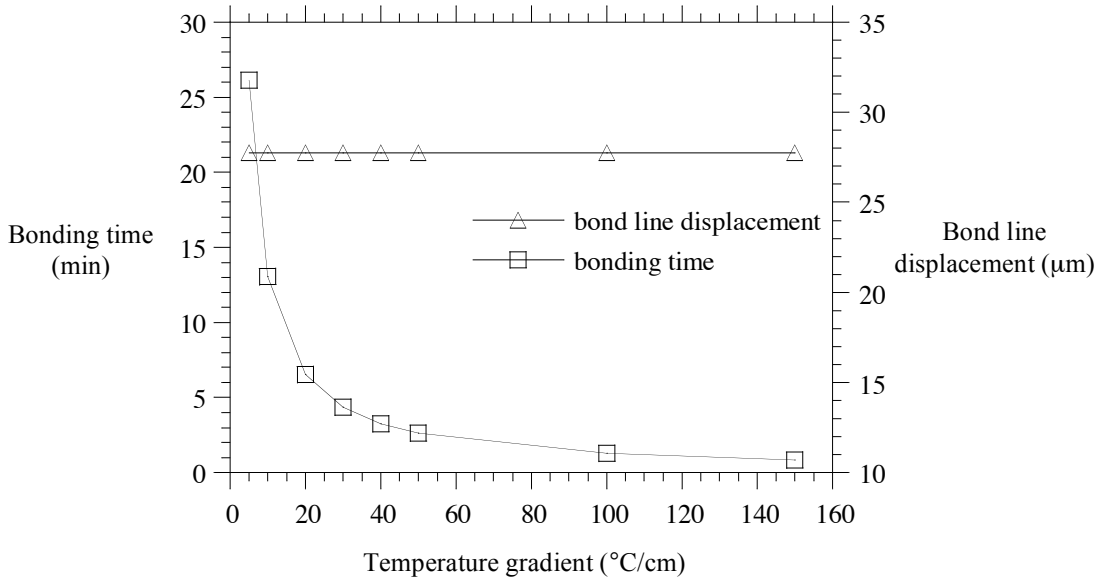

Fig. 6-10: Bond line displacement and bonding time versus temperature gradient for Al-Cu binary system at 550°C; calculated using the analytical model. Initial thickness of liquid phase was 5 μm (other parameters same as those in figure 6-4).

The displacement of the bond line when bonding pure aluminium with a copper interlayer using the above conditions is estimated to be about 27 μm (right-hand axis on figure 6-10). Figure 6-11 shows a cross section through the bond line of a bond in pure aluminium, made in 10 minutes using temperature gradient TLP diffusion bonding with the same interlayer, bonding temperature and bonding pressure as the samples in figure 6-9b. The upper piece in figure 6-11 (held at a lower temperature during bonding) has penetrated about 23 μm into the lower piece which was held at a higher temperature during bonding. This shows a 15% error between the measured (23 μm) and calculated (27 μm) values. Given the assumptions made in the model and also experimental errors, this shows good agreement between theoretical and experimental results.

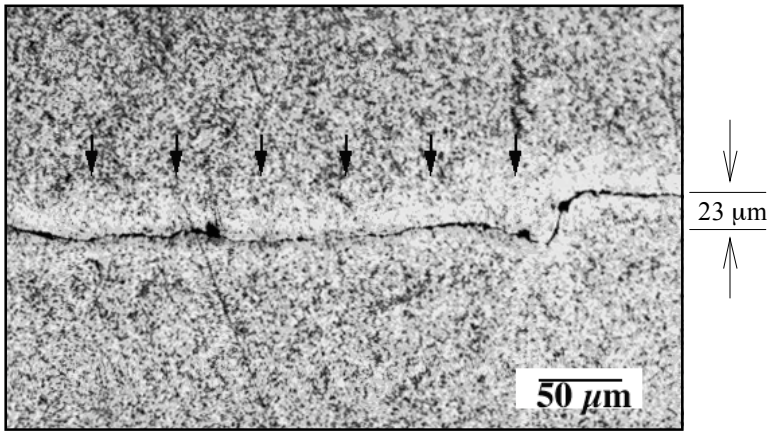

Fig. 6-11: Bond line in pure aluminium, made using temperature-gradient induced TLP diffusion bonding and a 12.5 μm copper interlayer. Arrows show the advancement of cold part (top) into the hotter part (bottom).

Accurate measurement of actual temperature gradients was found difficult. Two thermocouples were positioned as close as possible to the faying surfaces (about 2 mm below the each surface). Assuming a linear temperature gradient between the thermocouples, temperature gradients in the range of 20 to 30 °C/cm were measured.

Metallographic examination of the bonds made using a bonding time of 5 minutes or more showed that isothermal solidification was completed in all bonds as no evidence of retained eutectic phase was observed at the interfaces. This is consistent with the values predicted by the proposed model (left-hand axis on figure 6-10). Further investigations in this area will be undertaken in future work.

6.6 Summary

The analytical solution proposed for the new method of temperature gradient TLP diffusion bonding is in a good agreement with the experimental results for boundary displacement. It is evident that imposing a temperature gradient resulted in complete solidification in short bonding times; no evidence of the eutectic phase was observed when the bonding time was as short as 5 minutes. However, predicting bonding times, using the proposed method, requires accurate data regarding the actual temperature gradient across the liquid phase.

It is further believed that the model developed is applicable to conventional TLP diffusion bonding and may provide a more rigorous description of TLP diffusion bonding when, nominally, a temperature gradient is not imposed. This is because, in practice, a small difference is likely to exist between the temperatures at the two solid/liquid interfaces whenever TLP diffusion bonding is attempted. This means that bonding will take place as a consequence of the mechanism described above. This is a completely new way to describe the process and may be more consistent with the results that are achieved. Moreover, it provides a means to rigorously model TLP diffusion bonding, overcoming some of the assumptions required in previous models. Further work will be undertaken to demonstrate this.

Finally the initial experiments reported in this work showed that, as would be expected, bonding pressure has a drastic effect on the actual width of the liquid phase in TLP diffusion bonding. This has not been taken into account in previous analyses of the process.

Chapter 7

7. Methods V and VI: New methods for TLP diffusion bonding aluminium alloys in air

7.1 Introduction

Most alloys and metallic composites have stable oxide layers which can inhibit the interdiffusion of atoms across the interface when solid-state diffusion bonding. Therefore, diffusion bonding of these materials is normally conducted in vacuum in order to reduce the high temperature oxidation of the faying surfaces. Aluminium-based materials, in particular, are notoriously difficult to diffusion bond due to the presence of tenacious and chemically stable surface oxide layers.

Transient liquid phase (TLP) diffusion bonding has the potential to overcome the problem caused by the presence of stable surface oxides. However, the bonding process has to be carried out in vacuum, typically 10^{-3}-10^{-5} mbar, to prevent any increase in the thickness of surface oxide layers and also to avoid high temperature oxidation of the interlayer.

Although the new methods developed in this research are capable of reliably producing high strength bonds, the entire bonding process (when using methods I and IV) or part of it (when using methods II and III) needs to be carried out in vacuum. The necessity of conducting the joining process in vacuum requires complicated bonding equipment. Also, the overall bonding time increases substantially when a vacuum has to be established before bonding can start. As an example, the actual bonding time when using the fourth method, excluding the air evacuation stage, was about 10 minutes while

it normally takes an additional 20 minutes to evacuate the chamber down to a pressure of about 10^{-4} mbar. Thus, the overall bonding time is increased by a factor of three due to the time required to achieve a reasonable vacuum. The size of the parts to be joined is also limited by the size of the vacuum chamber. These limitations, associated with vacuum systems, become even more restrictive when conducting diffusion bonding on a commercial scale.

It can be concluded that the necessity of joining in vacuum in order to form bonds with reasonable mechanical strengths has restricted the application of TLP diffusion bonding. The initial investment, running and maintenance costs will be decreased if bonding is carried out in air.

In the research described in this chapter, two new methods for TLP diffusion bonding have been developed which are capable of producing high strength aluminium bonds in air. In contrast to most previous attempts to diffusion bond in air, the new methods do not exploit any particular surface preparation to prevent the oxidation of the faying surfaces, e.g. coating , roll-cladding etc. (see section 2.6).

In comparison to conventional TLP diffusion bonding in vacuum, the use of these new methods should drastically reduce the costs of the bonding process. There are also fewer limitations on the size of the parts to be joined in air. Therefore, a much wider range of applications for TLP diffusion bonding is anticipated.

Finally, bearing in mind that aluminium-based materials are among the most difficult materials to bond in air, the new methods are expected to be applicable to many other materials.

7.2 Method V: High heating rate TLP diffusion bonding in air

The initial attempts to carry out TLP diffusion bonding in air were similar to conventional TLP diffusion bonding except that, in addition to the main copper interlayer, an extra thin foil of copper in the form of a ring was inserted between the parts to be joined. The intention was to seal the interface by the copper ring during the bonding process. However due to a large amount of scatter in the results, and the lack of reproducibility, the tests were found inconclusive, see figure 7-1. In addition, making and positioning the copper ring was found difficult, therefore this method was not continued.

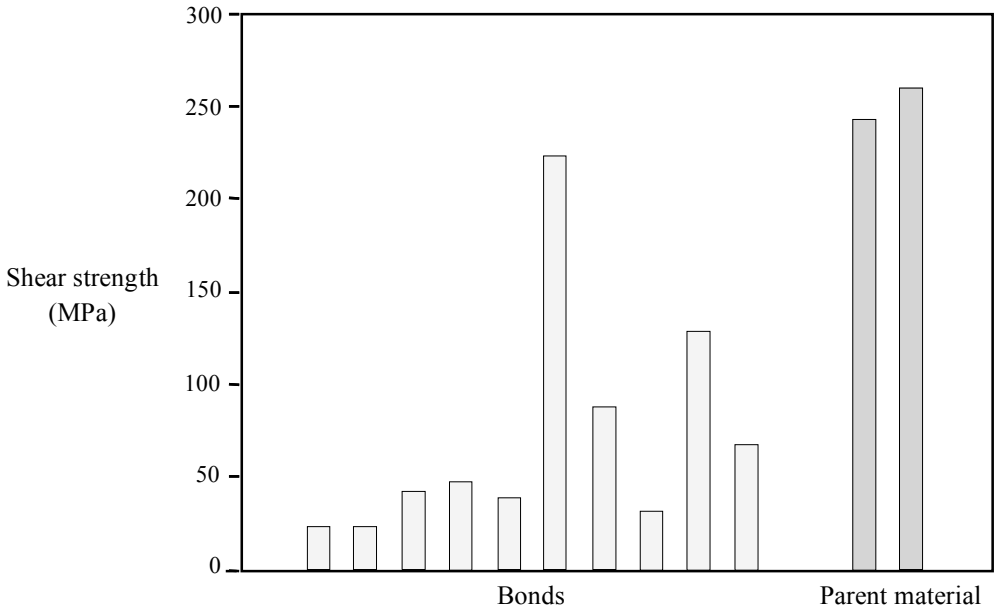

Fig. 7-1: Shear test results of TLP diffusion-bonded Al-6082 joints produced in air using ring-shape interlayers and different bonding conditions, compared with the maximum and minimum shear strengths of the parent material subjected to the same thermal cycle.

Consequently, another method was developed to overcome the problems associated with bonding in air. This new method (method V) is referred to as "High heating rate TLP diffusion bonding", see section 3.2.2 for experimental procedure.

Theoretical aspects of the new method are described below in terms of the major features of aluminium-based materials (as the parent material) and copper (as the interlayer). The method is, however, applicable to a much wider range of parent materials and interlayers.

Aluminium and oxygen have such a high chemical affinity that a new oxide layer effectively forms immediately after surface cleaning. A few nanometres of oxide are sufficient to isolate the base material from ambient oxygen, with the consequence that the rate of oxidation decreases rapidly following the initial oxidation. This intrinsic feature of aluminium-based materials has been considered to be an obstacle when diffusion bonding these materials. However, from a different point of view, it can be beneficial when TLP diffusion bonding in air! According to previous experience when TLP diffusion bonding aluminium alloys using a copper interlayer in vacuum, the liquid phase forms within a few seconds after reaching the eutectic temperature of the Al-Cu binary system (i.e. ~548°C). With the formation of the liquid phase, the interface then becomes sealed and so a vacuum is not required for the rest of the bonding process. It can be concluded that any increase in the thickness of the aluminium oxide layer from its initial condition occurs mostly during the heating stage and ceases when the liquid phase seals the interface. Theoretically, the relatively impermeable and chemically stable surface aluminium oxide layers should minimise further oxidation of the faying surfaces during the short heating stage. Accordingly, the higher the heating rate, the less the increase in the thickness of oxide layers – this is the main requirement for high heating rate TLP diffusion bonding in air (method V).

This approach is consistent with *Scamans & Butler's* report *(1975)* on the oxidation processes of pure aluminium and various aluminium alloys, in which they studied the effect of temperature (in the range of 400 to 520°C) on the morphology and structure of oxides formed in vacuum and air. Their *in situ* observations of oxidation showed that, apart from the already expected higher oxidation rate in air compared to that in vacuum, the morphology and structure of the oxide layers formed in air and vacuum are quite

similar. In addition, they reported that there was an incubation time for oxidation and this incubation period decreases drastically with increasing temperature. Even so, the incubation time for the formation of MgO crystallites on an Al-Mg-Zn alloy was reported to be as long as one minute at 500°C. Therefore, the surface composition and the initial thickness of a pre-existing oxide should not change markedly for a short time after reaching a high temperature. This brief delay in the onset of the oxidation process at the beginning of a heating cycle is the basis of the new approach for TLP diffusion bonding in air.

Copper is extensively used as a sealant in vacuums and pressurised systems. Hence the copper interlayer, used for TLP diffusion bonding, can act also as a sealant and so reducing the oxidation of itself and the aluminium alloy during the heating stage (provided the thickness of interlayer is adequate). Obviously, the faying surfaces should be flat and smooth to ensure proper contact between the interlayer and alloy. In this new method, good contact is required to reduce the oxidation due to the exposure of the interface to air (see section 3.2.1). Also, the higher the initial bonding pressure, the better is the sealing of the interface, providing that the bonding pressure does not subsequently exceed the yield stress of the parent material at the bonding temperature. Note that lack of good contact in the initial stage of conventional TLP diffusion bonding in vacuum can be tolerated as the liquid phase forms, normally with a thickness of a few times that of the thickness of the interlayer, and consequently fills any crevices.

Briefly, this new method relies on the combination of a rapid heating stage and excellent contact between the faying surfaces in order to minimise the detrimental effects of oxidation which may otherwise occur when diffusion bonding in air.

7.2.1 Results of method V and discussion

In the experimental verification of the method, Al-6082 was used as the parent material and copper foils as the interlayer. With a fairly constant heating rate of 20°C per second and a constant bonding temperature of 550°C for all specimens, the effects of time (5 and 10 minutes including 30 seconds for the heating stage) and the thickness of copper

interlayer (1 and 8 μm) on bond strength were investigated. Note that the rapid thermal expansion of the specimens during the heating stage increased the pressure up to 10 MPa for a short time before the loading system resumed the pre-set pressure (7 MPa).

To optimise the bonding conditions for this new method, up to 40 bonding trials were carried out. Having optimised the bonding conditions for Al-6082 using a 12.5 μm copper interlayer with a bonding condition of [T 550 / P 7 / t 5 / M V], samples were produced and shear tested in the fully aged condition. In figure 7-2, the shear strengths of Al-6082 bonds have been compared with that of the parent material subjected to the same thermal cycle. Bonds with shear strengths as high as 206 MPa (90% that of the parent material) were achieved. The minimum bond strength was 173 MPa (75% that of the parent material).

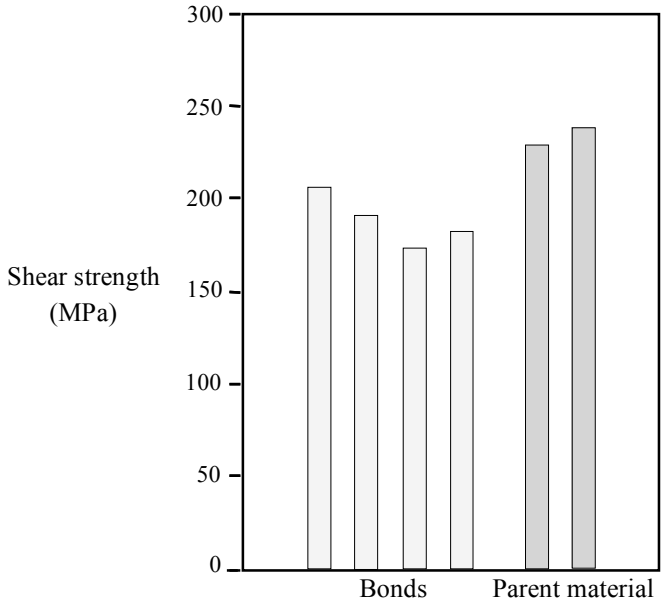

Fig. 7-2: Shear test results of the Al-6082 bonds produced using method V for TLP diffusion bonding in air, compared with the maximum and minimum shear strengths of the parent material subjected to the same thermal cycle (bonding condition: [T 550 / P 7 / t 5 / M V] using a 12.5 μm Cu interlayer).

Figure 7-3 shows the cross section of a sheared sample made using a 7 μm thick copper interlayer with a bonding condition of [T 550 / P 6 / t 5 / M V] which withstood an applied shear stress of 183 MPa (80% of the shear strength of the parent material in the

fully aged condition). This value is 10% lower that the maximum bond strength which was achieved using a thicker interlayer (12.5 μm) and slightly higher bonding pressure (7 MPa).

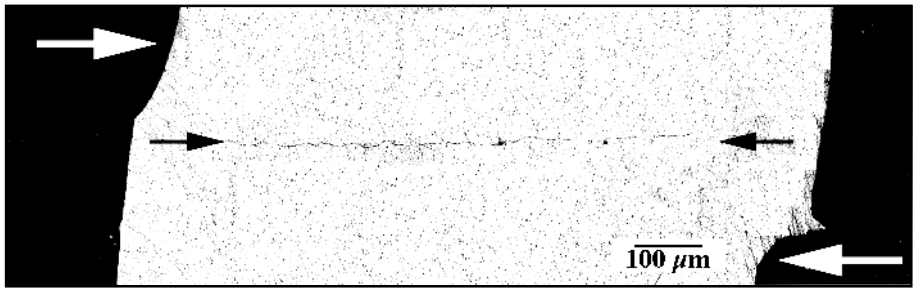

Fig. 7-3: Cross section of a shear tested Al-6082 bond (black arrows show the bond line) made in air using a 7 μm copper interlayer and bonding conditions of [T 550 / P 6 / t 5 / M V], which withstood 183 MPa in a shear test. White arrows show the direction of the applied shear force and the extent of lateral plastic deformation.

Effect of interlayer thickness and bonding time on bond strength

The effects of various bonding parameters (thickness of interlayer and time) on bond strength have been investigated. Increasing the thickness of the interlayer from 1 μm sputter coating to 8 μm (using an extra copper foil with a thickness of 7 μm) improved the bond strength very slightly, which is not unexpected. This is because, although the use of a thicker interlayer leads to the formation of more liquid at the interface, most of the excess liquid is expelled during the initial stage of the bonding process when a relatively high bonding pressure is applied. Therefore, the thickness of the interfacial liquid film, which is involved in the subsequent stages of the bonding process, does not increase when using thicker interlayers. This explanation does not contradict the previous conclusions regarding the effect of interlayer thickness on the microstructures and bond strengths of aluminium composites bonds made using methods I & II (see Chapter 4). The liquid phase formed in these cases had much higher viscosity due to the presence of reinforcement particles from the parent composite, and this resulted in

relatively less expulsion of the liquid phase from the interface. In addition, the applied pressures in the previous methods were lower then those in this fifth method. The effect of interlayer thickness on the bond strength when using method V is shown in figure 7-4.

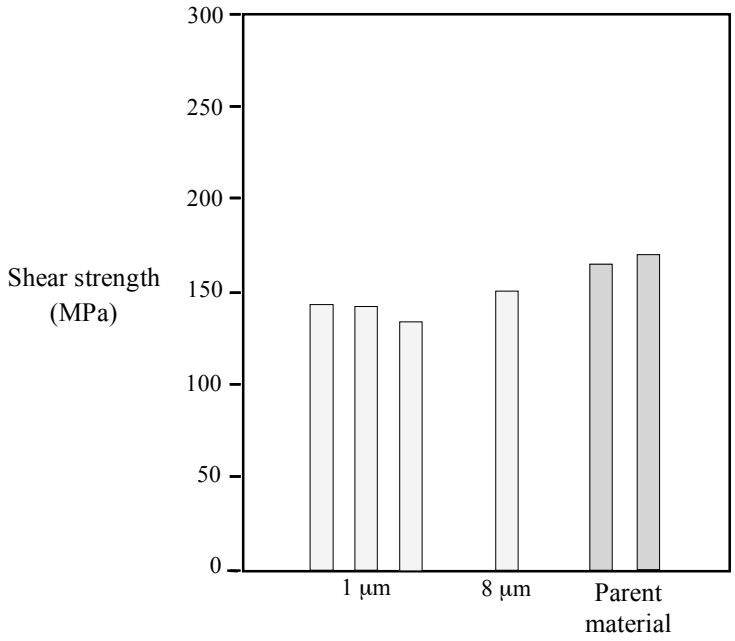

Fig. 7-4: The effect of interlayer thickness on shear strengths of Al-6082 bonds in as-bonded condition, made in air using method V, compared with the maximum and minimum shear strengths of the parent material subjected to the same thermal cycle (bonding conditions: [T 550 / P 5 / t 10 / M V]).

The slight increase in bond strength with increased thickness of interlayer was probably due to improved sealing when using thicker interlayer foils, rather due to an increase in the volume of the liquid phase. The thickness of the interlayer should be optimised for each individual parent alloy and interlayer combination.

Figure 7-5 shows that increasing the bonding time from 5 to 10 minutes did not improve the bond strength and the variation in bond strengths is within experimental error. This is consistent with the findings of the microstructural examination in which no trace of copper or eutectic phase was found at the interface of the bonds, showing that 5 minutes was enough for elimination of the liquid phase at the bonding temperature (Note that higher bond strengths for a bonding time of 5 minutes can be achieved using optimised

conditions as shown in figure 7-2). Traditionally, it has been accepted that the bonding time in TLP diffusion bonding is controlled by the diffusion rate of solute into the solid phase during the isothermal solidification stage. Note that this view has been questioned in the current research when a temperature gradient is imposed - see section 5.2. Whichever explanation is used, a shorter solidification time is expected with less liquid phase. On the other hand, the higher the bonding pressure, the thinner the liquid film at the interface. Therefore, it can be concluded that the use of higher pressures in this method indirectly reduces the bonding time.

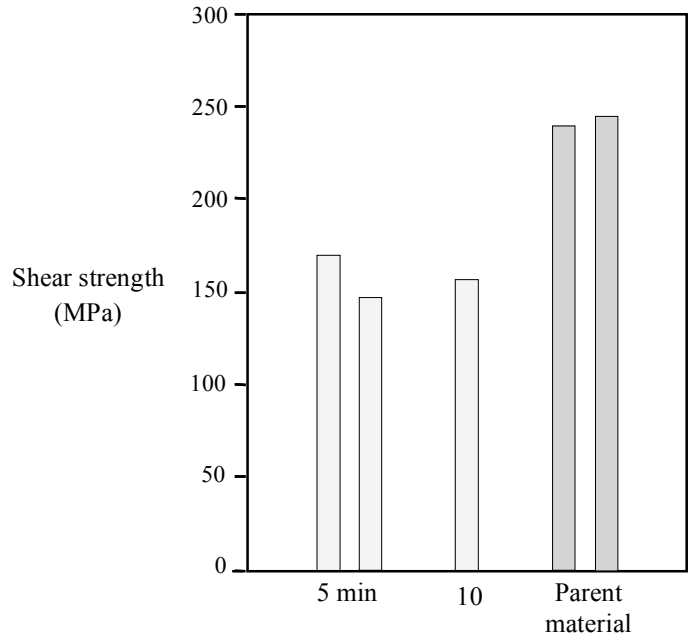

Fig. 7-5: The effect of bonding time on shear strengths of Al-6082 bonds, made in air using a 1 μm thick copper interlayer, compared with the maximum and minimum shear strengths of the parent material, all in the fully aged condition. Bonding condition: [T 550 / P 5 / t 5&10 / M V].

A typical microstructure of a heat-treated Al-6082 bond, made using this new method of TLP diffusion bonding in air, is shown in figure 7-6. Having etched the sample, a thin and discontinuous bond line can be seen. This bond line is more or less planar compared to those of the Al-6082 bonds made using temperature gradient TLP diffusion bonding (compare figures 5-4b and 7-6). However, some irregularities can be seen along the bond line which indicate a lack of uniform melting along the interface. This is due to the

fast heating stage which resulted in a non-uniform temperature distribution and, consequently, the formation of liquid along the interface was not uniform.

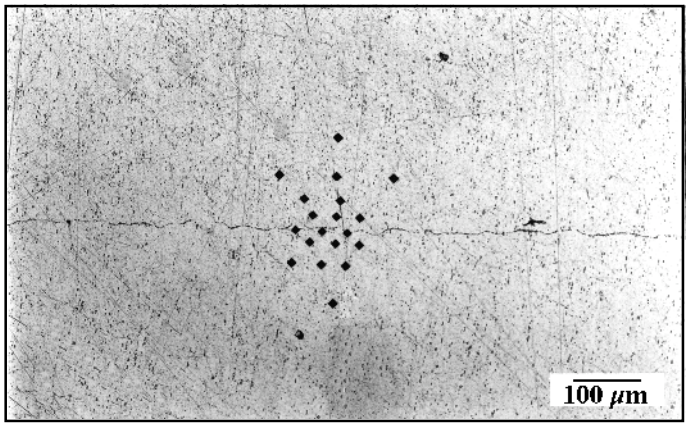

Fig. 7-6: Optical micrograph of an Al-6082 bond made using method V, and the results of micro-hardness testing at different distances from the bond line (bonding condition same as in figure 7-2).

Microhardness tests were carried out at various distances from the bond line, see figure 7-6. The hardness around the bond line is slightly higher than in the distant areas. The minimum and maximum hardnesses measured on the bond line were 137 and 144 HVN, respectively. The hardness decreases with distance from the interface (with a minimum of 116 HVN). This is probably because of a slightly higher copper content around the interface compared to the bulk alloy.

Briefly, the following steps are suggested for optimising the bonding conditions for TLP diffusion bonding in air using method V.

1. The bonding pressure should be set as close as possible to the maximum pressure that the parent material can withstand without substantial deformation at the bonding temperature. The presence of a high bonding pressure at the interface not only reduces the likelihood of oxidation but also expels excess liquid from the

interface during the bonding cycle. The effect of pressure on the thickness of the liquid phase results in shorter bonding times, compared to bonds made using lower bonding pressures.

2. The thickness of the interlayer should be chosen to provide sufficient liquid for complete bond formation. Increasing the interlayer thickness provides better sealing and also can result in slightly higher maximum bond strengths. However, thicker interlayers result in greater expulsion of liquid during bonding which is not desirable.

3. Having optimised the bonding pressure and interlayer thickness, the bonding time can be determined by microstructural examination of a few bonds, made using different bonding times, to ensure completion of the solidification stage, in order to achieve a virtually homogenous microstructure at the bond line.

4. The important role of surface preparation should be emphasised. A lack of complete contact between the faying surfaces and the interlayer leads to oxidation of the base alloy and the interlayer, and consequently the bond strength decreases drastically.

7.3 Method VI: Temperature gradient TLP diffusion bonding in air

TLP diffusion bonding under a temperature gradient (method IV) proved successful and, using that method, reliable bonds with shear strengths as high as those of the parent materials were produced. Using method IV, the evolution of the interface from planar to a sinusoidal structure improved the bond strength because of the increased surface area of the interface (see Chapter 5). Meanwhile, increasing the heating rate during TLP diffusion bonding in air (method V) resulted in bonds with up to 90% shear strength of that of the parent material. In light of these results, a sixth method, based on a combination of methods IV and V, was developed to achieve better results than those obtained using method V for bonding in air.

The sixth method relies on a fast heating stage to overcome the oxidation problem when bonding in air, and also on the presence of a temperature gradient across the interface in order to form a non-planar interface. However, imposing a temperature gradient during the bonding process reduces the effective heating rate as a consequence of substantial heat flux from the parts being joined into the heat sink (assuming the input power of the heat source is constant). As mentioned before, a delay in the formation of the liquid phase leads to oxidation of the interlayer and thickening of the oxide layer on the faying surfaces. Therefore it is not desirable, when imposing a temperature gradient, to cause an increase in the duration of the heating stage. In order to achieve a high heating rate under a temperature gradient, either the heat input has to be increased, or the heat sink should be modified to reduce the heat flux (see section 3.2.2 for experimental details). An optimal combination of the specimen set-up and bonding conditions is required to achieve high strength bonds, made in air.

7.3.1 Results of method VI and discussion

Initial experiments on temperature gradient TLP diffusion bonding in air (method VI), revealed that the use of a specimen set-up similar to the one used for method IV (temperature gradient TLP diffusion bonding) increased the duration of the heating stage substantially. The faying surfaces and the interlayer were therefore exposed to air for a long time before the formation of the liquid phase sealed the interface. Bonding processes with heating stages longer than one minute (in air) resulted in poor bond strengths, see figure 7-1.

Having designed a new specimen set-up for method VI, a few Al-6082 bonds were made and shear tested. A maximum bond strength of 195 MPa (85% that of the parent material) was achieved when using a 1 μm copper interlayer and bonding conditions of [T 550 / P 6 / t 10 / M VI]. The minimum shear strength was 183 MPa (80% that of the parent material). Although the maximum bond strength achieved in this method is slightly lower than that achieved using method V (195 MPa compared to 206 MPa), it seems that imposing a temperature gradient reduced the scatter in the results considerably (from ±8% in method V to ±3% in method VI). These results are promising and it seems that the presence of a temperature gradient was of benefit. However more experiments are required to obtain conclusive results.

Precise control of the heating rate was found difficult when using this method. The heating rate depends not only on the specimen set-up and the heat sink design but also on the bonding pressure. The higher the bonding pressure, the better the thermal conduction between the specimen and heat sink, leading to a slower temperature rise. This lack of control of a crucial bonding parameter (the heating rate) resulted in uncertainty when evaluating the effects of various other parameters. For example, the use of a 7 μm copper interlayer resulted in poor bonds; though due to the variation in the heating rate, it is not clear whether the increase in the thickness of the interlayer or the lack of a sufficiently high heating rate is responsible.

In light of the previous experiences with both methods IV and V, the crucial bonding parameters when using method VI can be ascertained. Table 7-1 compares crucial parameters between method VI and the previous methods. These comparisons can be used in future work as guide lines to optimise the bonding conditions when temperature gradient TLP diffusion bonding in air.

	Method IV	**Method V**
Surface preparation	-	same for VI
Loading	-	same for VI
Positioning of induction coil	same for VI	-
Bonding pressure	-	same for VI
Heating rate	-	as high as possible
Imposing temperature gradient	modified heat sink	-

Table 7-1: Common bonding parameters between Method VI (temperature gradient TLP diffusion bonding in air) and the previous methods, IV and V.

As can be seen in Table 7-1, all parameters except the heating rate and the design of the heat sink are similar to those in either method IV or V. As mentioned before, the basic problem in method VI is to provide a sufficient temperature gradient without prolonging the heating stage. This could be achieved by redesigning the heat sink and/or the induction system.

Alternatively, it should be possible to employ a more powerful heat source, e.g. laser beams, to increase the heating rate in method VI. A laser beam can be focused on a small area (close to the interface) which would result in shorter heating stages and higher temperature gradients, compared with those that can be achieved using conventional heating techniques. Investigations on the use of a laser beam when temperature gradient TLP diffusion bonding in air are strongly recommended for future work.

7.4 Summary

Method V*: High heating rate TLP diffusion bonding in air*

The new method for TLP diffusion bonding of aluminium-based materials in air has proved successful, and bonds with shear strengths comparable with that of the parent material have been made (up to 90% that of the parent material). This method relies on a rapid heating stage and also on the preparation of flat faying surfaces in order to overcome potential oxidation problems associated with bonding in air.

It should be emphasised that the surface preparation method and the bonding set-up used in this work should be regarded as guide lines since they were developed for laboratory purposes. Other approaches can be adopted. The following techniques are recommended to improve the results and to make the process more suitable for commercial exploitation.

1. The heating rate could be increased by improving the induction system or using other heating sources, e.g. a laser beam. The development of this approach is in progress.

2. Surface preparation could be improved by high precision grinding, preferably followed by a lapping process.

3. The loading arrangement should be designed according to the shape and size of the parts to be joined.

The bonding temperature, using this method and a copper interlayer, is close to the solution-treatment temperature of most aluminium alloys (i.e. ~540°C). In contrast to bonding in vacuum, it is feasible with this method to quench parts directly from the bonding temperature, so they are effectively solution treated. The parts can subsequently be aged to improve properties.

This method is expected to be applicable to the diffusion bonding in air of materials other than aluminium alloys.

Method VI: *Temperature gradient TLP diffusion bonding in air*

Temperature gradient TLP diffusion bonding in air (method VI) was developed to improve the reliability and strength of the aluminium bonds made in air. This new method takes advantage of inducing a temperature gradient (as in method IV) to reliably produce high strength joints, and at the same time, employs a fast heating stage (as in method V) to overcome the oxidation problems associated with bonding in air.

The results of preliminary experiments on joining Al-6082 alloy, using this sixth method, are promising. Compared to the results achieved using method V, the scatter in results was reduced when using method VI and similar bonding conditions (i.e. pressure, time, temperature and interlayer). Using this new method, bonds with shear strengths in the range of 183 to 195 MPa were produced. It seems the reliability of the bonds are improved by using method VI, even though the maximum bond strength was slightly lower than that of the bonds made using method V.

However, attaining a sufficiently high heating rate, and also precise control of this crucial factor, proved difficult; imposing a temperature gradient decreases the heating rate drastically (for a particular heating system and heat sink). The reduction and variation in the heating rate, when bonding in air, resulted in unfavourable scatter in the bond strengths. Therefore, the design of the heating system and heat sink become important factors when attempting to impose a sufficient temperature gradient, while maintaining a high enough heating rate.

Further investigation of this method, particularly on the use of other heat sources e.g. laser beams, is strongly recommended for future work.

Chapter 8

8. Conclusions and proposal for future work

Six new methods for TLP diffusion bonding of aluminium-based materials have been developed during the current work. A comprehensive analytical model for the fourth method has been also proposed and verified experimentally.

8.1 Experimental results

Method I

The first method (isostatic TLP diffusion bonding) relies on a simultaneous combination of isostatic compression and TLP diffusion bonding process in order to increase the bond strength. The use of this method for joining Al-8090/SiC composite proved successful. Bonds with shear strengths up to 221 MPa (85% that of the parent material) were produced using 3 μm thickness copper interlayers (the maximum shear strength obtained from bonds made using conventional TLP diffusion bonding was 105 MPa).

Method II

Method II consists of low pressure TLP diffusion bonding followed by solid-state diffusion bonding under isostatic pressure in air. The highest and lowest bond strengths for the Al-359/SiC bonds, using this method and a 7 μm thickness copper interlayer, were 242 and 212 MPa which are 92 and 80% of the strength of the parent material in the fully aged condition. These values are far beyond the highest diffusion bond strengths that have been reported for aluminium metal matrix composites to date.

The shear test results and examination of the microstructures showed that the thickness of the interlayer has a key role when TLP diffusion bonding Al-MMCs. The use of 1 μm thickness copper interlayers resulted in low bond strengths. On the other hand, the use of a thick interlayer (e.g. 12.5 μm) caused unfavourable agglomeration of the reinforcement particles about the bond line. Thicknesses of between 3 and 7 μm resulted in excellent strengths but the thickness of the interlayer should be optimised for each alloy.

Method III

The third method (method III) was developed to fabricate intricate components with minimal plastic deformation during the bonding process (particularly for superplastic materials with very low yielding strengths at the bonding temperature). In this method, low pressure TLP diffusion bonding is followed by hot isostatic pressing (HIP) without encapsulation. In contrast to conventional "HIP bonding" the complexity associated with encapsulation is avoided. Thus components with complicated shapes can be produced. The highest bond strength achieved for un-reinforced Al-6082, using a 7 μm thickness copper interlayer, was 200 MPa (89% of the shear strength of parent material).

Method IV

Imposing a temperature gradient when TLP diffusion bonding, as a novel approach for joining aluminium alloys, resulted in reliable bonds with shear strengths as high as those of the parent materials. The average shear strengths of the parent alloy and the Al-6082 bonds, made using copper interlayers with a thickness of 1.5 μm, were 250 MPa (with a scatter of less than ±2%). The shear strength of a dissimilar Al alloy and Al-MMC joint was comparable to that of the Al alloy, which confirms the potential of this method for the joining of dissimilar materials. It is assumed that the evolution of the interface from planar to a sinusoidal/cellular structure, as the result of imposing a temperature gradient, improves the bond strength because of the increased surface area of the interface.

The kinetics of this method rely on the diffusion of solute in the liquid phase. Therefore, the bonding times, using this method, are much shorter than for conventional TLP diffusion bonding. The analytical solution proposed in Chapter 6 for the new method is in good agreement with the experimental results.

It is believed that the model developed is also applicable to conventional TLP diffusion bonding. The approach outlined above may provide a more rigorous description of TLP diffusion bonding when, nominally, a temperature gradient is not imposed. In practice, a small difference is likely to exist between the temperatures at the two solid/liquid interfaces whenever TLP diffusion bonding is attempted. This is a completely new way of describing the process and is more consistent with the results that are achieved.

Finally, it is believed that temperature gradient TLP diffusion bonding is applicable to a wide range of aluminium-based alloys and composites. It is also likely to be of benefit when joining other materials and metallic alloys, particularly those with stable oxide films.

Method V

This new method for the TLP diffusion bonding of aluminium-based materials in air has proved successful, and Al-6082 bonds with shear strengths comparable with that of the parent material have been made (up to 90% that of the parent material). This method relies on a rapid heating stage and also on the preparation of flat faying surfaces in order to overcome potential oxidation problems associated with bonding in air.

In contrast to bonding in vacuum, it is feasible with this method to quench parts directly from the bonding temperature, so they are effectively solution treated. The parts can subsequently be aged to improve properties.

This method is expected to be applicable to the diffusion bonding in air of materials other than aluminium alloys.

Method VI

Temperature gradient TLP diffusion bonding in air (method VI) was developed to improve the reliability and strength of the aluminium bonds made in air. This new method takes advantage of inducing a temperature gradient (as in method IV) and at the same time, employs a fast heating stage (as in method V) to overcome the oxidation problems associated with bonding in air.

When using this method and similar bonding conditions as in method V, Al-6082 bonds with shear strengths in the range of 183 to 195 MPa were produced. The scatter in results was reduced, even though the maximum bond strength was slightly lower than that of the bonds made using method V.

The design of the heating system and heat sink are important factors when attempting to impose a sufficient temperature gradient while maintaining a high enough heating rate - see below for the suggestions for future work on this method.

Al-Li (UL-40) bonds

The aluminium-lithium alloy (UL-40) showed quite different bonding characteristics, probably because of the high percentage of lithium (4 wt.%) which forms a very stable surface layer. The maximum bond strength achieved, using method I and a copper interlayer of 12.5 μm thickness, was 155 MPa.

Method IV (temperature gradient TLP diffusion bonding) was used to break up the normally continuous bond line of this alloy. Imposing a temperature gradient has a dramatic effect on the microstructure of the UL-40 bond line, showing that the stable interface is disrupted. Although no assessment of mechanical properties has been carried out on the UL-40 bonds, it is expected that the use of the new method may lead to higher bond strengths than the previously reported values.

Summary:

In figure 8-1, the maximum bond strengths achieved using these new methods are compared with the average shear strength of the parent material given the same heat treatment.

• The use of method IV (temperature gradient TLP diffusion bonding) resulted in the highest bond strength, with excellent reliability, compared to the other five methods. Note that the maximum bond strength is slightly higher than the average shear strength of the parent material.

• Two new methods for TLP diffusion bonding in air (methods V and VI) are capable of producing bonds with shear strengths up to 90% that of the parent materials. Although these results are not as good as those obtained using method IV, the practicality and feasibility of these methods are definitely of interest since a vacuum system is not required.

• Despite the satisfactory results of the methods mentioned above, the methods based on applying isostatic pressure, particularly method III, remain an attractive solution for TLP diffusion bonding aluminium alloys and composites which have very low yield strengths at bonding temperatures. The use of the other methods can result in undesirable plastic deformation during the bonding process.

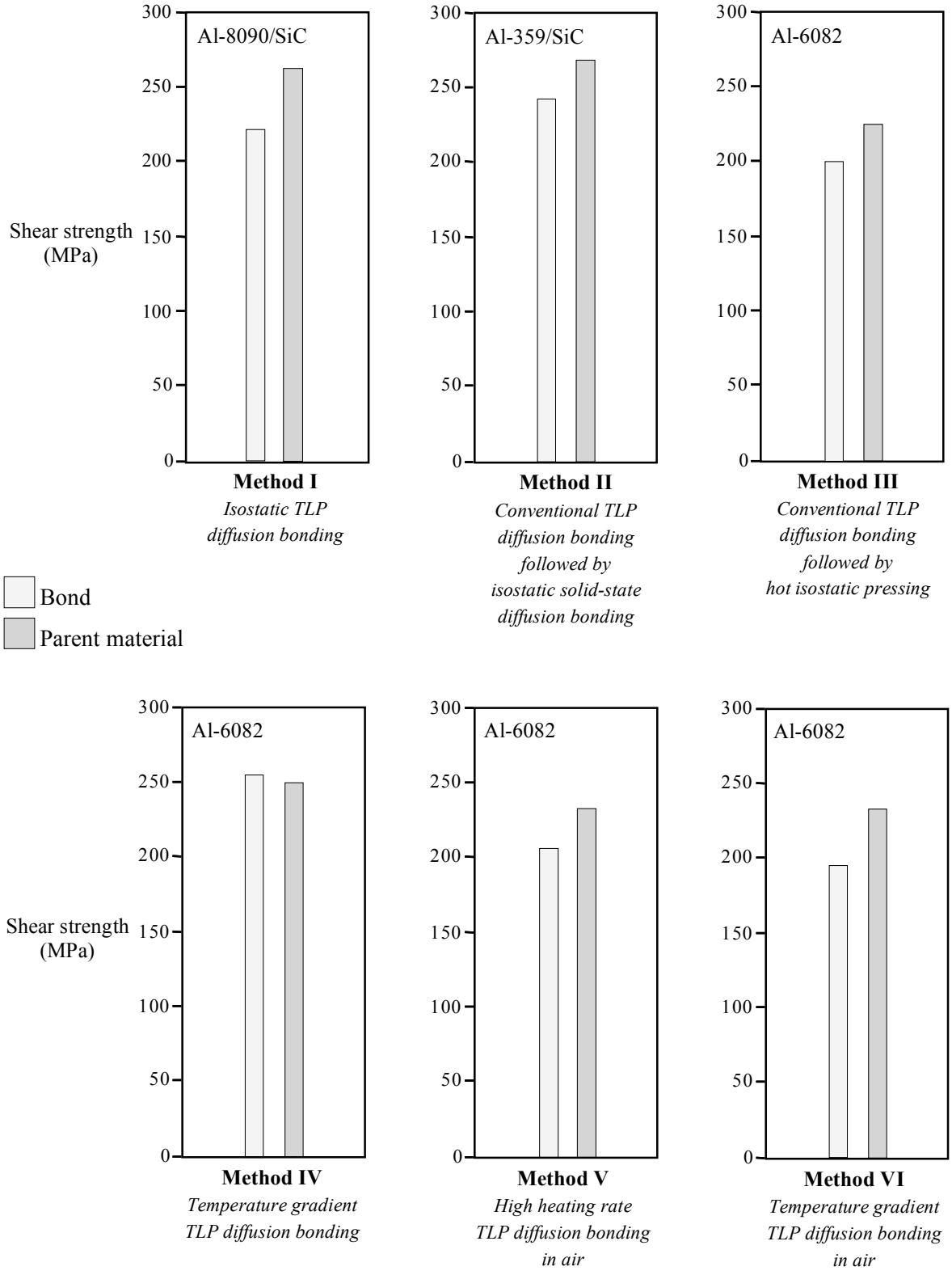

Fig. 8-1: Maximum bond strengths achieved using the six new methods compared with the average shear strength of the parent materials (all in the fully aged condition).

8.2 Modelling of method IV

Temperature gradient TLP diffusion bonding (method IV) is a new approach which cannot be theoretically analysed using the existing models for conventional TLP diffusion bonding. Therefore a new analytical model was developed to predict bonding times and interface displacements when using this method.

This new model provides precise solutions for predicting bonding times and interface displacement when TLP diffusion bonding under a temperature gradient. These solutions were simplified, using a mass balance approach and by applying some approximations, to provide less complicated solutions than the precise ones. The precise and approximate solutions are in excellent agreement for the range of bonding parameters likely to be used when TLP diffusion bonding.

Using a simple Al-Cu system, the accuracy of the analytical solutions were experimentally verified. The analytical solutions are in good agreement with the experimental results for boundary displacement and bonding time. Also, the experiments showed that bonding pressure has a drastic effect on the actual width of the liquid phase in TLP diffusion bonding. This has not been taken into account in previous analyses of the TLP diffusion bonding processes.

It is believed that the model is applicable to conventional TLP diffusion bonding even when, nominally, a temperature gradient is not imposed as a small temperature difference is likely to exist between the two solid/liquid interfaces. This provides a completely new way to describe and rigorously model TLP diffusion bonding, overcoming some of the assumptions required in previous models.

8.3 Future work

In light of the results achieved during the current work, the following topics are suggested for future work.

- **Further work on the scientific aspects and modelling of temperature gradient TLP diffusion bonding (method IV)**

The idea of introducing a temperature gradient when TLP diffusion bonding is a new approach for joining aluminium-based materials. In contrast to conventional explanations of TLP diffusion bonding which have relied on the diffusion of solute in the solid phase, the new approach is based on the diffusion of solute in the liquid phase. Further study of theoretical aspects (e.g. nature of solute rejection) is required in order to provide a better understanding of the new approach, and of the magnitude of the temperature gradients that can be used successfully.

This new approach may also provide a more rigorous and successful description of conventional TLP diffusion bonding when, nominally, a temperature gradient is not imposed. In addition, other isothermal processes associated with transient liquid phases, e.g. liquid phase sintering, may be reinvestigated using this different point of view.

According to the analytical solution proposed in this work, the bonding time can be controlled by the magnitude of the temperature gradient. The proposed analytical model now requires further development so that the bonding conditions can be optimised for different materials. For example, the effects of the temperature gradient on the microstructures of bond lines should be included in the analytical model. The model also needs further verification by comparing additional experimental results with theoretical values.

- **Further expansion and application of method IV**

Using temperature gradient TLP diffusion bonding (method IV), the microstructure of the bond line and the bonding time can be controlled favourably. The current work has examined several aluminium alloys and composites, and bonds could be made reliably with shear strengths as high as those of the corresponding parent materials. Further investigation is required to generalise the use of this new approach in the diffusion bonding of advanced materials which cannot be joined using conventional methods. This method should be of benefit when joining superalloys, particularly nickel-based alloys, as well as intermetallic and dissimilar materials.

- **Further expansion and application of method VI**

The preliminary results of the sixth method (Temperature gradient TLP diffusion bonding in air) were promising and bonds with shear strengths of 85% of that of the parent material (Al-6082) were produced. However, precise control of the duration of the heating stage was found difficult. Improvements to the design of the heat sink and heating source are required to achieve a high heating rate while a temperature gradient is imposed across the interface. Investigation of more powerful heating sources, e.g. laser beams, is recommended for future work.

- **Further expansion and application of method III**

Method III (Low pressure transient liquid phase diffusion bonding followed by hot isostatic pressing without encapsulation) allows the fabrication of intricate parts from superplastic materials with virtually no deformation during the bonding process, and so dimensional tolerances are preserved. However, this method needs to be further evaluated and developed. The first stage could be carried out using a temperature gradient in order to achieve a non-planar interface. Consequently, the sealing of the bond line, required for the second stage (HIP without encapsulation), is expected to be improved. Further work is necessary to optimise the bonding conditions in order to improve the reliability of the process.

- **The use of alloy interlayers rather than pure copper, in order to decrease the bonding temperature when TLP diffusion bonding of aluminium alloys**

The bonding temperature for TLP diffusion bonding of aluminium-based materials, using copper interlayers, is quite high (~550°C). Such a high temperature process can be associated with unfavourable phase transformations in some parent alloys, and also between reinforcement and the matrix when bonding composite materials. Therefore it will be beneficial to lower the bonding temperature (ideally < 450°C). This may be achieved using an alloy interlayer which forms a liquid phase with aluminium at lower bonding temperatures, e.g. using the Zn/Cu/Al ternary system with eutectic/peritectic reactions. Investigation of different alloy interlayers needs to be undertaken.

- **Development of method IV for joining dissimilar materials**

The joining of dissimilar materials has been of interest to combine alloys or composites with different mechanical-physical properties in order to optimise the exploitation of engineering materials. For example, the wear resistance of an aluminium alloy can be improved by up to 30 times when an aluminium matrix composite (with SiC particles) is used in components which are subjected to mechanical abrasion. The preliminary experiments to date have shown that temperature gradient TLP diffusion bonding is capable of producing strong bonds between aluminium-based alloys and composites. Further work is required to extend the application of the method to join dissimilar materials, e.g. joining steel to aluminium.

- **Use of electroplating for deposition of interlayers in TLP diffusion bonding**

Deposition of copper by electroplating techniques, rather than using foils or sputter coated interlayers, for TLP diffusion bonding of aluminium-based materials is also of interest. If this method is successful, then the scope for TLP diffusion bonding of these materials will be extended considerably, including the possibility of commercial exploitation, e.g. in the fabrication of honeycomb structures by the selective deposition of copper on the bonding areas of aluminium sheets.

References

Barta I.M. (1964), "Low temperature diffusion bonding of aluminium alloys", *Welding journal Research Supplement*, June, 241s-247s, June.

Bienvenu Y. and Koutny J.L. (1990), "Diffusion bonding of thin aluminium foils", Proc. Conf. *Diffusion Bonding 2*, Cranfield Institute of Technology, Cranfield, UK, 111-118, ed. Stephenson D.J, Amsterdam, Elsevier.

Bushby R.S. and Scott V.D. (1993), "Liquid phase bonding of aluminium and aluminium/Nicalon composite using copper interlayers", *Materials Science and. Technology*, Vol. 9, 417-423.

Bushby R.S. and Scott V.D. (1995a), "Liquid phase bonding of aluminium and aluminium/Nicalon composite using interlayers of Cu-Ag alloy", *Materials Science and. Technology*, Vol. 11, 643-649.

Bushby R.S. and Scott V.D. (1995b), "Joining of particulate silicon carbide reinforced 2124 aluminium alloy by diffusion bonding", *Materials Science and. Technology*, Vol. 11, 753-758.

Cailler M., Debbouz O., Dannawi M. and Latouche T. (1991), "Mechanical characterisation by dynamical tensile loading of 2017 aluminium alloy joints welded by diffusion bonding", *Journal of Materials Science*, Vol. 26, 4997-5003.

Church S., Day J. and Wild B. (1996), "Diffusion bonding of metals and alloys", *Materials World*, Vol. 4, No. 7, 385-386.

Cline C.L. (1966), "An analytical and experimental study of diffusion bonding", *Welding Journal Research Supplement,* November, 481s-489s.

Crank J. (1975), 'The mathematics of diffusion', Clarendon Press, Oxford.

Crank J. (1984), 'Free and moving boundary problems', Clarendon Press, Oxford.

Debbouz O. and Navai F. (1997), "Mechanical characterisation by dynamical tensile loading of 2017 aluminium alloy joints welded by diffusion bonding. New results and SEM observations of the failure surfaces", *Journal of Materials Science*, Vol. 32, 475-482.

Derby B. and Wallach E.R. (1982), "Theoretical model for diffusion bonding", *Metal Science*, Vol. 16, 49-56.

Derby B. and Wallach E.R. (1984), "Diffusion bonding: development of theoretical model", *Metal Science*, Vol. 18, 427-431.

Derby B. (1990), "Diffusion Bonding", in 'Joining of Ceramics', ed. Nicholas M.G., Chapman and Hall.

Dray A.E. (1985), "Diffusion bonding of aluminium", Ph.D. thesis, University of Cambridge, UK.

Dunford D.V. and Partridge P.G. (1987), "The peel strengths of diffusion bonded joints between clad Al-alloy sheets", *Journal of Materials Science*, Vol. 22, 1790-1798.

Dunford D.V., Partridge P.G. and Gilmore C.J. (1990), "Diffusion bonding of Al-Li alloys Proc. Conf. *Diffusion Bonding 2*, Cranfield Institute of Technology, Cranfield, UK, 130-143, ed. Stephenson D.J, Amsterdam, Elsevier.

Dunford D.V. and Partridge P.G. (1990), "Strength and fracture behaviour of diffusion-bonded joints in Al-Li (8990) alloy, Part 1: Shear strength", *Journal of Materials Science*, Vol. 25, 4957-4964.

Dunford D.V. and Partridge P.G. (1991), "Strength and fracture behaviour of diffusion-bonded joints in Al-Li (8990) alloy, Part 2: Fracture behaviour", *Journal of Materials Science*, Vol. 26, 2625-2629.

Dunford D.V. and Partridge P.G. (1992), "Diffusion bonding of Al-Li alloys", *Materials Science and Technology*, Vol. 8, 385-398.

Ellis M.B.D. (1992), "Solid-state joining of aluminium alloys and aluminium-based metal matrix composites (MMC)", in 'Aluminium Industry', Vol. 11, No. 5, 27-30.

Ellis M.B.D., Gittos M.F. and Threadgill P.L. (1994), "Joining aluminium based metal matrix composites", *Materials World*, Vol. 2, No. 8, 415-417.

Ellis M.B.D. (1996), "Joining of aluminium based metal matrix composites", *International Materials Review*, Vol. 41, No. 2, 41-58.

Enjo T., Ikeuchi K. and Akikawa N. (1978), "Study of microscopic process of diffusion welding by electric resistance measurement and transmission electron microscope", *Transaction of JWRI*, Vol. 7, No. 2, 97-100.

Enjo T. and Ikeuchi K. (1984), "Diffusion welding of Al-Cu-Mg series 2017 alloy", *Transactions of JWRI*, Vol. 13, No. 2, 63-68.

Escalera M.D., Urena A. and Gomez de Salazar J.M. (1997), "Solid state diffusion bonding of AA6061 matrix composites reinforced with alumina particles", ASM Proc. Conf. *Welding and Joining Science and Technology*, Madrid, Spain, 380-389.

Garmong G., Paton N.E. and Argon A.S. (1975), "Attainment of full interfacial contact during diffusion bonding", *Metallurgical Transactions A*, Vol. 6A, 1269-1279.

Gilmore C.J., Dunford D.V. and Partridge P.G. (1991), "Microstructure of diffusion-bonded joints in Al-Li 8090 alloy", *Journal of Materials Science*, Vol. 26, 3119-3124.

Gomez de Salazar J.M., Urena A. and Fernandez M.I. (1997), "Transient liquid phase diffusion bonding in aluminium-based composites", ASM Proc. Conf. *Welding and Joining Science and Technology*, Madrid, Spain, 397-406.

Harvey J., Partridge P.G. and Snooke C.L. (1985), "Diffusion bonding and testing of Al-alloy lap shear test pieces", *Journal of Materials Science*, Vol. 20, 1009-1014.

Harvey J., Partridge P.G. and Lurshay A.M. (1986), "Factors affecting the shear strength of solid state diffusion bonds between silver-coated clad Al-Zn-Mg alloy (Aluminium alloy 7010)", *Materials Science and Engineering*, Vol. 79, 191-199.

Hill A. and Wallach E.R. (1989), "Modelling solid-state diffusion bonding", *Acta Metallurgica*, Vol. 37, No. 9, 2425-2437.

Houldcroft P.T. (1977), 'Welding Process Technology', Cambridge University Press.

Ikeuchi K. and Asano K. (1993), "Development of intermediate layer for diffusion bonding of continuous alumina fibre reinforced aluminium matrix composite", *Transactions of JWRI*, Vol. 22, No. 1, 77-84.

Kazakov N.F(1985, English version), 'Diffusion Bonding of Materials', Pergamon Press.

Knight C.A. (1962), "Curved growth of ice on surfaces", *Journal of Applied of physics*, Vol. 33, No. 5, 1808-1815.

Kotani K., Ikeuchi K. and Matsuda F. (1996a), "Interfacial oxides in diffusion-bonded joints of Al-Mg alloys by TEM", Proc. *The 6th International Symposium of Japan Welding Society*, Nagoya, Japan, November, 95-100, Ed. Ushio M.

Kotani K., Ikeuchi K. and Matsuda F. (1996b), "Effects of interfacial phases on joint strength of diffusion-bonded aluminium alloys", *Quarterly Journal of the Japan Welding Society*, Vol. 14, No. 2, 382-388 (in Japanese).

Kuriyama K. (1992), "Joining of Composites", Ph.D. Thesis, University of Cambridge.

Lesoult G. (1976), Centre for Joining of Materials Report, Carnegie Mellon University, Pittsburgh, PA, USA.

Livesey D.W. and Ridley N. (1990), "Diffusion bonding of superplastic aluminium alloys using a transient liquid phase interlayer (zinc)", Proc. Conf. *Diffusion Bonding 2*, Cranfield Institute of Technology, Cranfield, UK, 83-100, ed. Stephenson D.J, Amsterdam, Elsevier.

Lloyd D.J. (1994), "Particle reinforced aluminium and magnesium matrix composites", *International Materials Review*, Vol. 39, No. 1, 1-23.

MacDonald W.D. and Eagar T.W. (1992), "Transient liquid phase bonding processes", in 'The Metal Science of Joining' 93-100, ed. Cieslak M.J. et al., The Minerals, Metals & Materials Society.

Maddrell E.R. (1989), "Diffusion bonding of aluminium alloys", Ph.D. Thesis, University of Cambridge.

Maddrell E.R., Ricks R.A. and Wallach E.R. (1989), "Diffusion bonding of aluminium alloys containing lithium and magnesium", Proc. Conf. *Aluminium-Lithium 5*, Williamsburg, Virginia, USA, 451-460, ed. Sanders Jnr. T.H. and Starke Jnr. E.A., MCEP Ltd. Birmingham, UK.

Maddrell E.R. and Wallach E.R. (1990), "Diffusion welding of aluminium-lithium alloys", Proc Conf. *Recent Trends in Welding Science & Technology*, 541-545, ed. David S.A. and Vitek V.M., ASM International.

Materials Progress (1997), "Aluminium composite reduces cost, improves performance", *Advanced Materials & Processes*, ASM International, Vol. 152, No. 4, 7.

Morley R.A. and Caruso J. (1980), "Diffusion welding of 390 aluminium alloy hydraulic valve bodies", *Welding Journal*, August, 29-34.

Nakagawa H., Lee C.H. and North T.H. (1991), "Modelling of base metal dissolution behaviour during transient liquid-phase brazing", *Metallurgical Transactions A*, Vol. 22A, 543-555.

Nicholas N.H., Nichting R.A., Edwards G.R. and Olson D.L. (1990), "The influence of surface topography on low temperature solid state bonding", Proc. Conf. *Recent Trends in Welding Science & Technology*, 547-550, ed. David S.A. and Vitek V.M., ASM International.

Niemann J.T. and Garrett R.A. (1974a), "Eutectic bonding of boron-aluminium structural components (Part 1)", *Welding Journal Research supplement*, April, 175s-184s.

Niemann J.T. and Garrett R.A. (1974b), "Eutectic bonding of boron-aluminium structural components (Part 2)", *Welding Journal Research supplement*, August, 351s-360s.

Osawa T. (1995), "Changes in the interface structure and strength of the diffusion brazed joints of Al-Si system alloy castings", *Welding Journal Research Supplement*, 206s-212s.

Partridge P.G. and Dunford D.V. (1991), "The role of interlayer in diffusion bonded joints in metal-matrix composites", *Journal of Materials Science*, Vol. 26, 2255-2258.

Peel C., Robertson J. and Tarrant A. (1995), "Have metal matrix composites proved their worth?", *Materials World*, Vol. 3, No. 1, 8-9.

Pfann W.G. (1955), "Temperature gradient zone melting", *Transactions AIME*, Vol. 203, 961-964.

Pilling J. and Ridley N. (1987), "Solid state bonding of superplastic AA 7475" *Materials Science and Technology*, Vol. 3, 353-359.

Ricks R.A., Winkler P.J., Stoklossa H. and Grimes R. (1989), "Transient liquid phase bonding of aluminium-lithium base alloy AA 8090 using roll-clad Zn based interlayers", Proc. Conf. *Aluminium-Lithium 5*, Williamsburg, Virginia, USA, 441-449, ed. Sanders Jnr. T.H. and Starke Jnr. E.A., MCEP Ltd. Birmingham, UK.

Ricks R.A., Mahon G.J., Parson N.C., Heinrich T. and Winkler P.J. (1990), "Development of diffusion bonding techniques for Al-Li base alloy AA 8090", Proc. Conf. *Diffusion Bonding 2*, Cranfield Institute of Technology, Cranfield, UK, 69-82, ed. Stephenson D.J, Amsterdam, Elsevier.

Sabathier V., Edwards G.R. and Cross C.E. (1994), "Kinetics study of low-temperature transient liquid phase joining of an aluminium-SiC composite", *Metallurgical and Materials Transactions A*, Vol. 25A, 2705-2714.

Scamans G.M. and Butler E.P. (1975), "In situ observations of crystalline oxide formation during aluminium and aluminium alloy oxidation", *Metallurgical Transactions A*, Vol. 6A, 2055-2063.

Sekerka R.F., Jeanfiles C.F. and Heckel R.W. (1975), in "Lectures on the theory of phase transformations", ed. Aaronson, New York, *AIME*, 117-169.

Sekerka R.F., Jeanfiles C.F. and Heckel R.W. (1975), Technical Report NO. 3, Carnegie Mellon University, Pittsburgh, PA, USA.

Singer C., Holmyard E.J., Hall A.R. and Williams T.I. (1958), 'A History of Technology', Oxford University Press.

Staley J.T., Liu J. and Hunt Jr. W.H. (1997), "Aluminium alloys for aerostructures", *Advanced Materials & Processes*, Vol. 152, No. 4, 17-20.

Takahashi Y., Ueno F. and Nishiguchi K. (1988), "A numerical analysis of the void-shrinkage process controlled by surface-diffusion", *Acta Metallurgica*., Vol. 36, No. 11, 3007-3018.

Takahashi Y., Takahashi K. and Nishiguchi K. (1991), "A numerical analysis of the void shrinkage processes controlled by coupled surface and interface diffusion", *Acta Metallurgica. et Materialia*, Vol. 39, No. 12, 3199-3216.

Takahashi Y. and Inoue K. (1992), "Recent void shrinkage models and their applicability to diffusion bonding", *Materials Science and Technology*, Vol. 8, 953-964.

Takahashi Y. and Tanimoto M. (1995a), "Effect of surface asperity on interfacial contact process controlled by power law creep-numerical study of viscoplastic adhering process", *Transactions of the ASME*, Vol. 117, 330-335.

Takahashi Y. and Tanimoto M. (1995b), "Experimental study of interfacial contacting process controlled by power law creep", *Transactions of the ASME*, Vol. 117, 336-340.

Tensi H.M., Wittmann M., Friedrich H.E. and Schmidt J.J. (1989), "Diffusion bonding of high strength aircraft and aerospace aluminium alloys", Proc. Conf. *Light alloys for aerospace applications*, Las Vegas, USA, 465-479, ed. Lee E.W. et al., The Minerals, Metals & Materials Society.

Tensi H.M. and Wittmann M. (1990), "Influence of surface preparation on the diffusion welding of high strength aluminium alloys", Proc. Conf. *Diffusion Bonding 2*, Cranfield Institute of Technology, Cranfield, UK, 101-110, ed. Stephenson D.J, Amsterdam, Elsevier.

Tiller W.A. (1963), "Migration of a liquid zone through a solid: part I", *Journal of Applied of physics*, Vol. 34, No. 9, 2757-2762.

Tuah-poku I., Dollar M. and Massalski T.B. (1988), "A study of the transient liquid phase bonding process applied to a Ag/Cu/Ag sandwich joint", *Metallurgical Transactions A*, Vol. 19A, 675-686.

Urena A. and Dunkerton S.B. (1989), "Diffusion bonding of an aluminium-lithium alloy (AA8090)" Report No. 403, 421-456, The Welding Institute, Abington, UK.

Urena A., Gomez de Salazar J. M. and Escalera M. D. (1995), "Diffusion bonding of discontinuously reinforced SiC/Al matrix composites: The role of interlayers", in metal matrix composite; Key Engineering Materials, Vol. 104-107, 523-540, ed. Newaz G.M., Trans Tech. Publications Ltd. Switzerland.

Urena A., Gomez de Salazar J.M., Quinones J. and Martin J.J. (1996a), "TEM characterisation of diffusion bonding of superplastic 8090 Al-Li alloy", *Scripta Materialia*, Vol. 34, No. 4, 617-623.

Urena A., Gomez de Salazar J.M. and Escalera M.D.(1996b), "Diffusion bonding of an aluminium-copper alloy reinforced with silicon carbide particles (AA2014/SiC/13p) using metallic interlayers", *Scripta Materialia*, Vol. 35, No. 11, 1285-1293.

Voller V.R. and Sundarraj S. (1993), "Modelling of microsegregation", *Materials Science and Technology*, Vol. 9, 474-481.

Wallach E.R. (1988), "Solid-state diffusion bonding of metals", *Transactions of. JWRI*, Vol. 17, No. 1, 135-148.

Welding Handbook (1976), 7th ed., Vol. 1, AWS.

Whitman W.G. (1926), "Elimination of salt from sea-water ice", *American Journal of Science*, 5th series, Vol. XI, No. 62, 126-132.

Yokota T., Otsuka M., Haseyama T., Ueki T. and Tokisue H. (1997), "Solid phase welding of alloy AA6061 and SiC_p reinforced alloy AA6061 at intermediate temperature", *Materials Science Forum*, Vol. 242, 225-230.

Zhai Y. and North T.H. (1997), "Counteracting particulate segregation during transient liquid-phase bonding of MMC-MMC and Al_2O_3-MMC joints", *Journal of Materials Science*, Vol. 32, 5571-5575.

Zhou Y. (1994), "Numerical modelling of process kinetics during TLP bonding and other diffusion-controlled processes.", Ph.D. Thesis, University of Toronto.

Zhou Y, Gale W.F. and North T.H. (1995), "Modelling of transient liquid phase bonding", *International Materials Reviews*, Vol. 40, No. 5, 181-196.